CHALMERS
UNIVERSITY OF TECHNOLOGY

Minimizing the Climate Impact of Slab-on-Grade Foundations Through Life Cycle Analysis

Considering energy performance and material use across different building types and material configurations

Master's thesis in Master Program Structural Engineering and Building Technology

ANGELICA ANDERSSON AND LINE JENSEN

DEPARTMENT OF ARCHITECTURE AND CIVIL ENGINEERING

CHALMERS UNIVERSITY OF TECHNOLOGY
Gothenburg, Sweden 2025
www.chalmers.se

Master's thesis 2025

Minimizing the Climate Impact of Slab-on-Grade Foundations Through Life Cycle Analysis

Considering energy performance and material use across different building types and material configurations

ANGELICA ANDERSSON
LINE JENSEN

CHALMERS
UNIVERSITY OF TECHNOLOGY

Department of Architecture and Civil Engineering
Division of Building Technology
Chalmers University of Technology
Gothenburg, Sweden 2025

Minimizing the Climate Impact of Slab-on-Grade Foundations Through Life Cycle Analysis
Considering energy performance and material use across different building types and material configurations
ANGELICA ANDERSSON
LINE JENSEN

Supervisor and examiner: Angela Sasic Kalagasidis, Department of Architecture and Civil Engineering
Supervisor: Martina Stockhaus, PE Teknik & Arkitektur

Master's Thesis 2025
Department of Architecture and Civil Engineering
Division of Building Technology
Chalmers University of Technology
SE-412 96 Gothenburg
Telephone +46 31 772 1000

Cover: Illustration of different building types analyzed in this thesis.
Figures: The illustrations in this master thesis are the authors' own unless otherwise stated.

Gothenburg, Sweden 2025

Minimizing the Climate Impact of Slab-on-Grade Foundations Through Life Cycle Analysis
Considering energy performance and material use across different building types and material configurations
ANGELICA ANDERSSON, LINE JENSEN
Department of Architecture and Civil Engineering
Chalmers University of Technology

Abstract

While it is commonly perceived that increasing insulation thickness improves performance by reducing heat loss through the foundation, this also increases material use and environmental impact. In parallel, interest in alternative foundation materials has grown, driven by the need to reduce embodied carbon and enhance energy efficiency. This thesis investigates the thermal and climate performance of slab-on-grade foundations across three building types: warehouse, residential building, and school/preschool. Three foundation systems, concrete, cross-laminated timber, and the Koljern system, are evaluated under two heating scenarios: heat pump and district heating. The study combines energy simulations in IDA Indoor Climate and Energy with Life Cycle Assessment covering material use (A1–A3) and operational energy (B6).

Thermal transmittance, zone-wise insulation configurations, and total climate impact measured as Global Warming Potential are determined for each combination of system and scenario. U-values are calculated in accordance with Sandin's model, which accounts for the influence of thermal zones in slab-on-grade constructions. Results are presented through line diagrams, stacked bar charts, and supporting tables. The analysis highlights how varying insulation thickness across different thermal zones influences the balance between emissions from material use and emissions from operational energy.

The results show that the cross-laminated timber system consistently achieves the lowest total climate impact across all buildings and heating scenarios. For the other two systems, the lowest climate impact varies depending on building type and heating system. Further, the results show that the most climate-efficient foundation design is not necessarily the one with the lowest U-value, but the one that effectively balances material use and operational energy. In summary, the study shows that strategic choices, such as selecting a different slab-on-grade system or aligning insulation strategy with the heating system, can lower a building's overall climate impact. However, the results also indicate that in certain cases, such as buildings with a relatively small slab-on-grade area, the benefits of insulation optimization are limited.

Keywords: slab-on-grade foundation, cross-laminated timber, concrete, Koljern, life cycle assessment, material use, operational energy, insulation optimization, thermal transmittance, global warming potential.

Acknowledgements

This master's thesis was conducted from January to June 2025 at the Department of Architecture and Civil Engineering, Chalmers University of Technology. It accounts for 30 credits and serves as the final project of the Master's program in Structural Engineering and Building Technology. The thesis was carried out in collaboration between Chalmers University of Technology and PE Teknik & Arkitektur.

We would like to express our gratitude to everyone who supported us throughout the thesis process.

A special thanks to our supervisor Martina Stockhaus at PE Teknik & Arkitektur for her support, encouragement, and the genuine interest she showed in our work throughout the thesis process. Her insights and guidance have truly helped shape our work. We're also very grateful to PE Teknik & Arkitektur for the opportunity to collaborate and for warmly welcoming us into the office.

We are grateful to our examiner Angela Sasic Kalagasidis for her support and feedback, as well as to our opponents, Maja Lageson and Therese Haar, for their thoughtful comments and contributions.

We would also like to thank Patrik Folkerman for input on structural feasibility, Thu Svensson for assistance with Revit modeling, and Emma Wahlfridsson for support with IDA Indoor Climate and Energy simulations.

Lastly, we extend our thanks to our friends and families for their continued encouragement and support throughout this journey.

Angelica Andersson, Gothenburg, June 2025
Line Jensen, Gothenburg, June 2025

List of Acronyms

Below is the list of acronyms that have been used throughout this thesis listed in alphabetical order:

AHU	Air handling unit
Boverket	Swedish National Board of Housing, Building, and Planning
CAD	Computer aided design
CAV	Constant air volume
CLT	Cross-laminated timber
COP	Coefficient of performance
DH	District heating
EPBD	Energy Performance of Buildings Directive
EPD	Environmental product declaration
EPS	Expanded Polystyrene
FTX	Supply and extract ventilation
GWP	Global Warming Potential
HP	Heat pump
HVAC	Heating, ventilation and air condition
IDA ICE	IDA Indoor Climate and Energy
LCA	Life cycle assessment
PCR	Product category rules
SFP	Specific fan power
VAV	Variable air volume

Nomenclature

Below is the nomenclature of indices, parameters, and variables that have been used throughout this thesis.

Indices

i	Index for thermal zones
j	Index for material layers
k	Index for material
l	Index for layer
m_l	Number of materials in layer l
n	Number of layers in the construction

Parameters

CO_2e	CO2 equivalents
$T_{exterior}$	Exterior temperature
$T_{interior}$	Interior temperature
A_{slab}	Slab-on-grade area
A_{gross}	Gross area
A_{temp}	Floor area heated above 10 °C
$A_{envelope}$	Thermal envelope area

Variables

d	Thickness of material layer
f	Fractional areas of each section
R_{tot}	Thermal resistance

$U_{average}$	Average thermal transmittance
U_{tot}	Thermal transmittance
Q	Ventilation air flow
λ	Thermal conductivity

Contents

List of Figures

List of Tables

1
Introduction

This chapter introduces the context, objectives, and methodological framework of this thesis. It begins by outlining the climate impact of the construction sector, emphasizing the growing regulatory and environmental focus on foundation systems, particularly slab-on-grade. The chapter then presents the aim of this thesis and the research questions, which guide the investigation of energy performance and climate impact across different foundation systems and building categories. The methodology section describes the structured approach taken, covering literature review, modeling, optimization, and environmental assessment, to evaluate foundation performance. Finally, the limitations section clarifies the boundaries and assumptions. Together, these sections establish the foundation for this thesis by defining its relevance, scope, and approach.

1.1 Background

The construction and real estate sector is a major contributor to global resource consumption and greenhouse gas emissions, therefore playing a crucial role in the transition toward sustainable built environments (Fossilfritt Sverige, 2024). In Sweden, the sector accounted for approximately 22% of national greenhouse gas emissions in 2021, with emissions arising from various stages of a building's lifecycle, including material extraction, construction, operation, and demolition. Historically, most of a building's lifecycle emissions originated from operational energy use, primarily due to fossil fuel-based heating. As fossil fuels have been phased out for heating and electricity, the relative share of operational emissions has decreased. However, heating still accounts for approximately one-quarter of the sector's total emissions and further reductions can be achieved through improved energy efficiency. Given the long lifespan of buildings, reducing emissions in both the material and operational stages is essential to meet climate targets and moving toward more environmentally sustainable buildings.

As of 2022, newly constructed buildings in Sweden requiring a building permit must submit a climate declaration to assess and report their environmental impact (Boverket, 2023b). This declaration includes all building components, such as the slab-on-grade foundation and its insulation, with the primary aim of reducing emissions from the construction phase. However, current regulations do not yet specify threshold values for acceptable climate impact. Recognizing the urgency of emission reductions, the Swedish National Board of Housing, Building and Planning, commonly

referred to as Boverket, is preparing to introduce mandatory climate impact limits in 2025. These limits will serve as a prerequisite for obtaining building permits and will apply to all new construction projects. Additionally, by 2027, climate declarations and their associated limits are expected to expand to cover the entire lifecycle of buildings, incorporating both operational and end-of-life emissions. These national initiatives align with broader European policies, such as the Energy Performance of Buildings Directive (EPBD), which establishes energy and emission performance requirements for buildings. This initiative is expected to be integrated into Swedish law in 2026 (Boverket, 2024a). The directive mandates that all new buildings constructed from 2030 onward must qualify as zero-emission buildings, while the entire EU building stock aims to achieve zero-emission status by 2050. A zero-emission building is defined as one with high energy performance and minimal greenhouse gas emissions from fossil fuel-based energy sources during operation.

As a fundamental component of the building envelope, slab-on-grade foundations affect thermal efficiency, moisture control, and structural stability, all of which contribute to overall performance. Fossilfritt Sverige (2024) highlights that slab-on-grade foundations represent a significant portion of the total climate impact, particularly in low-rise buildings. The thickness of the slab, which includes both the load-bearing material and insulation, directly affects embodied carbon and resource consumption. While it is commonly perceived that increasing insulation thickness improves performance by reducing heat loss through the foundation, this also increases material use and environmental impact. This underscores the importance of strategic material selection and design optimization to enhance environmental sustainability. Concrete slab-on-grade foundations are the most commonly used type, valued for their structural strength, durability, and ease of construction. However, according to Malmqvist et al. (2023), this foundation system contributes substantially to a building's total climate impact. Furthermore, building with a uniform insulation thickness across the entire slab area is common practice. However, optimizing thermal performance and material use can be achieved by applying different insulation thicknesses in different thermal zones of the slab-on-grade.

In recent years, alternative materials have gained attention as potential replacements for concrete in slab-on-grade foundations, driven by the need to reduce embodied carbon emissions and improve energy efficiency. However, this transition presents challenges related to structural performance, durability, and compatibility with existing construction techniques. One alternative is Cross-laminated timber (CLT). This renewable and low-carbon material offers structural integrity while significantly reducing environmental impact compared to the traditional concrete slab-on-grade (Gustafsson, 2017). Another alternative is Koljern, a prefabricated system consisting of cellular glass insulation, commonly referred to as Foamglas, and embedded steel beams, offering a lightweight and thermally efficient solution compared to conventional slab-on-grade designs (Evia, 2024b). As the construction industry moves toward lower-carbon solutions, understanding the potential and limitations of these alternatives is crucial for sustainable foundation design.

1.2 Aim and research questions

This master thesis aims to evaluate and compare the energy performance and climate impact of different slab-on-grade foundation systems across various building categories, including a combined school and preschool, warehouse, and residential building. For simplicity, the combined school and preschool will be referred to as school/preschool. By analyzing the effects of insulation placement and thickness as well as material selection, this thesis seeks to identify foundation solutions that reduce Global Warming Potential (GWP) from both material use and operational energy use over the building's lifetime, 50 years. An additional objective is to assess the extent to which the slab-on-grade contributes to the total GWP of the building. The aim is to provide insights and practical recommendations that support foundation selection, contributing to more sustainable construction practices. To achieve this, the following research questions will be addressed:

1. How do insulation thickness and placement affect the GWP, considering both material use and operational energy use?
2. How do the environmental impacts of various slab-on-grade systems differ when considering both material use and operational energy use?
3. To what extent can an optimized foundation design, in terms of insulation thickness and material selection, reduce the overall environmental impact of a building?

By addressing these questions, the aim is to evaluate how foundation choices influence sustainability in the built environment. Given the increasing focus on emissions, optimizing foundation design is crucial for reducing embodied carbon and improving energy efficiency. This research contributes to the transition toward environmentally responsible construction by identifying resource-efficient foundation solutions that align with evolving sustainability regulations and industry goals.

1.3 Limitations

This study is limited to buildings with slab-on-grade foundations, assuming stable soil conditions and negligible risk of elevated groundwater levels, thus eliminating the need for additional structural support such as piles. Structural calculations or analyses are excluded from the scope, but a validity assessment is conducted in collaboration with structural engineers from PE Teknik & Arkitektur and manufacturers to validate practical applicability. Acoustic analyses are also excluded. In this thesis, the foundation is parametrically optimized, which is the only element of the climate envelope analyzed.

The environmental impact of the foundation materials is assessed using Life Cycle Assessment (LCA), focusing on selected life cycle stages and using GWP as the climate impact indicator. For the construction stage, only the product stage (A1 to A3), comprising raw material extraction, transport, and manufacturing, are quantitatively analyzed to determine GWP. Due to data limitations, the construction process stage (A4 to A5), encompassing transport to the site and construction, are

not included in the quantitative analysis and is instead briefly addressed within the discussion. For the use phase (stage B), only B6 (operational energy) is quantified through energy simulations, assuming a building lifespan of 50 years. For this thesis, the focus is specifically on the energy used for the heating of the building. Therefore, the energy demand for domestic hot water and property electricity are not considered or included in the analysis. Other components of the use phase, such as maintenance and repair, are excluded from quantitative evaluation and considered only at a general level in the discussion. Similarly, stages C and D, which include demolition, waste processing, and potential reuse or recycling, are only mentioned in general terms due to data constraints and uncertainties surrounding future conditions. Furthermore, LCA calculations for the entire building are only conducted for the cases where input data is provided by PE Teknik & Arkitektur. No whole-building LCA calculations is carried out independently by the authors as part of this thesis.

1.4 Ethical aspects

To ensure the reliability and academic integrity of this thesis, several ethical aspects have been taken into account. Academic integrity has been maintained throughout the thesis process. The AI tool ChatGPT has been utilized primarily for improving the clarity and readability of the authors' written text, such as checking grammar, spelling, and language formulation. However, the tool has not been employed to generate content, write sections of the thesis, or conduct research and gather information. All research findings, analyses, and interpretations presented in the thesis are the result of the authors' work. Furthermore, to support the reliability of the results, all calculations have been performed in accordance with relevant regulations and industry standards, with all assumptions stated. Environmental aspects are a central focus of the thesis, to identify slab-on-grade systems for various building types that minimize GWP over the life cycle.

1.5 Overview of methodology

The methodology of this master thesis is structured into four phases: the initial phase, the modeling phase, the optimization phase, and the environmental impact assessment phase. A flowchart is presented in Figure 1.1 outlining the phases of the study, each phase includes specific tasks and simulations.

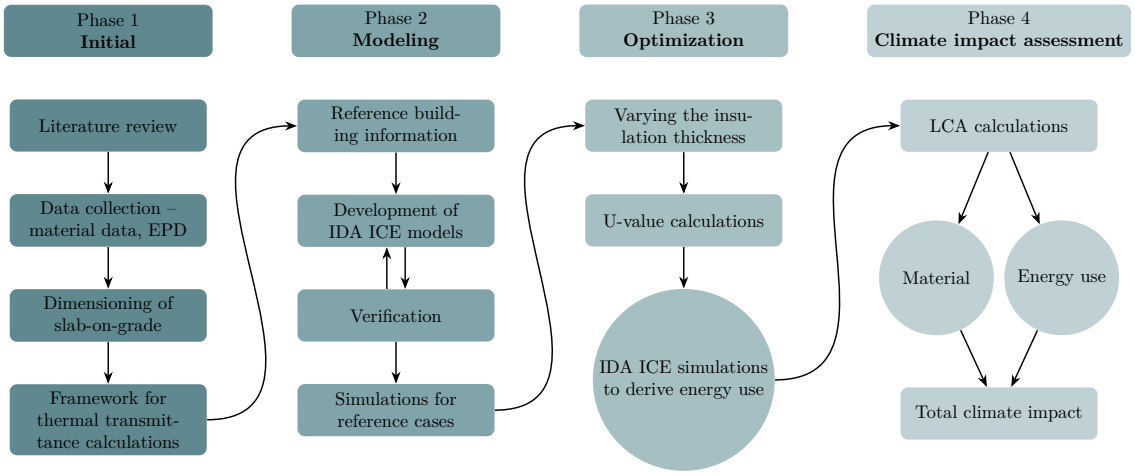

Figure 1.1: Flowchart outlining the four phases of the methodology: initial research, modeling, optimization and climate impact assessment.

The initial phase focused on establishing a theoretical and technical foundation through an extensive literature review and preliminary design calculations. The literature review investigated existing research on slab-on-grade foundations, with particular emphasis on the structural, thermal, and material properties of concrete, Expanded Polystyrene (EPS), CLT, and the Koljern system. This review incorporated peer-reviewed articles, industry standards, and technical reports to ensure a comprehensive understanding of each foundation type's performance attributes and suitability for the three building categories. In parallel, this phase involved dimensioning slab-on-grade foundations to the three reference building types, addressing preliminary load-bearing capacity and thermal insulation requirements. Additionally, a computational framework was developed in MATLAB to calculate the two-dimensional thermal transmittance of a slab-on-grade foundation. The framework is based on the method proposed by Sandin, referred to as Sandin's model in this thesis, enabling quantitative assessment of heat transfer properties to support parametric analysis in the optimization phase (Sandin, 2010).

The modeling phase entailed the development of energy simulation models for the three reference building types using IDA Indoor Climate and Energy (IDA ICE), a dynamic building performance simulation software. Each type of building was modeled with the three different slab-on-grade foundations, integrating site- and building-specific information such as climate data, internal gains, and characteristics of the Heating, Ventilation and Air Conditioning (HVAC) system. The output

of this phase was a set of baseline models that served as a reference for the optimization process. These models were verified to ensure accuracy and reliability in the simulation results.

The optimization phase aimed to systematically refine the thermal performance of the slab-on-grade foundations by varying the insulation thickness for each slab-on-grade type across the three building models. A parametric approach was adopted, where insulation thickness was incrementally adjusted, guided by the U-value calculations from the initial phase. For each iteration, energy simulations were conducted in IDA ICE to determine the annual energy demand.

The environmental impact assessment phase evaluated the performance of the foundation designs by integrating data on energy and material use. The environmental impact was quantified using LCA, in which operational carbon emissions were calculated from the energy demand, derived from the optimization phase. Simultaneously, embodied carbon emissions associated with material use in the optimized designs were estimated using emission factors derived from established Environmental Product Declarations (EPDs). These metrics were analyzed to assess trade-offs between operational energy efficiency and material-induced environmental impacts, ultimately identifying the design solution with the lowest GWP for each building type.

2
Theory

This chapter establishes the theoretical foundation for the thesis by introducing structural and thermal principles related to slab-on-grade foundations. It presents three different foundation systems, concrete with EPS, CLT with EPS, and the Koljern system, highlighting their construction methods and material properties. The chapter then explains heat transfer mechanisms, including thermal resistance and U-value calculations, using Sandin's model. Finally, it outlines the LCA methodology used to evaluate environmental impact, with a focus on GWP. Together, these sections form a framework that connects construction principles, thermal performance, and environmental evaluation, supporting the comparative analysis in later chapters.

2.1 Slab-on-grade

As described by TräGuiden (2020), a slab-on-grade foundation consists of a structural slab placed directly on the ground, providing the base for the building. This foundation method is widely used across various building types. The primary function of a slab-on-grade is to offer structural stability, transfer loads from the building to the underlying soil, and act as a component of the building envelope. Because the slab-on-grade is in direct contact with the ground, it influences the building's heat transfer characteristics and long-term durability. The system is susceptible to thermal and moisture dynamics, making it essential to address these factors in the design. To enhance energy efficiency and protect against moisture-related issues, slabs are typically insulated beneath and around the perimeter. This insulation helps maintain comfortable indoor temperatures, minimizes the risk of thermal bridges, and reduces overall heat loss. Additionally, it ensures the slab-on-grade remains warm, thereby supporting the long-term performance and durability of both the foundation and the building.

2.1.1 Requirements and construction

The design and construction of a slab-on-grade must fulfill several structural and thermal requirements to ensure stability and energy efficiency. A key consideration is load-bearing capacity, as the slab must support both imposed loads from occupants and furnishings as well as the dead loads of the building itself. According to TräGuiden (2020), edge beams are integrated into the slab to support load-bearing walls, distribute loads evenly, and minimize the risk of settlement. To

enhance thermal performance and prevent heat loss at the slab perimeter, these beams are typically insulated using specialized masonry blocks or cellular plastic elements with pre-fabricated plinth cladding. Their dimensions vary depending on the building category, reflecting the specific structural requirements of different construction types. Additional support elements such as beams or footings may be incorporated to enhance structural stability. Footings are typically placed where load-bearing walls and columns are located to provide adequate load distribution and prevent settlement. See Figure 2.1 for an illustration of both an edge beam and a footing.

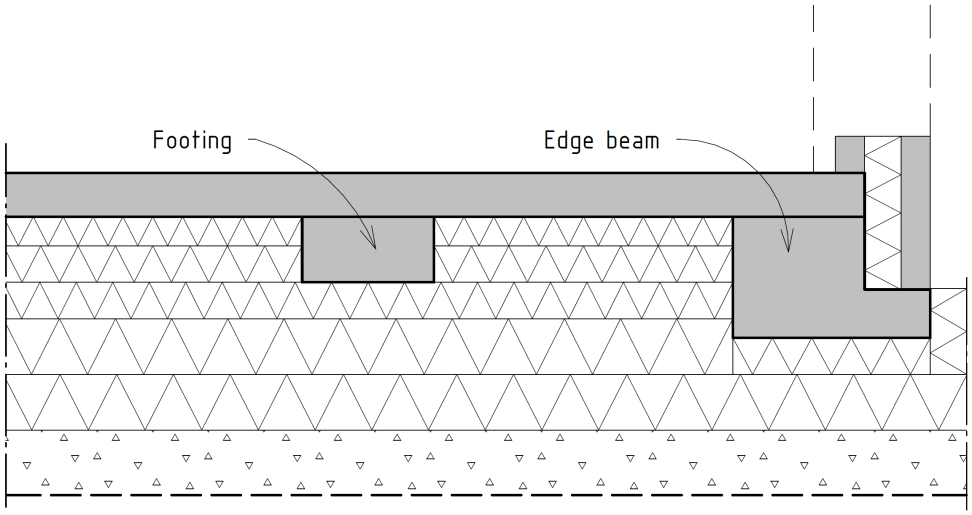

Figure 2.1: Illustration of a slab-on-grade showing an arbitrary footing and edge beam.

Additionally, moisture control measures, such as a moisture barrier or a capillary-breaking layer, are essential in preventing water ingress, reducing the risk of mold growth, and material deterioration. In cold climates, frost protection is particularly crucial, as insufficient insulation can lead to frost heave and structural damage (Roots & Hagentoft, 2004). Furthermore, thermal insulation plays an important role in minimizing heat loss and ensuring compliance with energy efficiency standards, helping to maintain indoor comfort and prevent frost-related damage to the foundation. Both load-bearing capacity and thermal insulation are crucial factors as they directly impact material use and energy efficiency.

2.1.2 Slab-on-grade systems and materials

This master thesis explores the environmental benefits of alternative foundation systems by using a concrete slab with EPS insulation, the most widely used slab-on-grade foundation, as a reference. Additionally, two emerging alternative foundation systems are analyzed: CLT with EPS insulation and the Koljern system, composed of Foamglas and steel beams. For simplicity, the concrete slab with EPS insulation and CLT with EPS insulation types are hereafter referred to as the concrete system and CLT system, respectively. These systems are gaining attention for their sustainability potential and have already been implemented in several Swedish construc-

tion projects. For instance the Koljern system was used in the fossil-free preschool project Hoppet in Gothenburg (FOAMGLAS, 2025), and also in the Rosendalsgatan preschool project (Göteborgs Stad, 2025), illustrating its growing application in building foundations. The CLT system has been applied in several residential buildings where the system is delivered by the manufacturer Klara Byggsystem (Klara Byggsystem, 2025b). The construction process of a slab-on-grade foundation, regardless of the specific system used, follows a systematic approach to ensure proper load distribution, thermal insulation, and durability. The process begins with soil preparation, where the subgrade is compacted to create a stable and uniform bearing surface. If soil conditions require additional stabilization, a gravel or crushed stone layer is introduced beneath the insulation to enhance drainage and prevent excessive moisture accumulation. Once the subgrade is prepared, insulation is installed directly on the compacted soil or gravel layer, with its thickness determined by thermal performance and structural load requirements. A waterproof membrane is often applied above the insulation to further reduce moisture ingress. Following insulation placement, load-bearing elements are installed in accordance with structural design specifications. Additional moisture protection measures, such as sealants and protective coatings at connection points and around penetrations, may be implemented. Proper site drainage management, including sloped grading around the foundation and perimeter drains, is essential to minimize the risk of moisture-related deterioration.

2.1.2.1 Concrete system

Concrete exhibits excellent compressive strength but limited tensile capacity, which necessitates the use of steel reinforcement to resist both vertical and lateral loads. In slab-on-grade foundations, reinforcement is essential for controlling cracking, distributing loads, and ensuring structural stability under various service conditions. Concrete has relatively low thermal insulation capacity, therefore EPS is incorporated beneath the slab to minimize heat loss and improve energy efficiency. EPS, a lightweight closed-cell polymeric foam, serves a dual function in slab-on-grade applications: it acts as a thermal insulator, reducing heat transfer between the ground and indoor environment, and functions as a capillary-breaking layer, mitigating moisture ingress from the underlying soil. EPS have different compressive strengths depending on the type, for example, EPS S200 has a higher compressive strength than EPS S100. In some cases, extruded polystyrene (XPS) is used instead of EPS, particularly where higher compressive strength is required. By preventing capillary rise, EPS helps reduce the risk of frost heave in cold climates and enhances the long-term durability of the foundation system. Once the EPS layer is installed, concrete is poured, leveled, and finished to achieve the required surface characteristics. To enhance structural integrity and service life, crack control measures, such as appropriate reinforcement layout, are implemented. Curing is a critical step to prevent premature drying, which could otherwise lead to shrinkage cracking and reduced durability. Furthermore, optimizing the water-cement ratio and selecting a suitable exposure class based on site-specific conditions help ensure long-term performance. To mitigate the environmental impact of cement production, low-carbon concrete alternatives, such as mixes with lower clinker content or supplementary cementitious

materials, are increasingly used in foundation systems. Depending on the specific mix design and production method, these alternatives can result in varying levels of GWP reduction. A commonly used low-carbon concrete mix typically achieves around a 20% reduction in GWP compared to conventional concrete (A. Akram, Personal communication, 5 Maj 2025).

2.1.2.2 CLT system

The CLT slab examined in this master thesis is based on a system developed by Klara Byggsystem, see Figure 2.2. The system is a prefabricated alternative to traditional concrete slab-on-grade constructions, utilizing CLT as the primary load-bearing material and omitting the use of concrete (Klara Byggsystem, 2025a). In this system, CLT is combined with EPS insulation to optimize thermal performance and minimize heat loss through the foundation. According to Gustafsson (2017), CLT has a significantly lower embodied carbon footprint than concrete due to the renewable nature of timber. It exhibits high strength and stiffness, allowing it to support structural loads while offering design flexibility. However, its vulnerability to moisture necessitates additional protective measures to ensure long-term durability and energy performance. Preventing capillary rise is crucial, as excessive moisture exposure can lead to swelling, reduced mechanical strength, and biological degradation such as mold or fungal growth. According to E. Goverde (Personal communication, 25 April 2025) the system includes a weather-resistant coating (labelled as No.3 in Figure 2.2) designed to enhance moisture protection during transportation, assembly and construction. This self-adhesive protective layer remains on the element after installation and is designed to shield wood-based materials from moisture-related degradation by forming a barrier that prevents liquid water infiltration while allowing controlled vapor diffusion. Before floor installation, a gas- and vapor-tight membrane is applied (labelled as No.4 in Figure 2.2). It consists of a reinforced polymer material with a thin aluminum layer, which serves as an effective barrier against gaseous emissions and moisture ingress. This membrane acts as a complete barrier against both odors and moisture, ensuring that the foundation system meets indoor environmental requirements related to emissions from biological processes in the soil as well as radon.

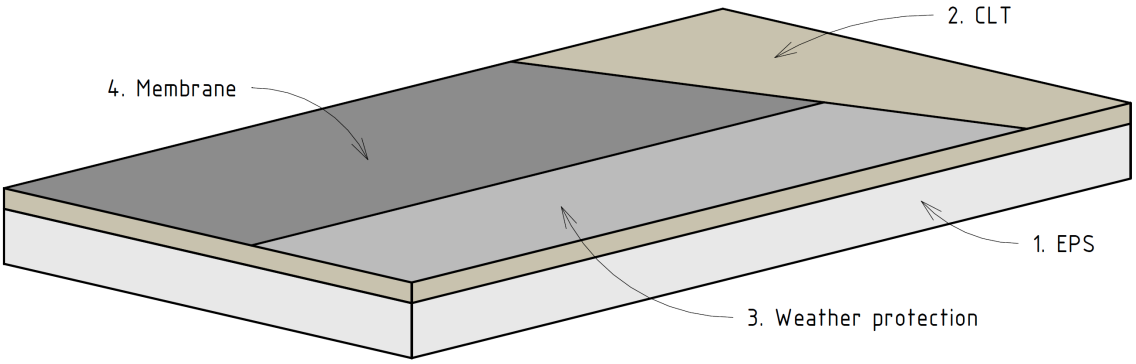

Figure 2.2: Illustration of a CLT slab-on-grade, detailing the materials and placement used in this master thesis. Inspired by figure from Klara Byggsystem (2025a).

In this type of foundation, the load-bearing elements, such as beams or footings, are typically constructed from concrete. In cases where higher compressive strength is required, an additional concrete screed may be applied. A concrete screed is a thin layer of self-leveling concrete that distributes load more evenly and enhances the foundation's structural performance. Additionally, careful consideration of site-specific conditions is crucial in designing a robust foundation system (Gustafsson, 2017). The load-bearing capacity of the CLT panels is influenced by their thickness, lamination configuration, and the overall building design.

2.1.2.3 Koljern system

The Koljern system is a prefabricated foundation solution that replaces the traditional concrete slab-on-grade, as described by Evia (2024b). This system entirely eliminates the use of concrete and cellular plastic. Koljern is composed of Foamglas and galvanized steel light-gauge beams, making it an inhomogeneous system. See Figure 2.3 for an illustration of an element and the placement of the steel beams. The steel beams are embedded between the Foamglas panels to ensure adequate compressive strength. Foamglas handles 500–1600 kPa of pressure depending on the product (Evia, 2024a). The assembly forms a structural element with standard dimensions of 12 m × 4 m. The elements are assembled together on-site to form a complete slab-on-grade foundation. Typically, Foamglas T3+ is used for this type of system (N. Holmquist, Personal communication, 18 February 2025). According to Evia (2024a), the Koljern foundation exhibits similar properties to a conventional concrete slab-on-grade while offering high performance, long durability and a significantly lower environmental impact. The system is designed for buildings with a timber structure of up to five stories. In this type of foundation, the support elements, beams or footings, are typically made of steel (Evia, 2024a). However, CLT and concrete alternatives are also viable (N. Holmquist, Personal communication, 18 February 2025). A concrete screed can also be included in this system, when the compressive strength is insufficient.

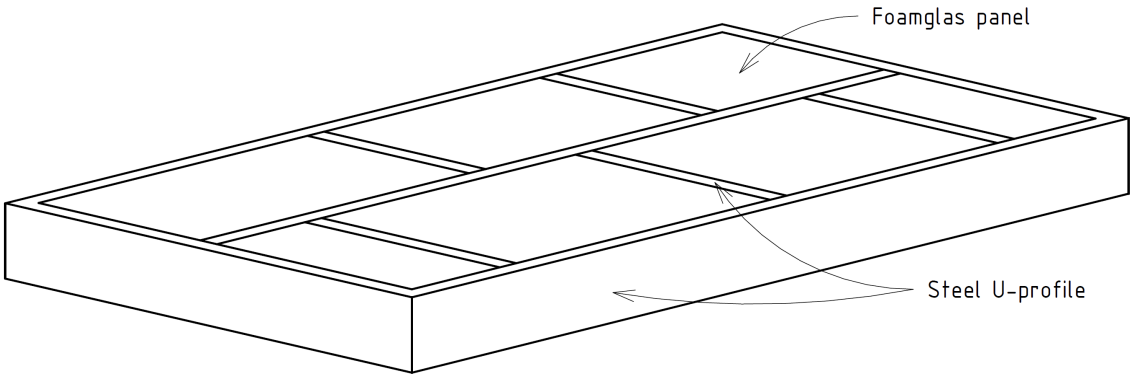

Figure 2.3: Illustration of a Koljern system with Foamglas panels and steel beams. Based on figure from Evia (2024b).

According to Evia (2024a), the top layer of the subgrade must be carefully leveled to ensure even load distribution and to account for varying soil conditions. The ground must have a bearing capacity of at least 150 kPa to provide a reliable foundation. Following subgrade preparation, foamglas elements are placed directly on the compacted surface, serving as an additional insulation layer beneath the Koljern element. Due to their closed-cell glass structure, the panels provide complete resistance to capillary water absorption, preventing moisture accumulation within the foundation and mitigating risks associated with freeze-thaw cycles.

2.2 Heat transfer analysis

Understanding heat transfer mechanisms in slab-on-grade foundations is essential for accurately predicting energy performance in buildings. Rantala (2005) describes how a slab-on-grade structure is unique within the building envelope, as it is in direct contact with the soil, which serves as a heat sink, continuously transferring heat away from the building. The heat exchange between the slab and the ground is a complex three-dimensional process influenced by indoor temperatures, outdoor climate conditions, and the thermal properties of the subsoil. The rate of heat flow into the ground is determined by the indoor temperature, potential thermal stresses from floor heating systems and the thermal resistance of the slab structure. Near the building perimeter, the impact of seasonal outdoor temperature variations is more pronounced, particularly at corners, where heat loss is typically higher. This increased heat loss at building corners is an example of a thermal bridge.

Further supporting these observations, Carl-Eric Hagentoft (2001) defines thermal bridges as regions of increased heat loss that typically occur at junctions between structural elements, such as at the intersection of two walls or at the connection between a wall and a slab-on-grade. The thermal bridges not only amplify conductive heat losses but also contribute to a reduction in internal surface temperatures, potentially leading to condensation and moisture-related degradation. Given that the floor represents a large portion of the building envelope, a significant fraction of the total heat loss occurs downward into the soil. Additionally, the presence of a thermal pillow beneath the foundation, a zone where ground temperatures remain elevated due to sustained heat dissipation from the structure, demonstrates the complex heat transfer mechanisms occurring within the soil.

As described by Sandin (2010), thermal bridges in structural elements, such as edge beams in slab-on-grade constructions, introduce additional heat loss that cannot be accurately estimated using simple analytical methods. Due to the complexity of the geometry and varying material properties, numerical methods are often required for precise calculations. Thermal bridges occur where materials with high thermal conductivity disrupt the continuity of the insulation layer. This is particularly evident at the edges of slab foundations, where heat loss becomes more pronounced due to the interaction between the foundation, surrounding ground, and structural elements. The heat transfer in these areas is often two- or even three-dimensional, increasing the overall thermal loss of the building. Additionally, support elements

of the slab, such as footings, further contribute to thermal bridging effects. These elements have a significantly higher thermal conductivity leading to localized heat loss. The impact of thermal bridges in slab-on-grade constructions is relevant when considering overall building energy efficiency. If not properly managed, they can contribute to increased heating demand, condensation risks, and discomfort due to uneven indoor surface temperatures.

2.2.1 Sandin's model

Sandin's model provides a detailed explanation of the complexities involved in heat transfer for building components in direct contact with the ground. When heating begins, a thermal pillow develops beneath the building because the ground's high heat capacity delays heat flow from the interior. The maximum heat flux aligns with the period when the temperature difference between the interior and exterior is highest. The steady-state heat flow through a slab-on-grade is illustrated in Figure 2.4, demonstrating how the heat flow varies depending on the distance from the center of the slab. In the figure, T_{interior} represents the indoor temperature maintained within the heated space, while T_{exterior} refers to the outdoor ground surface temperature. This temperature difference drives the heat loss from the building, with the largest gradients and the greatest heat flow occurring near the slab edges. Sandin's model presented in this section is based on Sandin (2010).

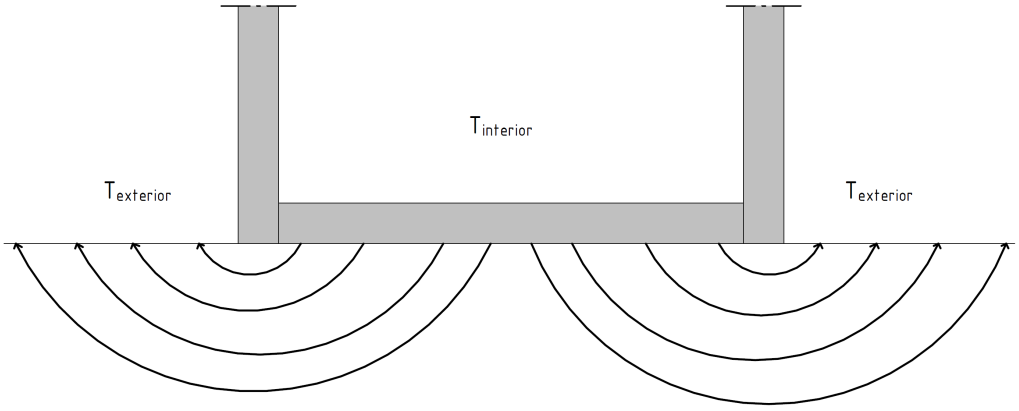

Figure 2.4: Illustration of the heat flow through a slab-on-grade. Figure from Sandin (2010).

To accurately calculate the heat flow, it is necessary to integrate the flow over the entire slab surface. Since a point near an exterior wall has a significantly shorter path to the outdoor air than a point at the center, the thermal resistance near the wall is considerably lower. This variability makes exact calculations more complex and typically requires advanced computer simulations. For practical purposes, a slab-on-grade is typically divided into three thermal zones, each assigned a specific thermal resistance depending on the distance from the building edge and the underlying soil conditions, as illustrated in Figure 2.5. Zone 1 (0–1 m) represents the slab edge closest to the outdoor environment and is most exposed to heat loss. Zone 2 (1–6 m) covers the intermediate area, while Zone 3 (>6 m) represents the central, least

exposed part of the slab. This zoning reflects the varying heat transfer characteristics across the slab and is used in both modeling and insulation optimization.

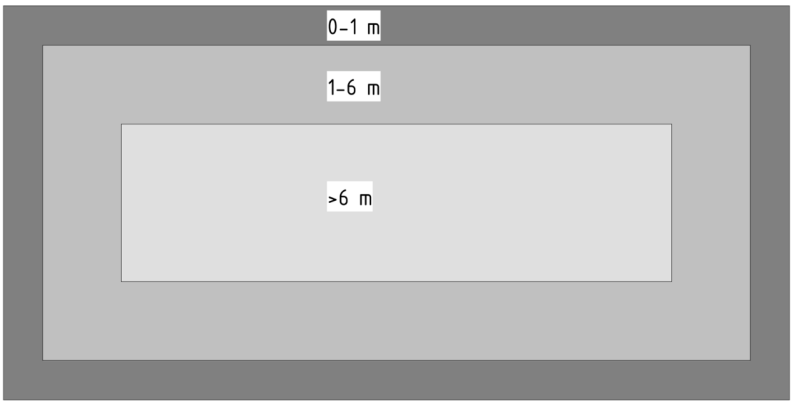

Figure 2.5: Illustration of three different thermal zones for a slab-on-grade. Figure from Sandin (2010).

Practically applicable thermal resistance values for ground conditions are provided in Table 2.1. These values exclude surface heat transfer resistance at the interfaces, which is essential to account for in the calculations. The provided values assume that no snow is present on the ground. Additionally, a drainage layer with a minimum thickness of 150 mm can contribute with an extra thermal resistance of $0.20\,\mathrm{m}^2 \cdot \mathrm{K/W}$.

Table 2.1: Thermal resistance values for different soil types.

Key performance indicators			
Soil Type	Thermal resistance $[\mathrm{m}^2 \cdot \mathrm{K/W}]$		
	0-1 m	1-6 m	>6 m
Clay, drained sand and gravel	1.00	3.40	4.40
Silt, moraine, undrained sand and gravel	0.70	2.20	2.70
Crushed stone	0.60	1.80	2.20
Bedrock	0.50	1.40	1.80

In practice, the construction sector primarily relies on the methodology described by Sandin (2010) for calculating heat transfer in slab-on-grade foundations. This method is used by PE Teknik & Arkitektur, as it provides a practical and empirically validated approach that aligns with real-world applications. An alternative method is outlined in SS-EN ISO 13370:2017, which offers a standardized framework for determining thermal transmittance, U_{tot}, and thermal resistance, R_{tot} (Swedish Standards Institute [SIS], 2017). However, its application in the industry is limited compared to Sandin's approach. To ensure alignment with established practice and to produce results relevant for practical implementation, this master thesis adopts the method described by Sandin (2010), which is presented below.

Thermal resistances of material layers
The total thermal resistance of a zone is composed of multiple material layers, each contributing to the overall resistance. The thermal resistance, $R_{\text{layer},j}$, of an individual material layer j within a given zone is calculated with Equation 2.1, where the sum of all layer resistances is included in the total thermal resistance.

$$R_{\text{layer},j} = \frac{d_j}{\lambda_j} \tag{2.1}$$

where	$R_{\text{layer},j}$	Thermal resistance of material layer j, in $\text{m}^2 \cdot \text{K/W}$
	d_j	Thickness of material layer j, in m
	λ_j	Thermal conductivity of material layer j, in $\text{W/(m} \cdot \text{K)}$

Thermal resistance for each thermal zone
For practical calculations, the foundation is divided into three thermal zones, see Figure 2.5, based on the distance from the exterior wall, with corresponding ground resistances $R_{\text{ground},i}$. The total thermal resistance for each thermal zone is given by:

$$R_{\text{tot},i} = R_{\text{si}} + \sum_{j=1}^{n} R_{\text{layer},j} + R_{\text{drainage}} + R_{\text{ground},i} + R_{\text{se}} \tag{2.2}$$

where	$R_{\text{tot},i}$	Total thermal resistance of zone i, in $\text{m}^2 \cdot \text{K/W}$
	$R_{\text{si}}, R_{\text{se}}$	Internal and external surface resistances, 0.04 and 0.17 respectively, in $\text{m}^2 \cdot \text{K/W}$
	$R_{\text{layer},j}$	Thermal resistance of material layer j within thermal zone i, in $\text{m}^2 \cdot \text{K/W}$
	R_{drainage}	Thermal resistance provided by the drainage layer, in $\text{m}^2 \cdot \text{K/W}$ (assumed to be $0.20\,\text{m}^2 \cdot \text{K/W}$)
	$R_{\text{ground},i}$	Ground resistance for thermal zone i, in $\text{m}^2 \cdot \text{K/W}$ (values can be found in Table 2.1)
	n	Total number of layers in the construction

The total heat transmittance for each thermal zone is then calculated as:

$$U_i = \frac{1}{R_{\text{tot},i}} \tag{2.3}$$

where	U_i	Thermal transmittance (U-value) of thermal zone i, in $\text{W/(m}^2 \cdot \text{K)}$

Weighted average U-value
To obtain the overall thermal transmittance of the slab-on-grade foundation, a weighted average U-value is computed based on the area distribution of each thermal zone:

$$U_{\text{tot}} = \frac{A_1 U_1 + A_2 U_2 + A_3 U_3}{A_{\text{tot}}} \tag{2.4}$$

where A_1, A_2, A_3 Areas of the three thermal zones, in m^2
A_{tot} Total slab area, in m^2

This method provides a structured approach to determining the U-value of slab-on-grade foundations, accounting for varying thermal resistances across different zones. The mathematical framework presented here serves as a basis for evaluating the thermal performance of different foundation configurations. However, this approach is applicable only to homogeneous components. If a component consists of both homogeneous and inhomogeneous layers, the thermal resistance, $R_{\text{layer},j}$ must be computed using a different method, see Section 2.2.2.

2.2.2 Thermal resistance of inhomogeneous layers

According to SS-EN ISO 6946:2017, for a slab-on-grade consisting of both homogeneous and inhomogeneous layers, the total thermal resistance is calculated with Equation 2.5 as the mean value of the upper and lower thermal resistances (SIS, 2017). This thermal resistance should replace $\sum_{\text{j=1}}^{\text{n}} \text{R}_{\text{layer,j}}$ in Equation 2.2.

$$R_{\text{layer, inhomogeneous}} = \left(\frac{R_{\text{tot, upper}} + R_{\text{tot, lower}}}{2} \right) \tag{2.5}$$

where $R_{\text{tot, upper}}$ Upper limit of the total thermal resistance, in $\text{m}^2 \cdot \text{K/W}$
$R_{\text{tot, lower}}$ Lower limit of the total thermal resistance, in $\text{m}^2 \cdot \text{K/W}$

The upper limit of the total thermal resistance is given by:

$$R_{\text{tot, upper}} = \sum_{l=1}^{n} \sum_{k=1}^{m_l} f_{k,l} \cdot R_{k,l} \tag{2.6}$$

where $f_{k,l}$ Area fraction of material, k, in layer l (dimensionless), with $\sum_k f_{k,l} = 1$
$R_{k,l}$ Thermal resistance of material, k, in layer l, in $\text{m}^2 \cdot \text{K/W}$

m_l Number of materials in layer l

The lower limit of the total thermal resistance is given by:

$$R_{\text{tot, lower}} = \sum_{l=1}^{n} R_l \tag{2.7}$$

For homogeneous sections:

$$R_l = \frac{d_l}{\lambda_l} \tag{2.8}$$

For inhomogeneous sections:

$$R_l = \frac{d_l}{\lambda_{\text{eq},l}} \tag{2.9}$$

where the equivalent thermal conductivity is:

$$\lambda_{\text{eq},l} = \sum_{k=1}^{m_l} \lambda_{k,l} \cdot f_{k,l} \tag{2.10}$$

where
- $\lambda_{k,l}$ Thermal conductivity of material, k, in layer l, in $\text{W}/(\text{m} \cdot \text{K})$
- d_l Thickness of layer l, in meters (m)
- R_l Thermal resistance of layer l, in $\text{m}^2 \cdot \text{K}/\text{W}$

2.2.3 Thermal performance of slab-on-grade types

The thermal performance of slab-on-grade foundations plays a crucial role in a building's overall energy efficiency and indoor climate stability. Different slab-on-grade construction methods utilize various materials, each with distinct thermal characteristics that impact heat loss, thermal bridges, and temperature regulation. This section examines the three different slab-on-grade types focusing on their respective thermal properties and insulation solutions.

2.2.3.1 Concrete system

The thermal conductivity of concrete is relatively high compared to insulation materials, making it a poor thermal insulator on its own. To address this, EPS insulation is incorporated beneath the slab to enhance energy efficiency and indoor thermal comfort. The thickness and density of EPS are determined based on the required U-value, which dictates the slab's ability to minimize heat loss. The combination of concrete and EPS is homogeneous and exhibits uniform thermal properties. For the calculation model used to determine thermal transmittance, see Section 2.2.1. EPS insulation plays a critical role in reducing thermal bridges. Additionally, the thermal mass of concrete helps stabilize indoor temperatures by storing and slowly releasing heat, reducing temperature fluctuations. The long-term performance of

EPS is influenced by factors such as moisture resistance, compression strength, and durability. In practice, the thermal conductivity (λ) of EPS typically ranges from $0.033 - 0.041\,\mathrm{W/(m \cdot K)}$, depending on its density, with a specific heat capacity of approximately $1.400\,\mathrm{J/(kg \cdot K)}$. In contrast, concrete has a significantly higher thermal conductivity of approximately $1.7\,\mathrm{W/(m \cdot K)}$ and a specific heat capacity of around $900\,\mathrm{J/(kg \cdot K)}$, which highlights the necessity of incorporating insulation to reduce heat loss in concrete slab-on-grade constructions.

2.2.3.2 CLT system

CLT provides both structural integrity and thermal performance in slab-on-grade constructions. The combination of CLT and EPS is homogeneous. For the calculation model used to determine thermal transmittance, see Section 2.2.1. According to Gustafsson (2017), CLT exhibits minimal thermal expansion, making it stable under varying temperatures. Its thermal conductivity is relatively low, typically ranging from $0.12 - 0.13\,\mathrm{W/(m \cdot K)}$. Additionally, CLT has a high specific heat capacity of approximately $1.300\,\mathrm{J/(kg \cdot K)}$. To optimize energy efficiency and reduce heat loss to the ground, EPS insulation is often incorporated beneath the CLT slab. The thickness and density of EPS are selected based on the required U-value, ensuring an effective insulation layer.

2.2.3.3 Koljern system

The Koljern system composed of foamglas and galvanized steel light-gauge beams is inhomogeneous and exhibits non-uniform thermal properties. For the calculation model used to determine thermal transmittance, see Section 2.2.2. Foamglas has a low λ, typically around $0.036\,\mathrm{W/(m \cdot K)}$. The prefabricated nature of Koljern slabs ensures consistent quality and thermal properties, reducing onsite variability in insulation performance. In practice, cellular glass has a specific heat capacity of approximately $800 - 1000\,\mathrm{J/(kg \cdot K)}$. The combination of insulation and structure in a single element reduces the overall thickness of the foundation while maintaining high energy efficiency. However, to further enhance thermal performance, additional layers of foamglas insulation is added beneath the load-bearing Koljern element.

2.3 Environmental impact

Environmental impact refers to any change to the environment, whether positive or negative, resulting from human activities, products, or services. This includes impacts associated with material production, energy use, and emissions throughout a system's life cycle. These impacts are typically quantified using LCA methodologies. In this thesis, climate impact is evaluated using GWP as the primary metric, where the values of construction materials are obtained from EPDs. Additionally, the GWP of different heating sources is assessed to account for the emissions associated with operational energy use.

2.3.1 Life Cycle Assessment

LCA is a standardized method for assessing the environmental impact of a building or product over its entire life cycle. As defined in SS-EN 15978:2011, this includes raw material extraction, production, use, and end-of-life processes (SIS, 2011). By analyzing these stages, LCA enables the identification of the most environmentally significant stages, providing valuable insights for reducing a building's overall environmental footprint. The life cycle is divided into four stages: construction (A), operation (B), end-of-life (C), and beyond-system-boundary effects (D). Table 2.9 provides an overview of the various life cycle stages and presents the modules within each stage.

Table 2.9: Overview of the building life cycle stages.

A: Product stage	**A1:** Raw material supply **A2:** Transport **A3:** Manufacturing
A: Construction process stage	**A4:** Transport **A5:** Construction process
B: Use stage	**B1:** Use **B2:** Maintenance **B3:** Repair **B4:** Replacement **B5:** Refurbishment **B6:** Operational energy use **B7:** Operational water use
C: End-of-Life stage	**C1:** Deconstruction, demolition **C2:** Transport **C3:** Waste processing **C4:** Disposal
D: Benefits and loads beyond the system boundary	**D:** Reuse, recovery, recycling

LCA can incorporate multiple environmental impact indicators, including global warming-, acidification-, eutrophication- and ozone depletion potential. As stated by Boverket (2024b), GWP is widely regarded as the most critical indicator due to the urgency of climate change. Consequently, it is common practice to focus LCA studies of buildings primarily on GWP, see Section 2.3.2 for more detailed information about GWP. Notably, the potential to minimize environmental impact, including the GWP, is greatest during the early stages of the building process, where design decisions can significantly influence resource efficiency, material selection, and overall sustainability.

The construction stage begins with the product stage (A1–A3), covering raw material extraction, transport to manufacturing, and production of building components (Gervasio & Dimova, 2018). Impacts from this phase include resource depletion, energy use, and emissions, contributing significantly to GWP. In LCA, the environmental performance of this stage is typically assessed using standardized data sources, such as EPDs, which provide verified data on a product's life cycle impacts, enabling comparisons across different materials. The construction process stage (A4–A5) includes transport to the site and on-site work. Module A4 include transport-related emissions, depending on distance, fuel type, and material mass, while A5 covers on-site activities like slab installation, involving electricity and fuel use. Due to high variability and site-dependency, especially in A5, estimates often rely on generalized or qualitative assessments.

The use stage, defined in SS-EN 15978:2011, covers the building's operational life from handover to deconstruction (SIS, 2011). It includes modules B1–B7, addressing environmental impacts related to the building's use, maintenance, and operation. This encompasses the performance of construction products and systems essential for indoor comfort, such as heating, cooling, ventilation, lighting, and water supply. It also covers activities like maintenance, repair, and refurbishment. According to Boverket (2025a) a significant contributor to environmental impact in this stage is operational energy (B6). Energy consumption encompasses heating, cooling, ventilation, and electricity use. The environmental footprint of these processes is influenced by factors such as energy efficiency measures, thermal performance, and choice of energy source. The environmental impact of the energy source depends on whether electricity, district heating (DH), or other energy carriers are used, as different sources have varying GWP.

The end-of-life stage (C1–C4) begins when the building reaches the end of its service life, covering deconstruction (C1), transport to processing facilities (C2), waste processing (C3), and final disposal (C4) (SIS, 2011). Environmental impacts vary depending on demolition methods, transport distances, treatment techniques, and the share of materials that can be reused or recycled. Residual materials are disposed of through landfill or incineration, contributing to long-term emissions. The choice of selective demolition versus traditional demolition techniques can significantly influence recovery rates and total environmental impact. Lastly, module D accounts for net environmental impacts or benefits from reuse, recycling, and energy recovery beyond the system's life cycle (SIS, 2011). It considers components intended for reuse and materials suitable for recycling or energy recovery as resources contributing to future material cycles. Accurate assessment requires consideration of degradation, composition, and recovery efficiencies. However, due to limited standardized return rates and regional variation, assumptions are often generalized, complicating precise life cycle assessments.

2.3.2 Global Warming Potential

According to Makhnatch (2014) GWP is a standardized metric used to evaluate the climate impact of greenhouse gases by comparing their radiative forcing to that of carbon dioxide over a specified time period, typically 100 years. This metric quantifies the total energy a given mass of a greenhouse gas contributes to global warming relative to an equivalent mass of CO_2. CO_2, which has a GWP of 1 by definition, other gases are assigned higher factors based on their heat-trapping capacity and atmospheric persistence. For instance, methane's GWP of 25 indicates that one tonne of methane emissions equals 25 tonnes of CO_2 equivalents (CO_2e) in terms of warming effect. By converting emissions into CO_2e using these gas-specific GWP values, the cumulative contribution of diverse greenhouse gases to global warming can be uniformly assessed, providing a basis for evaluating the environmental performance of materials and energy use across a building's life cycle.

2.3.3 Environmental Product Declaration

An EPD describes the environmental impact of a product throughout its entire life cycle. The development and structure of EPDs are governed by the standard SS-EN 15804:2012+A2:2019, which establishes the methodological framework and requirements for the construction sector (SIS, 2019). According to this standard, an EPD must adhere to defined calculation principles and methodological rules to ensure consistency and comparability. The purpose is to provide transparent, verifiable, and comparable information on the environmental performance of a product, enabling scientifically based assessments and comparisons between different products. An EPD consists of three main components: a product description, which presents information about the product and its technical properties, a methodology section, which outlines the assumptions and calculation principles used in the LCA and an impact assessment, which quantifies the environmental effects of the product across defined categories, such as GWP, resource consumption and acidification. To ensure methodological consistency, product-category rules (PCR) must be followed when conducting the LCA. These rules, also defined within the standard, provide guidelines concerning system boundaries, methodological choices, and calculation principles for different product categories, such as insulation materials. For a comparison between two products to be valid, their EPDs must be based on the same PCR, ensuring equivalent assessment criteria. To guarantee reliability, an EPD undergoes independent review and verification by an external party. The validity of an EPD is typically three to five years, after which it must be updated to reflect potential changes in production processes, raw material sourcing, or regulatory requirements.

2.3.4 Heat sources

Heating systems play a crucial role in the overall energy performance and environmental impact of buildings. The choice of heat source significantly influences operational energy demand and GWP. In this thesis, various heat sources are incorporated, including district heating and various types of heat pump (HP).

2.3.4.1 District heating

District heating is an efficient and environmentally sustainable energy system that supplies heat to more than half of all commercial and residential buildings in Sweden (Rydegran, 2023). Heat production for district heating networks can originate from different sources, including dedicated heat plants, which generate heat solely through combustion. Another common source is combined heat and power plants, which produce both electricity and heat. Additionally, surplus heat from industrial processes can be recovered and supplied to the district heating network, further reducing energy waste. The fuel mix for district heating in Sweden primarily consists of renewable and recycled energy sources. A significant portion of the energy comes from biomass residues from the wood industry, excess heat from industrial facilities and data centers, as well as non-recyclable municipal waste. The reliance on fossil fuels in district heating production has declined markedly since the 1980s, with fossil fuels now accounting for only two percent of the total fuel mix. This transition has resulted in a substantial reduction in carbon dioxide emissions, making district heating one of the most sustainable large-scale heating solutions available. According to climate data derived from Boverket (2025b), the Swedish average GWP of district heating is 0.056 kg CO_2e per kWh.

2.3.4.2 Heat pumps

Heat pumps are thermodynamic systems designed to transfer heat stored in air, water, or soil to the interior of a building. By utilizing electricity, heat pumps achieve a coefficient of performance (COP) greater than one, meaning they can deliver more heat energy than the electricity consumed. The selection of heat pump type is influenced by factors such as the heat source, the building's energy requirements, and local climate conditions, including seasonal temperature variations and the availability of natural heat sources. Heat pump systems are known for their energy efficiency, however, their environmental impact largely depends on the source of electricity used to operate them. When powered by renewable energy, heat pumps can significantly reduce greenhouse gas emissions. According to Boverket (2025c), the CO_2e per kWh for the Swedish electricity mix is 0.037 kg.

There are various types of heat pumps, each optimized for specific heating and cooling requirements (Svenska kyl och värmepumpföreningen, n.d.). Air-to-air heat pumps, for example, extract heat from outdoor air and transfer it to indoor air. These systems are particularly beneficial for buildings that currently rely on direct electric heating, as they offer a more energy-efficient alternative by reducing electricity demand. However, an additional heating system is required because the

air-to-air heat pump serves only as a complement and does not provide domestic hot water. Another variant is the extract-air heat pump, which recovers heat from the exhaust air, making it suitable only for buildings equipped with mechanical exhaust ventilation. This type of heat pump supplies extracted heat to both a water-based heating system and domestic hot water. Since an extract-air heat pump can only recover energy present in the ventilated air, supplementary energy from an additional heat source, often an electric heater within the system, is required. Another commonly used type is the air-to-water heat pump, which extracts heat from the air and transfers it to a water-based heating system, such as underfloor heating or radiators, as well as to provide domestic hot water. Ground-source (geothermal) heat pumps, on the other hand, utilize solar energy stored in the ground, bedrock, or groundwater. These systems operate through boreholes or horizontal loops embedded in the soil and require a water-based distribution system to deliver heat. Geothermal heat pumps are particularly well-suited for buildings with substantial heating requirements and for regions characterized by cold climates, as the temperature of the ground remains relatively constant throughout the year.

3
Method

This chapter details the methodology applied to evaluate the energy performance and environmental impacts of slab-on-grade foundations in the three building types. The analysis utilized IDA ICE simulation software, which modeled each building's heating demand. Following the simulation setup, the U-value and LCA methodology is presented. This includes an explanation of the insulation optimization process and the zone-based U-value modeling using Sandin's method, which allows for variable insulation thickness across thermal zones. The chapter also describes how both material and operational emissions were quantified, incorporating GWP-values from EPDs and simulated energy use. Furthermore, an LCA for the whole building is presented. Together, the energy modeling and LCA form the foundation for evaluating how different slab-on-grade designs influence GWP over a 50-year lifecycle.

3.1 Reference models

The reference buildings examined in this master thesis include a school/preschool, a warehouse, and a residential building. These buildings serve as case studies for evaluating energy performance. Their design and input parameters are based on reference projects provided by PE Teknik & Arkitektur, including the computer aided design (CAD) model and input data from the project stakeholders. The input data includes characteristics of the building envelope, ventilation system, and climate data. Data that was not provided by PE Teknik & Arkitektur has been estimated based on generalized data and industry standards.

To assess energy performance, each building was individually modeled and simulated in IDA ICE, a building energy simulation software, well validated and widely used in practice (EQUA Simulation AB, n.d.). IDA ICE specializes in analyzing the thermal indoor climate, its interaction with the surrounding environment, and the energy use of the entire building. The software utilizes dynamic thermal zone modeling, where the building is divided into various zones that reflect differences in usage, internal heat gains, and ventilation. These simulations generate detailed energy balance assessments, providing insights into the annual energy consumption and thermal performance of the buildings. Since this master thesis specifically focuses on the slab-on-grade foundation, the simulations were structured to isolate the effects of this component. Variations in the slab-on-grade geometry and material composition were systematically introduced by varying the U-value to evaluate their influence on energy performance. To ensure that these effects could be clearly

assessed, the rest of the building envelope was kept constant across all simulation scenarios. Within IDA ICE, only the materials in the slab-on-grade with a significant effect on thermal performance were included in the model. Non-thermally relevant components, such as the interior floor layer, were excluded to maintain focus on heat transfer dynamics. Additional construction layers, such as a geotextile or radon membrane (if required by site-specific conditions), are not included in simulations or shown in the illustrations of the various slab-on-grade configurations. Note that the drainage layer is automatically included in the U-value calculations within IDA ICE.

It is important to highlight that according to Boverket (2025a) the energy demand of a building corresponds to the total energy required for heating, ventilation, domestic hot water, and property electricity over a typical year. However, for the purpose of this thesis, the focus is specifically on the energy used for the heating of the building. Therefore, the energy demand for domestic hot water and property electricity are not considered or included in the analysis. For each reference building two heating sources was evaluated, a HP and DH, to account for varying energy supply scenarios.

3.1.1 School/preschool

The analyzed school/preschool is a two-story structure located in an urban area of Trollhättan, with a maximum height of 7.4 m. It is designed to accommodate a maximum occupancy of 260 individuals. Figure 3.1 illustrates the south-west and north-east facades of the building.

(a) South-west facade.

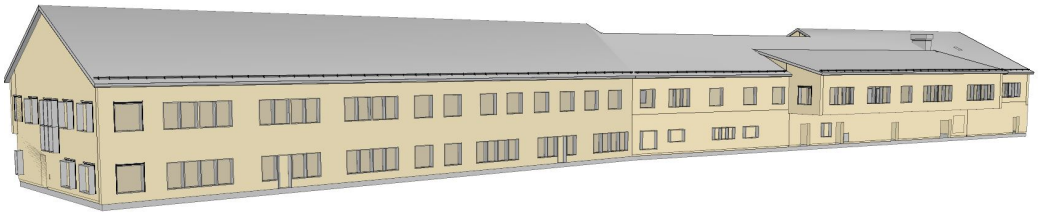

(b) North-east facade.

Figure 3.1: The reference school/preschool from two different perspectives.

The southern section houses preschool facilities, while the northern section is designated for the primary school. Centrally located within the building is a kitchen and dining hall and a technical room is situated on the first floor in the northern section. Geometry and key performance indicators for the school/preschool are presented in Table 3.1. The table includes essential building characteristics, such as area specifications, the average thermal transmittance and the total heating energy demand simulated in IDA ICE. To more accurately simulate the thermal dynamics of the building, the energy model was divided into zones representing functional areas such as the kitchen, dining halls, the technical room, and school and preschool spaces. This zoning enables a realistic representation of internal heat gains, occupancy patterns, and ventilation needs.

Table 3.1: Geometry and key performance indicators for the school/preschool.

Key performance indicators		
Parameter	**Value**	**Unit**
A_{slab}	2121	m^2
A_{gross} [1)]	4321	m^2
A_{temp}	4081	m^2
$A_{envelope}$	6845	m^2
$U_{average}$	0.20	$W/(m^2 \cdot K)$
Operational energy demand (HP)	61146	kWh
Operational energy demand (DH)	228074	kWh

[1)] Note that the corresponding Swedish term is *bruttoarea (BTA)*.

3.1.1.1 Climate envelope

The building features a well-insulated timber structure for both the exterior walls and roof. The reference slab-on-grade foundation for the school/preschool is constructed from concrete and EPS insulation, which are the main materials used in its design. Figure 3.2 illustrates the slab-on-grade construction used in the simulation model, detailing the materials and design layers.

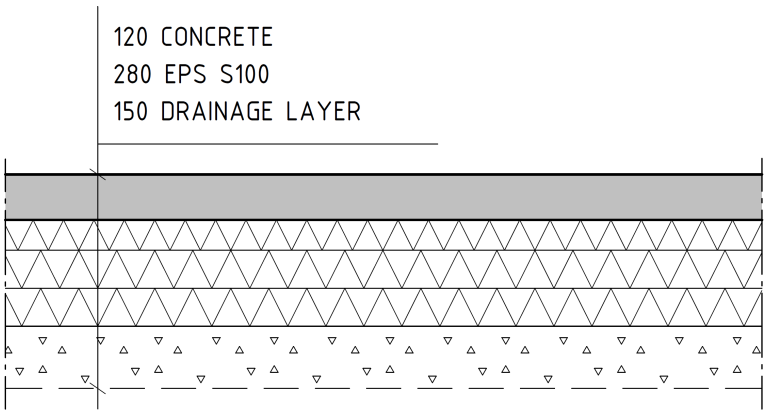

Figure 3.2: Illustration of the slab-on-grade construction for the reference building.

Table 3.2 presents the areas and U-values for each building part, along with the corresponding transmission losses. The impact of thermal bridges is accounted for, contributing an additional 15 % to the total heat loss. Additionally, the table shows the relative contribution of each construction component, such as walls, roof and floor, to the overall transmission losses, showing the thermal performance of each element. Further, the energy model includes solar shading, with external shading devices applied to the south and west facades and internal shading on the north and east facades. The shading system is set to activate when solar irradiance exceeds $100\,\mathrm{W/m^2}$ on the windows.

Table 3.2: Input data for the IDA ICE energy model including thermal bridges for the reference school/preschool.

U-values and transmission losses				
Part	**Area**	**U-value**	**U·A**	**Transmission loss**
	[m^2]	[$W/(m^2 \cdot K)$]	[W/K]	%
Exterior walls	1603	0.13	208	15.4
Roof	2336	0.09	210	15.6
Slab-on-grade	2121	0.10	212	15.7
Windows	532	0.94	500	37.2
Entrance doors	9	1.09	10	0.7
Thermal bridges	-	-	207	15.4
Total	6601	0.20	1347	100

3.1.1.2 Ventilation and heating system

The ventilation system was modeled based on provided specifications, consisting of two mechanical supply and extract ventilation systems with heat recovery (FTX). One unit serves the kitchen and two dining halls, while the other covers the assigned school and preschool areas. The ventilation system operates with variable air volume (VAV) control for airflow distribution. In the energy model, the ventilation operation is assumed to follow the schedules for school/preschool outlined in Boverkets guidelines BFS 2017:6 (2017). The only exception is the technical room, which is modeled with a constant air volume (CAV) control of $0.35\ \mathrm{L/(s \cdot m^2)}$. The building is modeled with balanced ventilation, meaning the extract airflow matches the supply airflow. Furthermore, the building's air tightness was specified as 0.3 $\mathrm{L/(s \cdot m^2}$ ext.surf) at 50 Pa. The minimum indoor temperature is set to 22 °C for all areas, except for the technical room, where it is set to 18 °C according to Boverkets guidelines BFS 2017:6 (2017). A maximum indoor temperature of 27 °C is assumed throughout the building. To enhance energy efficiency, a geothermal heat pump with a COP of 3.7 was integrated into the system, transferring heat from the soil. The parameters governing the ventilation and heating system, as implemented in the energy model, are detailed in Table 3.3. These include the FTX unit efficiency, airflow characteristics, and specific fan power (SFP) for both air handling units. The ventilation system in the energy model was assumed to operate according to the schedule presented in Table 3.4. During all other hours, as well as during weekends

and summer weeks, the ventilation rate was reduced to a minimum airflow.

Table 3.3: Ventilation system data for the reference school/preschool.

Ventilation system data			
Parameter	**AHU 01**	**AHU 02**	**Unit**
Efficiency FTX	83.8	80.7	%
Min. supply airflow	0.592	0.61	$L/(s \cdot m^2\, A_{temp})$
Max. supply airflow	1.316	2.41	$L/(s \cdot m^2\, A_{temp})$
Min. supply air temperature	17	17	°C
SFP	1.51	1.57	$kW/(m^3/s)$

Table 3.4: Ventilation schedule for air handling units one and two.

Ventilation schedules for air handling units			
Parameter	**AHU 01** School	**AHU 01** Preschool	**AHU 02** Kitchen/ Dining hall
Hours with 55% of max. air flow	09-16	07-17	06-18

3.1.1.3 Internal heat gains

The operational energy consumption and internal heat gains from occupants have been modeled according to the guidelines provided by Boverket, BFS 2017:6 (2017). for schools and preschools, incorporating values for lighting, equipment, as well as their respective operating hours. Similarly, the internal heat gains from occupants have been modeled by accounting for the duration of occupancy and the distribution of heat generation across various areas of the building. The power distribution for internal gains from both operational energy use and occupants in the school/preschool is assumed to follow the schedules presented in Table 3.5. The technical room is modeled in accordance with the guidelines provided by Boverket, BFS 2017:6 (2017), which prescribes zero internal heat gains from both operational energy use and occupancy throughout all hours.

Table 3.5: Hourly power distribution of internal gains from operational energy and occupants in the school/preschool.

Power distribution for operational energy and occupants		
Parameter	**School**	**Preschool**
Operational Energy		
Hours with 50 % power	07–08, 17–18	06–08, 16–18
Hours with 100 % power	08–17	08–16
Occupants		
Hours with 50 % presence	08–09:30, 15:30–17	07–11, 13–17
Hours with 100 % presence	09:30–15:30	11–13

3.1.2 Warehouse

The examined warehouse is a single-story, heated storage facility with a pitched roof, designed exclusively for goods storage without the need for continuous worker presence. It features entrance doors, windows, and industrial doors on the north-facing facade and does not accommodate forklifts or vehicles inside. A detailed 3D model of the reference warehouse is presented in Figure 3.3, providing a visual representation of the building's design and layout.

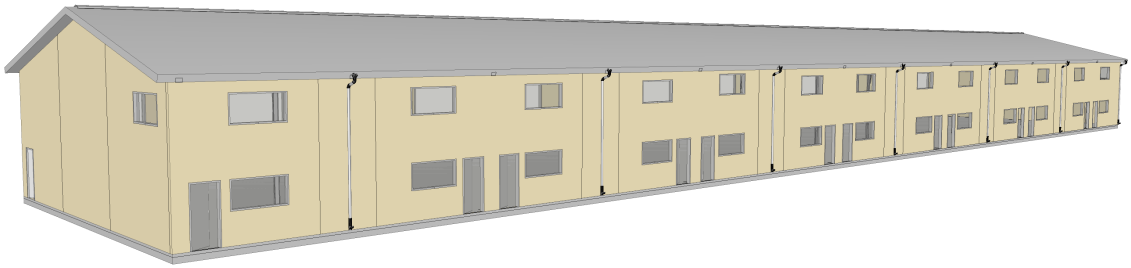

Figure 3.3: Reference warehouse, south- and west facade.

The reference warehouse is situated in a rural, open-country area outside Gothenburg, where the lack of surrounding buildings and vegetation results in high exposure to wind loads, potentially increasing infiltration rates and convective heat losses. The building has a maximum height of approximately 7.6 meters. The geometry and key performance indicators for the reference warehouse are presented in Table 3.6.

Table 3.6: Geometry and key performance indicators for the warehouse derived from the energy model in IDA ICE.

Key performance indicators		
Parameter	**Value**	**Unit**
A_{slab}	1264	m^2
A_{gross} [1)]	1264	m^2
A_{temp}	1236	m^2
$A_{envelope}$	3535	m^2
$U_{average}$	0.37	$W/(m^2 \cdot K)$
Operational energy demand (HP)	27466	kWh
Operational energy demand (DH)	126343	kWh

[1)] Note that the corresponding Swedish term is *bruttoarea (BTA)*.

3.1.2.1 Input data and energy model configuration

The energy model in IDA ICE was divided into five zones, each representing different storage rooms and areas separated by internal walls. This was implemented to provide a more accurate representation of the building's thermal behavior, despite all zones serving similar functions and being assumed to have identical requirements for ventilation and internal heat gains.

3.1.2.2 Climate envelope

The building is constructed with an insulated timber structure for both exterior the walls and roof. The reference slab-on-grade foundation for the warehouse consists of concrete and EPS insulation, following the same design as that used for the school/preschool, see Figure 3.2, with the exception of the EPS compressive strength class, which is replaced with EPS S200. Table 3.7 presents the U-values and corresponding transmission losses used in the simulations for the reference warehouse construction components. Based on these transmission losses, the impact of thermal bridges was quantified as an additional heat loss of 16.7 %. Furthermore, the table illustrates the relative contribution of each construction component to the total transmission losses, providing insight into their respective thermal performance.

Table 3.7: Input data for the reference warehouse energy model in IDA ICE, including thermal transmittance values and thermal bridges.

U-values and transmission losses				
Part	**Area**	**U-value**	**U·A**	**Transmission loss**
	[m^2]	[$W/(m^2 \cdot K)$]	[W/K]	%
Exterior walls	647	0.30	194	15
Roof	1283	0.19	244	18.7
Slab-on-grade	1264	0.09	114	8.7
Windows	56	1.20	67	5.1
Industrial doors	260	1.47	382	29.3
Entrance doors	55	2.0	110	8.4
Thermal bridges	-	-	194	14.8
Total	3565	0.37	1305	100

3.1.2.3 Ventilation and heating system

The heating and cooling setpoints were estimated at 18 °C and 25 °C, respectively. Further, the building's air tightness was specified as 0.5 $L/(s \cdot m^2$ ext.surf) at 50 Pa, reflecting assumed air leakage characteristics of a warehouse. The ventilation system used in the energy model is an exhaust-only system, meaning that air is mechanically extracted while fresh air enters through passive inlets or leaks in the building envelope. This system operates with a CAV strategy, where the ventilation rates remain fixed regardless of occupancy or internal loads. The ventilation flow rate was determined using Equation 3.1, which calculates the required airflow based on a combination of floor area and occupant density, in accordance with Boverket's guidelines, BFS 2017:6 (2017). The calculated ventilation flow was then distributed across the respective thermal zones in the model. For the reference warehouse, where continuous occupancy is not expected, the airflow was set to a constant value of 0.35 $L/(s \cdot m^2)$.

$$Q = 0.35\frac{L}{s \cdot m^2} + 7\frac{L}{s \cdot person} \tag{3.1}$$

Additionally, an extract-air heat pump was incorporated into the system to improve energy efficiency, by transferring heat from the exhaust air. The parameters defining the ventilation system, as implemented in the energy model, are detailed in Table 3.8. This includes the airflow characteristics, SFP, and heat pump COP, which together influence the overall energy performance.

Table 3.8: Ventilation system parameters used in the warehouse energy model.

Ventilation and heating system data		
Parameter	**Value**	**Unit**
Supply airflow	0.025	$L/(s \cdot m^2\, A_{temp})$
Exhaust airflow	0.35	$L/(s \cdot m^2\, A_{temp})$
Exhaust fan SFP	0.1875	$kW/(m^3/s)$
Heat pump COP	4.6	-

3.1.2.4 Internal heat gains

The reference warehouse was modeled without internal heat gains from people and equipment, as it is designed specifically for storage purposes, with no additional equipment or continuous worker presence assumed. The building's primary function does not involve regular occupancy or active use of machinery, which justifies the exclusion of such internal gains. Internal heat gains from lighting were assumed to be 5 kWh/m^2, reflecting the energy consumption typical of warehouse lighting systems.

3.1.3 Residential building

The examined residential building is a multi-family residential house, designed to accommodate multiple households with shared and private spaces. A 3D model is presented in Figure 3.4, offering a representation of the layout of the building. The model highlights features such as balconies, window placements, and entrances, as well as the sloped roof design. The reference building is part of a larger structure, but its design has been simplified to more accurately represent a typical standalone apartment building. Additionally, the building includes dedicated spaces for waste management and storage.

(a) South- and west facade. **(b)** North- and east facade.

Figure 3.4: The reference residential building from two different perspectives.

The residential building is located in an urban area on Orust. The building has a maximum height of approximately 19 meters, accommodating multiple households across its six stories. Geometry and key performance indicators for the reference building are presented in Table 3.9. In the residential building, the COP is 3.5.

Table 3.9: Geometry and key performance indicators for the residential building derived from the energy model in IDA ICE.

Key performance indicators		
Parameter	**Value**	**Unit**
A_{slab}	332	m^2
A_{gross} [1)]	2014	m^2
A_{temp}	1921	m^2
$A_{envelope}$	1757	m^2
$U_{average}$	0.35	$W/(m^2 \cdot K)$
Operational energy demand (HP)	12547	kWh
Operational energy demand (DH)	43916	kWh

[1)] Note that the corresponding Swedish term is *bruttoarea (BTA)*.

3.1.3.1 Input data and energy model configuration

The energy model in IDA ICE was divided into a number of different zones to accurately capture the thermal dynamics of the buildings. These zones includes bathroom, bedroom, kitchen/living room, the elevator and staircase, waste management areas, storage rooms, shared corridors, and bi-areas.

3.1.3.2 Climate envelope

The residential building features a well-insulated steel frame for the exterior walls and a timber structure for the roof. The reference slab-on-grade foundation for the residential building consists of concrete and EPS insulation, following the same design as that used for the school/preschool, see Figure 3.2. Table 3.10 presents the U-values and corresponding transmission losses. Based on these transmission losses, the impact of thermal bridges was quantified as an additional heat loss of 23 %. Furthermore, the table illustrates the relative contribution of each construction component to the total transmission losses, providing insight into their respective thermal performance.

Table 3.10: Input data for IDA ICE including thermal bridges.

U-values and transmission losses				
Part	**Area**	**U-value**	**U·A**	**Transmission loss**
	$[m^2]$	$[W/(m^2 \cdot K)]$	[W/K]	%
Exterior walls	786	0.15	118	19.5
Roof	354	0.09	32	5.3
Slab-on-grade	332	0.10	33	5.5
Windows	234	1.01	236	38.8
Entrance doors	52	1.09	57	9.4
Thermal bridges	-	-	130	21.5
Total	1758	0.35	606	100

3.1.3.3 Ventilation and heating system

The ventilation system used in the energy model is a FTX system. This system operates with a CAV airflow strategy, where the ventilation rates remain fixed regardless of occupancy or internal loads. The ventilation flow rates were calculated using Equation 3.1 and vary across different building zones, depending on both the area and the number of occupants in each zone. To account for demand-controlled ventilation, the energy model includes a kitchen exhaust fan boost, which operates at a flow rate of 40 L/s for 30 minutes per day. This additional exhaust airflow is incorporated into the model, influencing the heating demand. For modeling purposes, the boost is scheduled daily between 17:00 and 17:30 (Levin et al., 2024). The parameters defining the ventilation system are presented in Table 3.11 and includes the efficiency of the FTX system, airflow characteristics, and the SFP, which together influence the overall energy performance.

Table 3.11: Ventilation data for the reference residential building.

Ventilation and heating system data		
Parameter	**Value**	**Unit**
Efficiency FTX	82.2	%
Min. supply airflow	0.35	$L/(s \cdot m^2\, A_{temp})$
Max. supply airflow	0.607	$L/(s \cdot m^2\, A_{temp})$
Min. exhaust airflow	0.35	$L/(s \cdot m^2\, A_{temp})$
Max. exhaust airflow	1.907	$L/(s \cdot m^2\, A_{temp})$
SFP	1.35	$kW/(m^3/s)$

Additionally, according to Levin et al. (2024), the heating and cooling setpoints for a residential building should be 21 °C and 25 °C, respectively. The building is also equipped with a floor heating system in all bathrooms. The infiltration rate of the building was specified as 0.35 $L/(s \cdot m^2$ ext.surf) at 50 Pa, reflecting the assumed air leakage characteristics of a residential building.

3.1.3.4 Internal heat gains

The household electricity consumption is modeled based on a standardized annual specific energy use of 21 $kWh/(m^2\, A_{temp})$, which allows comparison with measured consumption data (Levin et al., 2024). Of the total household electricity use, 70 % is assumed to contribute to indoor heating, while the remaining 30 % is considered lost. Furthermore, see Table 3.12 for the recommended values of occupant heat gains, which are based on standardized data defining reference parameters for energy performance calculations in residential buildings.

Table 3.12: Occupancy parameters for the residential building.

Occupancy patterns		
Parameter	**Value**	**Unit**
Power per person	80	W
Presence time per day	14	h
Number of people, 2-room apartment	1.63	-
Number of people, 3-room apartment	2.18	-

3.2 Optimization process

To assess the thermal performance and the environmental impact of the various slab-on-grade configurations, calculations were conducted. The calculations include U-value estimations, insulation optimization, and LCA. Optimization refers to identifying the insulation thickness that results in the lowest total GWP over the building's lifetime, while still being reasonable to construct in practice, considering standard material dimensions and construction feasibility. MATLAB scripts were developed for each of the studied buildings, tailored to the specific characteristics of the three slab-on-grade systems. U-value calculations for all slab-on-grade systems were performed using Sandin's model for zone-dependent insulation strategies, see Section 2.2.1. For the Koljern system, the method for inhomogeneous layers was used in combination with Sandin's model, see Section 2.2.2. Sandin's model divides the slab into three thermal zones to allow for varying insulation thicknesses across the slab. The insulation thickness in each thermal zone serves as the variable parameter in the optimization process. The thermal zone areas for each building are presented in Table 3.13.

Table 3.13: Thermal zone areas for the slab-on-grade for each building.

Thermal zone areas				
Building	**Zone 1** [m^2]	**Zone 2** [m^2]	**Zone 3** [m^2]	**Total slab area** [m^2]
School/preschool	149	933	1039	2121
Warehouse	186	813	265	1264
Residential	36	153	143	332

The insulation optimization process explored a wide range of zone-specific insulation thickness combinations (non-uniform). Uniform insulation thicknesses (the same in all zones) were also evaluated, as this configuration is representative of typical construction practices in the building industry. The optimization adhered to industry-relevant constraints to ensure practical applicability:

1. U-values must be within the range $0.07{-}0.20\,\mathrm{W/(m^2 \cdot K)}$.
2. For the non-uniform configurations:
   - Insulation thicknesses were varied from 0 to 700 mm in 100 mm increments.
   - For the Koljern system, a finer resolution of 50 mm was used.
3. For the uniform configurations:
   - Insulation thicknesses were varied in 50 mm increments.
   - The maximum allowed thickness did not exceed the highest thickness used in the non-uniform configurations.
4. Insulation in Zone 1 must be equal to or thicker than in Zones 2 and 3.
5. The maximum allowable insulation thickness difference between thermal zones was 300 mm.

Following the application of the defined constraints, several combinations with varying insulation thicknesses across the thermal zones of each slab-on-grade were identified for each U-value. A complete overview of all theses combination for each building and slab-on-grade system is provided in Appendix A, Appendix B, and Appendix C. These appendices detail the number of combinations for each U-value and insulation thickness in each zone. For further analysis, the non-uniform combination with the lowest climate impact corresponding to each specific U-value was selected, together with uniform configurations. Additionally, a constraint was applied such that none of the thermal zones could have 0 mm insulation thickness. All U-value calculations assume steady-state thermal conditions, constant material properties, and exclude moisture effects. Only materials that directly influence thermal performance are included in the calculations. According to Sandin's model, a drainage layer of 150 mm is included in all slab designs, contributing $0.20\,\mathrm{m}^2 \cdot \mathrm{K/W}$ in thermal resistance. Soil conditions below the slabs are modeled using the typical value for moraine, silt, or undrained sand and gravel, see Table 2.1.

The total climate impact over a 50-year lifetime includes both embodied emissions from construction materials and operational emissions from energy used for space heating, expressed per square meter of gross floor area. In accordance with the guidelines provided by Boverket (2023a), certain components were excluded from the embodied carbon assessment, although the drainage layer is included in the U-value calculations as per Sandin's method, it is not considered in the climate declaration. Similarly, the geotextile layer was excluded from the LCA. The operational heating demand, part of module B6 in LCA, was simulated using IDA ICE. The resulting energy use for space heating was then translated into CO_2e and included in the overall climate impact. The GWP factors applied for the various heating source are presented in Table 3.14. The embodied emissions of the construction materials were assessed individually for each slab-on-grade system and are presented in Sections 3.2.1, 3.2.2, and 3.2.3. The CO_2e used in the assessment represent average GWP data from life cycle stages A1–A3, compiled from multiple manufacturers. For materials with significant variation, an average GWP value was calculated, to get a more accurate representation. All GWP values for the selected materials are presented in Appendix D. Based on the calculated total GWP, the most optimized insulation configuration for each slab-on-grade system could then be identified.

Table 3.14: GWP-values for heating sources used in the assessment.

GWP-values for the heating sources	
Heating source	**GWP (A1-A3)** $\mathrm{kg\,CO_2e/kWh}$
Heat pump[1)]	0.037
District heating[2)]	0.056

[1)] Electricity, Swedish mix from Boverket.
[2)] District heating, Swedish average from Boverket.

3.2.1 Concrete system

This configuration represents a conventional concrete slab-on-grade construction, for which both standard and low-carbon concrete variants have been evaluated. All buildings feature the same concrete slab design, consisting of a 120 mm concrete layer and a 280 mm EPS insulation layer, see Figure 3.5. The only exception is the warehouse, where the standard EPS is replaced with EPS S200 to meet higher compressive strength requirements. The associated material properties used in the calculations are listed in Table 3.15. The thickness of the EPS insulation is the variable parameter adjusted in the MATLAB script to evaluate its influence on thermal performance and environmental impact.

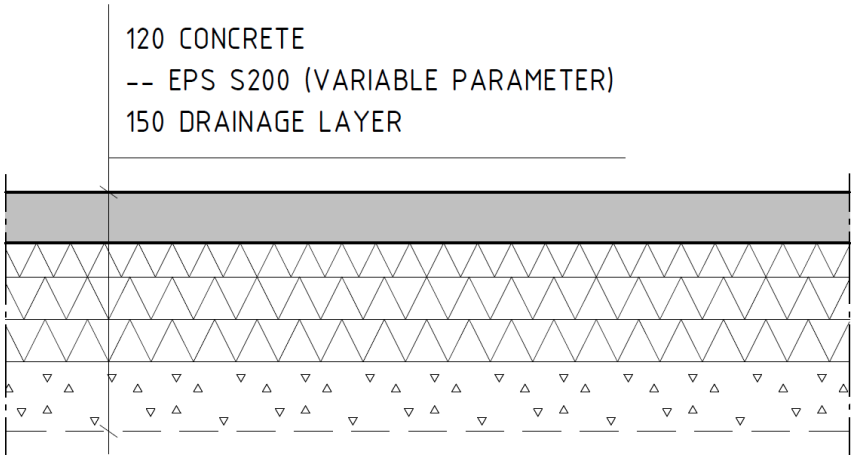

Figure 3.5: Illustration of the concrete system for the warehouse.

The climate impact includes emissions from the concrete slab and the varying EPS insulation. For the concrete slab, emissions associated with steel reinforcement were also included. The amount of reinforcement required for each building type was estimated using simplified structural calculations in consultation with a structural engineer. For the school/preschool and for the residential building, the reinforcement content was assumed to be 60 kg/(m^3concrete), while for the warehouse, a higher value of 90 kg/(m^3concrete) was used to reflect increased structural demands. These values were used as input for calculating the GWP from reinforcement steel.

Table 3.15: Thermal conductivity and CO_2-equivalent values for materials used in the concrete system.

Material properties for the concrete system		
Material	**Thermal conductivity** $[W/(m \cdot K)]$	**GWP** $[kg\,CO_2e/m^3]$
Concrete	1.7	225
Low-carbon concrete (20%)	1.7	175
Reinforcement[1)]	–	557 ($kg\,CO_2e$/ton)
EPS S100	0.037	63.1
EPS S200[2)]	0.034	103.4

[1)] Note that the unit for the reinforcement is given in $kg\,CO_2e$/ton.

[2)] Only used in the warehouse slab-on-grade, where higher compressive strength requirements led to the replacement of EPS S100 with EPS S200.

For EPS S100, GWP values are based on EPDs from Finja Betong (2022) and Finnfoam (2021), while for EPS S200, values are taken from EPDs by the same manufacturers (Finja Betong, 2021; Finnfoam, 2021). The data for conventional concrete and low-carbon concrete, with an estimated 20% reduction in GWP and a compressive strength class of C25/30, is based on information provided by Skanska (A. Akram, Personal communication, 5 Maj 2025). The GWP for the reinforcement integrated in the concrete slab is derived from the EPD published by Stena Stål (2024). More detailed information on the GWP values and associated data is provided in Appendix D.

3.2.2 CLT system

Based on the slab-on-grade system from Klara Byggsystem, this master thesis presents a system consisting of a CLT slab with an underlying EPS insulation layer, which is the variable parameter in the IDA ICE simulations. Figure 3.6 illustrates the CLT slab-on-grade system used for the warehouse. The CLT element is assumed to have fixed geometry and material properties for each building type: 100 mm for all the buildings. For the warehouse reference, a concrete screed is added to the slab to accommodate the increased compressive strength demands of the building. In this context, EPS S200 is used as the insulation material due to its higher compressive strength, matching the requirements of the warehouse. This screed is not included in the residential building or the school/preschool, where the structural loads are lower and such reinforcement is unnecessary. For these buildings, EPS S100 is used as the insulation material. It should also be noted that the figure highlights only the components that affect thermal transmittance or are considered in the climate impact assessment. Note that additional construction layers, such as a geotextile and a radon membrane (if required by site conditions), are not shown in the illustration.

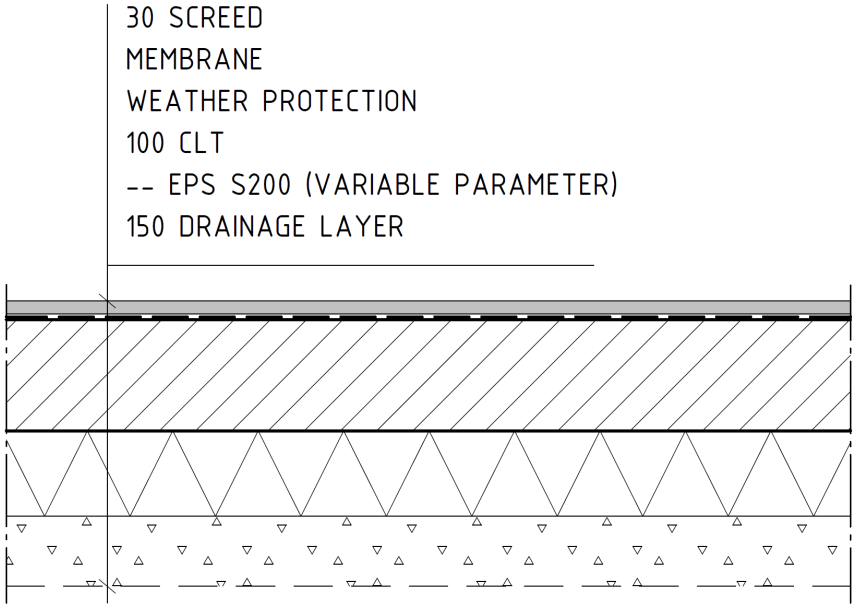

Figure 3.6: Illustration of the CLT system for the warehouse.

The climate impact assessment includes emissions from the CLT, varying EPS insulation, the concrete screed (where applicable), and the weather protection. Due to the lack of available EPD data, the membrane with a thin aluminum layer was excluded from the assessment. The associated material properties used in the calculations are listed in Table 3.16.

Table 3.16: Thermal conductivity and CO_2-equivalent values for materials used in the CLT system.

Material properties for the CLT system		
Material	**Thermal conductivity** $[W/(m \cdot K)]$	**GWP** $[kg\,CO_2e/m^3]$
Screed[1)]	1.7	225
Membrane[2)]	–	– $(kg\,CO_2e/m^2)$
Weather protection[2)]	–	1.1 $(kg\,CO_2e/m^2)$
CLT	0.12	0
EPS S100	0.037	63.1
EPS S200[1)]	0.034	103.4

[1)] Only used in the warehouse slab-on-grade, where higher compressive strength requirements led to the use of a concrete screed and the replacement of EPS S100 with EPS S200.
[2)] Note that the units for the membrane and the weather protection are given in $kg\,CO_2e/m^2$.

For EPS S100 and EPS S200, the average values are based on EPDs from Finja and Finnfoam, as previously stated in Section 3.2.1. The concrete screed is based on the same C25/30 data used for the concrete system. The weather protection is based on the EPD from SIGA Cover AG (2022). The CLT in this thesis is assigned a climate impact value of zero, even though it may have negative GWP values in certain EPDs. Embodied emissions from the CLT slab are assumed negligible. While

CLT can function as a temporary carbon sink, biogenic carbon is not credited in this assessment. According to RISE Research Institutes of Sweden (2023), carbon storage in wood products may only be considered if the storage duration exceeds the forest regeneration cycle, typically 80-120 years for pine and 65-110 years for spruce, which is longer than the 50-year analysis period applied here. More detailed information on the GWP values and associated data is provided in Appendix D.

3.2.3 Koljern system

This configuration is based on the Koljern prefabricated foundation system developed by Evia. The Koljern element has a fixed geometry and material composition, with standard panel sizes of 12 m × 4 m. For additional thermal insulation and moisture protection, a layer of Foamglas is typically placed beneath the element and this is the variable parameter in the U-value calculations, which is then varied in the IDA ICE simulations. Figure 3.7 illustrates the Koljern slab-on-grade configuration used for the warehouse in this master thesis. For the warehouse, an additional concrete screed is included to meet the higher compressive strength requirements. In contrast, such a screed is not required for the residential building or the school/preschool, where the compressive forces are significantly lower. Note that the figure only shows materials that influence thermal transmittance. In practice, a layer of geotextile is also required during construction and a radon membrane may be necessary depending on the location of the building.

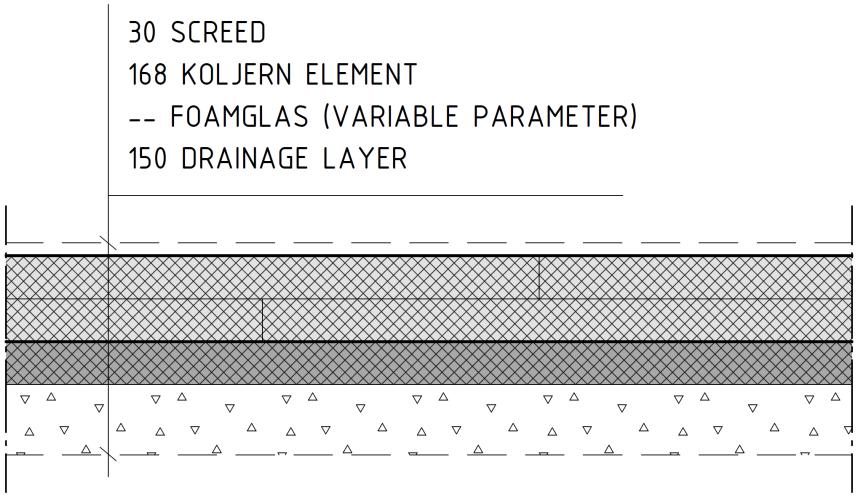

Figure 3.7: Illustration of the Koljern system for the warehouse.

An illustration of the structural layout of the Koljern element is shown in Figure 2.3 in Section 2.1.2.3. Each element consists of a Foamglas T3+ core for thermal insulation and light-gauge steel beams that provide structural support. Due to the inhomogeneous nature of the Koljern system, the method described in Section 2.2.2 was used to calculate its thermal resistance, which results in an approximate value of 5.6 $m^2 \cdot K/W$. The geometry and material composition of the Koljern element remain constant across the three building types, while the thickness of the Foamglas insulation layer beneath the element is varied in this configuration. The associated

material properties used in the calculations are listed in Table 3.17. The climate impact assessment includes emissions from the concrete screed, Koljern element, and the Foamglas insulation.

Table 3.17: Thermal conductivity and GWP values (A1–A3) for materials used in the Koljern system.

Material properties for the Koljern system		
Material	**Thermal conductivity** $[\mathrm{W/(m \cdot K)}]$	**GWP (A1–A3)** $[\mathrm{kg\,CO_2e/m^3}]$
Screed[1)]	1.7	225
Koljern element[2)]	–	33.5 $(\mathrm{kg\,CO_2e/m^2})$
Foamglas T3+	0.045	137.8

[1)] Only used in the warehouse slab-on-grade, where higher compressive strength requirements led to the use of a concrete screed.
[2)] Includes steel beams and Foamglas; thermal resistance calculated separately due to inhomogeneous structure, see Section 2.2.2. Also note that the unit for the Koljern element are given in $\mathrm{kg\,CO_2e/m^2}$.

The GWP value for the concrete screed is derived from the same data source used for the screed in the CLT system. For the Koljern element, the GWP value is based on data from EVIA (2024), but has been adapted to match the specific dimensions used in this study and to allow for variations in the insulation thickness beneath the Koljern element. This adaptation incorporates GWP values for the Foamglas insulation (Pittsburgh Corning Europe, 2021) and for the galvanized steel beams from Lindab Profil (2020). More detailed information on the GWP values and associated data is provided in Appendix D.

3.2.4 Foundation supports

To enable a consistent comparison between the different foundation alternatives, all supporting foundation elements responsible for distributing vertical loads into the ground, such as edge beams and footings, were assumed to be constructed from standard concrete across all slab-on-grade systems. This assumption also applies to the slab-on-grade using the low-carbon concrete variant. For the reference buildings with conventional concrete slabs, the dimensions of these elements were derived from architectural and structural drawings, allowing for an estimate of the total concrete volume required. For the CLT slab-on-grade system, the same volume of concrete for supporting foundation elements was assumed as in the reference concrete slab design. In contrast, the Koljern slab-on-grade system was assumed to require a reduced volume of concrete in these elements, based on the higher compressive strength of the system. Specifically, the volume was reduced by a factor of 2.5, based on calculations provided by the structural engineer at PE Teknik & Arkitektur. All assumptions related to the design and quantity of supporting foundation elements were made in consultation with a structural engineer to ensure consistency with standard structural design practice.

3.2.5 LCA of total building

Tables 3.18 and 3.19 present the GWP (modules A1–A3) associated with the building components of the school/preschool and warehouse, respectively. The data is based on input provided by PE Teknik & Arkitektur and corresponds to the reference slab-on-grade configuration for each building. It should be noted that the input data varies slightly between the two buildings. These differences reflect the varying equipment levels and functional requirements of each building type. Corresponding data for the residential building is currently unavailable and is therefore excluded from the analysis presented in this section.

Table 3.18: GWP values (A1–A3) for building components in the school/preschool.

LCA school/preschool	
Component	**GWP (A1–A3)** $[\mathrm{kg\,CO_2e/(m^2\,A_{gross})}]$
Slab-on-grade	45.4
Structural frame	56.8
Climate envelope	37.8
Internal walls	34.2
HVAC	10.1
Tap water and sewage	3.5
Electrical and telecommunications systems	12.7
Total building	200.5

Table 3.19: GWP values (A1–A3) for building components in the warehouse.

LCA warehouse	
Component	**GWP (A1–A3)** $[\mathrm{kg\,CO_2e/(m^2\,A_{gross})}]$
Slab-on-grade	37.4
Structural frame	76.2
Climate envelope	59.7
Internal walls	4.0
Total building	177.3

4

Results and observations

This chapter presents the thermal and climate impact results for the three slab-on-grade systems across the three building types. Each building is analyzed for concrete, CLT, and Koljern systems under heat pump and district heating scenarios. Results include U-values, insulation configurations, and total GWP, split into material and operational emissions. Visualizations include line and bar charts alongside summary tables. The chapter concludes with a cross-building comparison and evaluates the foundation's contribution to total building GWP, highlighting how insulation choices impact the environmental impact.

4.1 Context and overview

The following sections present the total climate impact for various slab-on-grade foundation configurations across the three reference buildings. Each result includes emissions from both material use and operational energy over a 50-year building lifespan. The insulation configurations analyzed are labeled according to zone-wise thickness distribution in millimeters, using the format "Zone 1–Zone 2–Zone 3." For example, "300-200-100" indicates 300 mm insulation in Zone 1, 200 mm in Zone 2, and 100 mm in Zone 3. Furthermore, all U-values are presented with two significant figures according to industry standard. Note that some tables may show multiple configurations with identical total GWP values. In such cases, additional decimal precision was used to identify the most optimized alternative, and only the configuration with the lowest total climate impact was selected for presentation. The x-axes in the figures are sorted by increasing total insulation thickness across the three thermal zones, rather than by U-value. This allows clearer insight into how additional material use influences embodied emissions. Furthermore, it should be noted that the line plots presented for each reference building have different maximum values on the y-axis, which must be taken into account when comparing GWP between figures.

4.2 School/preschool

The resulting range of uniform and non-uniform insulation configurations, developed according to the defined design constraints for the school/preschool, is presented in Table 4.1, Table 4.2, and Table 4.3. These three tables each correspond to one slab-on-grade foundation system and provide an overview of the analyzed insulation thicknesses across the three thermal zones, along with the corresponding calculated U-values. The configurations presented are those that met the defined constraints in the optimization process, including all uniform cases and the best-performing non-uniform configurations. In addition, the tables show the calculated GWP for all configurations, separately for HP and DH. The most optimized insulation configuration, defined as the one with the lowest GWP, for each heating system and foundation system is highlighted in red. For some U-values, multiple insulation configurations are possible, including both uniform and non-uniform alternatives.

Table 4.1: U-value, zone-wise insulation configuration and total GWP-values for the concrete system in the school/preschool, organized by increasing U-value and divided by HP and DH.

Concrete system			
U-value [W/(m^2 · K)]	**Insulation configuration** [mm]	**GWP** [$kg\,CO_2\,e/(m^2\,A_{gross})$]	
		HP	**DH**
0.07	500-400-400	55.6	171.9
	400-400-400	55.3	171.6
0.08	350-350-350	54.1	171.5
	400-400-300	54.1	171.5
0.09	400-300-300	53.0	171.6
	300-300-300	52.7	171.3
0.10	400-300-200	52.1	173.7
	250-250-250	51.9	173.5
0.11	300-300-200	52.2	175.2
0.12	300-200-200	51.2	175.9
	200-200-200	50.9	175.6
0.13	300-300-100	51.3	177.3
0.14	400-200-100	50.5	178.0
0.15	150-150-150	49.8	176.2
	200-200-100	49.8	176.2
0.17	300-100-100	49.4	178.8
0.18	200-100-100	49.8	180.1
	100-100-100	49.2	179.9

Table 4.1 presents that the most optimized insulation configurations for the concrete system using a HP and DH is 100-100-100 and 300-300-300, respectively, resulting in GWP values of 49.2 and 171.3 kg CO_2e/(m^2 A_{gross}). The table also demonstrates that identical U-values can be achieved with both uniform and non-uniform insulation configurations, though these alternatives result in varying GWP outcomes. For

example, the uniform configuration 250-250-250 and the non-uniform 400-300-200 both reach a U-value of 0.10 $W/(m^2 \cdot K)$, despite their differences in insulation distribution. In some cases, uniform configurations are more favorable, while in others, non-uniform ones result in lower emissions.

Table 4.2: U-value, zone-wise insulation configuration and total GWP-values for the CLT system in the school/preschool, organized by increasing U-value and divided by HP and DH.

CLT system			
U-value $[W/(m^2 \cdot K)]$	**Insulation configuration** [mm]	**GWP** $[kg\,CO_2\,e/(m^2\,A_{gross})]$	
		HP	**DH**
0.07	500-500-300	40.7	157.0
	400-400-400	40.7	157.0
0.08	400-300-300	38.1	155.5
	350-350-350	39.4	156.8
0.09	400-400-200	38.1	156.7
	300-300-300	38.1	156.7
0.10	300-300-200	37.3	158.9
	250-250-250	37.2	158.8
0.11	300-200-200	36.2	159.2
	200-200-200	36.0	159.0
0.12	300-300-100	36.3	161.0
0.13	200-200-100	35.1	161.1
	150-150-150	35.0	161.0
0.15	200-100-100	33.8	160.2
0.16	100-100-100	34.0	162.4

For the CLT slab-on-grade system, Table 4.2 identifies 200-100-100 as the most optimized insulation configuration for HP and 400-300-300 for DH, resulting in GWP values of 33.8 and 155.5 $kg\,CO_2e/(m^2\,A_{gross})$, respectively. As with the concrete system, identical U-values can be reached through both uniform and non-uniform configurations, yet the resulting GWP varies depending on the distribution.

Table 4.3: U-value, zone-wise insulation configuration and total GWP-values for the Koljern system in the school/preschool, organized by increasing U-value and divided by HP and DH.

Koljern system			
U-value [W/(m^2 · K)]	**Insulation configuration** [mm]	**GWP** [$kg\,CO_2\,e/(m^2\,A_{gross})$]	
		HP	**DH**
0.07	300-200-150	54.6	170.9
	200-200-200	55.8	172.1
0.08	150-150-100	51.1	168.5
	150-150-150	52.7	170.1
0.09	200-100-50	48.4	167
	100-100-100	49.5	168.1
0.10	100-50-50	47.1	168.7
	50-50-50	46.9	168.5

The insulation configurations and corresponding U-values for the Koljern slab-on-grade system are presented in Table 4.6. The most optimized configurations are identified as 50-50-50 for the HP and 200-100-50 for DH. Compared to the concrete system, both the CLT and particularly the Koljern system offer fewer viable insulation configurations, indicating that a lower insulation thickness is sufficient to achieve the minimum U-value of 0.07 W/(m^2 · K) in these systems.

The insulation configurations illustrated in Figure 4.1 represent a selected subset of those presented in Table 4.1, Table 4.2, and Table 4.3. This subset includes all uniform insulation configurations, along with the most optimized setups, highlighted in red in the respective tables. Figure 4.1 displays the total GWP associated with the three slab-on-grade systems under varying insulation configurations and heating sources. Solid lines indicate results for HP, while dashed lines correspond to DH. The most optimized insulation configuration for each system and heating source is highlighted in red. In addition, the figure includes a low-carbon concrete variant (20% reduction), which was analyzed using the same insulation configurations as the standard concrete system. The results show that the low-carbon concrete system follows a similar trend but exhibits a lower total GWP for each configuration, due to the reduced material emissions associated with the use of low-carbon concrete.

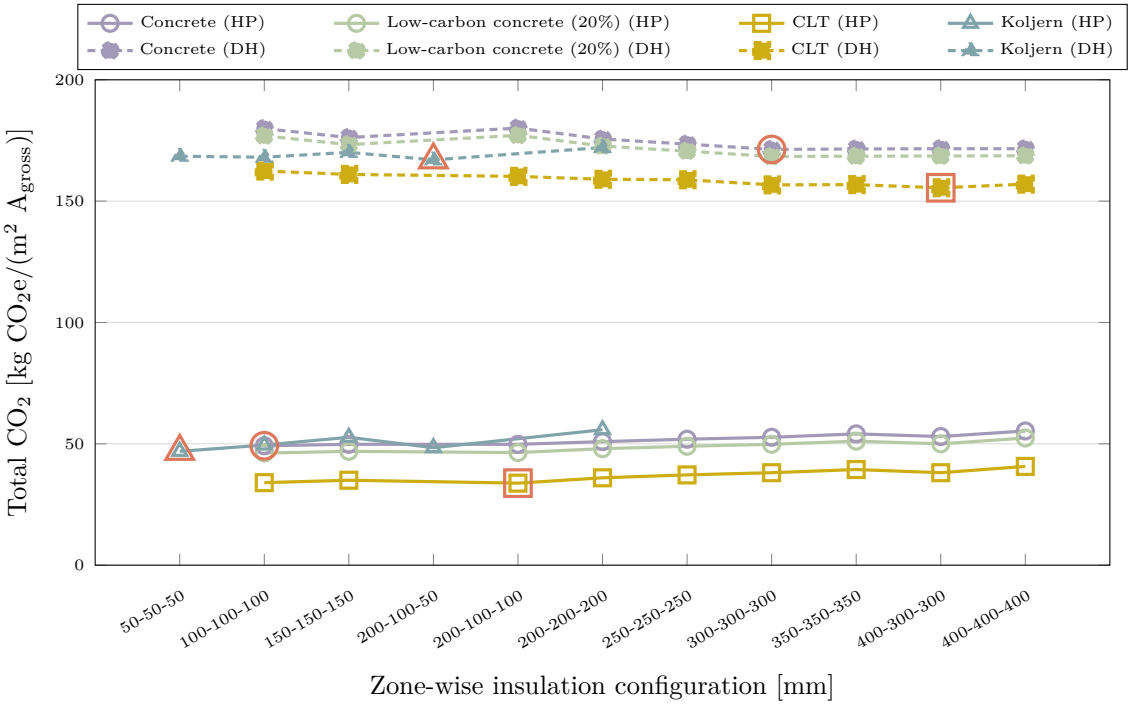

Figure 4.1: Line plot of total GWP as a function of zone-wise insulation configuration for the school/preschool, comparing HP and DH. The x-axis is ordered by increasing total insulation thickness across zones. The most optimized insulation configuration for each heating source and slab-on-grade system is marked in red.

Figure 4.1 presents the total GWP for the three slab-on-grade systems across various insulation configurations and heating sources. As shown, the GWP is consistently higher for all systems when DH is used, compared to HP systems. For DH, GWP values range from approximately 155 to 180 kg CO_2e/(m^2 A_{gross}), while for HP, values range from around 30 to 55 kg CO_2e/(m^2 A_{gross}). The GWP trend differs between the two heating sources: DH slopes slightly downward with increasing insulation thickness, while the curve for HP slopes slightly upward. This indicates that for DH, thicker insulation can reduce operational energy emissions sufficiently to compensate the material emissions, whereas for HP systems, the already relatively low operational emissions make added insulation less beneficial, resulting instead in higher total GWP due to increased material use. For HP, the most optimized configurations for the Koljern and concrete systems are those with minimal insulation thickness, while the CLT system requires a thicker insulation to reach its minimum GWP. For DH, the optimal insulation thickness varies more between systems. The Koljern system achieves its lowest GWP with the 200-100-50 configuration, while both the concrete and CLT system require higher insulation levels to minimize GWP. However, in none of the systems does the configuration with the thickest insulation yield the lowest GWP. The figure also illustrates that the CLT system consistently exhibits the lowest GWP across all insulation configurations for both heating systems. In contrast, the Koljern system yields lower GWP values than the concrete systems with DH, but for the HP scenario, it performs better than concrete only for certain configurations. Furthermore, the figure confirms that, for both heating

sources, the most optimized configurations for the concrete and CLT systems consistently involve thicker insulation than those for the Koljern system. This aligns with the U-values reported in Table 4.1, Table 4.2, and Table 4.3, where the Koljern system demonstrates better thermal performance, achieving lower U-values with less insulation.

Figure 4.2 and Figure 4.3 present the total GWP associated with the most optimized insulation configurations for each slab-on-grade system, evaluated separately for HP and DH. These results are compared against the reference case representing the conventional concrete slab-on-grade solution currently used in the school/preschool. Each bar in the figures are divided into two components: embodied emissions from material use and emissions associated with operational energy use. This enables a comparison of how both material selection and heating strategy affect the overall climate impact of each slab-on-grade system.

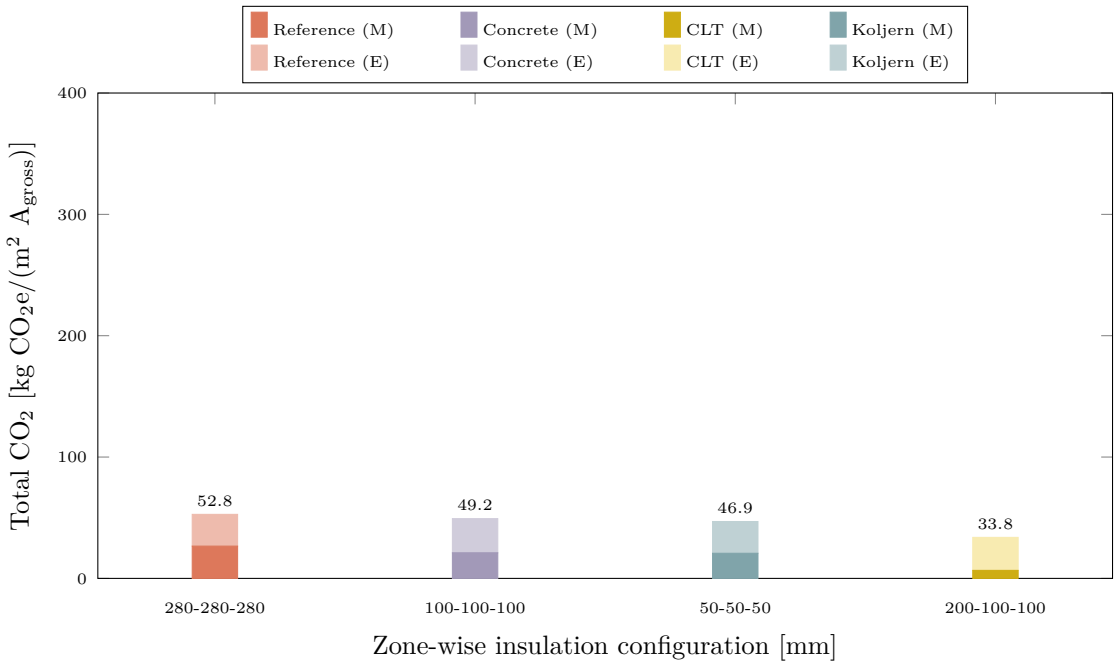

Figure 4.2: GWP for each optimized slab-on-grade system in the school/preschool with a HP. (M) denotes material emissions; (E) denotes operational energy.

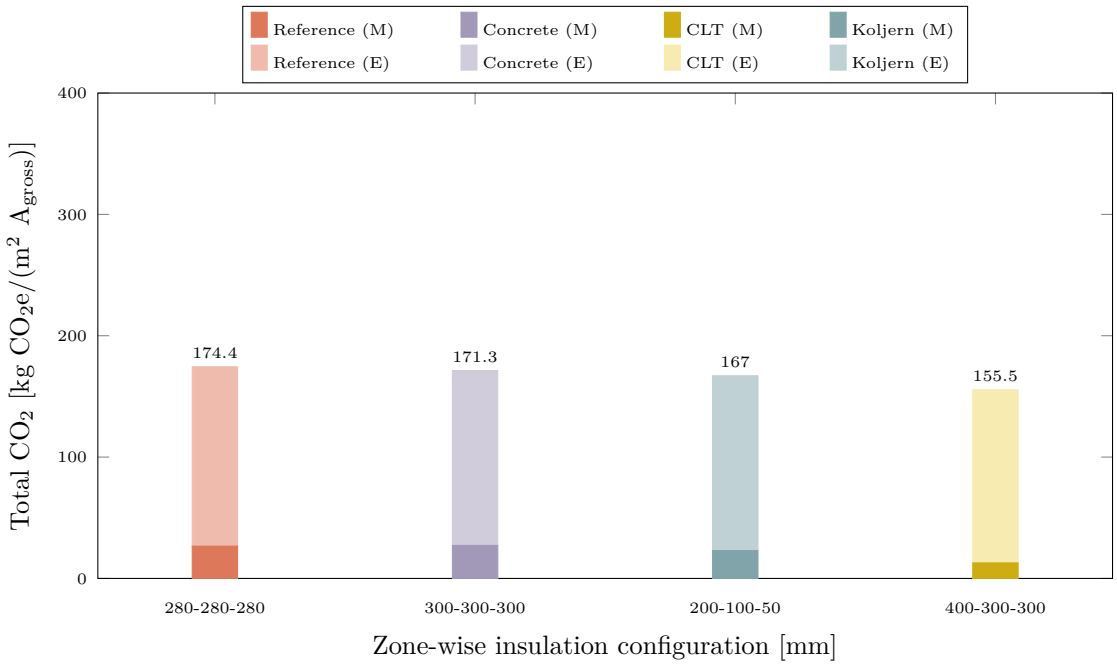

Figure 4.3: GWP for each optimized slab-on-grade system in the school/preschool with DH. (M) denotes material emissions; (E) denotes operational energy.

The most optimized slab-on-grade configurations presented in Figure 4.2 and Figure 4.3 show that the CLT system yields the lowest total GWP across all systems and heating source combinations. All optimized slab-on-grade systems also perform better in terms of GWP than the reference concrete system with 280-280-280 mm insulation, regardless of the heating source. When using a HP, the balance between operational and material-related emissions is relatively even for the reference and standard concrete systems, as well as the Koljern system, while the CLT system shows a higher proportion of emissions from operational energy use. Under DH conditions, however, operational energy dominates the total GWP for all systems, including the reference, highlighting the notably higher climate impact of district heating compared to heat pump use. The figures also show a trend in insulation distribution. For HP, most optimal configurations are uniform, with the exception of the CLT system. In contrast, when using DH, non-uniform insulation configurations are more commonly among the most optimized solutions, as seen for both the CLT and Koljern systems. This suggests that non-uniform insulation may offer greater potential for reducing GWP under DH conditions in the school/preschool. The low-carbon concrete variant is excluded from these figures, as its most optimized configuration matches that of the standard concrete system. However, as shown in Figure 4.1, it results in a consistently lower total GWP, approximately 6.1% lower for HP and 1.7% lower for DH, primarily due to its reduced embodied emissions.

4.3 Warehouse

The different insulation configurations for all the systems analyzed for the warehouse are summarized in Table 4.4, Table 4.5, and Table 4.6, each corresponding to one of the slab-on-grade systems. The tables include insulation thicknesses across the three thermal zones, the resulting U-values, and the calculated GWP for each configuration, shown separately for HP and DH. The configuration with the lowest GWP per heating and foundation system is marked in red.

Table 4.4: U-value, zone-wise insulation configuration and total GWP-values for the concrete system in the warehouse, organized by increasing U-value and divided by HP and DH.

Concrete system			
U-value $[W/(m^2 \cdot K)]$	**Insulation configuration** [mm]	**GWP** $[kg\,CO_2\,e/(m^2\,A_{gross})]$	
		HP	**DH**
0.07	400-400-400	117.2	354.5
	400-400-300	115.1	352.4
0.08	350-350-350	112.3	350.4
	400-300-300	108.6	346.7
0.09	300-300-300	107.3	347.0
	300-300-200	105.1	344.8
0.10	300-300-100	103.3	344.6
	250-250-250	102.4	343.7
0.11	300-200-200	99.0	341.5
0.12	200-200-200	97.7	341.9
	300-200-100	97.0	341.2
0.13	200-200-100	95.8	341.2
0.14	150-150-150	93.0	339.9
0.16	300-100-100	91.5	342.1
0.17	200-100-100	90.1	341.8
0.18	100-100-100	88.8	341.7

Table 4.4 shows that the most optimized insulation configuration for the concrete system is 100-100-100 for the HP and 150-150-150 for DH. These configurations correspond to GWP values of 88.8 kg CO_2e/(m^2 A_{gross}) and 339.9 kg CO_2e/(m^2 A_{gross}), respectively. The table also shows that both uniform and non-uniform configurations can achieve the same U-value, though with different GWP outcomes.

Table 4.5: U-value, zone-wise insulation configuration and total GWP-values for the CLT system in the warehouse, organized by increasing U-value and divided by HP and DH.

CLT system			
U-value [W/(m^2 · K)]	**Insulation configuration** [mm]	**GWP** [$kg\,CO_2\,e/(m^2\,A_{gross})$]	
		HP	**DH**
0.07	400-400-200	87.7	325.0
0.08	300-300-300	81.9	320.0
	400-300-200	81.3	319.4
0.09	400-300-100	79.3	319.0
	250-250-250	77.0	316.7
0.10	300-200-200	73.6	314.9
0.11	200-200-200	72.3	314.8
	300-200-100	71.6	314.1
0.12	200-200-100	70.3	314.5
0.13	150-150-150	67.6	313.0
0.14	300-100-100	65.7	312.6
0.15	200-100-100	64.5	313.1
0.16	100-100-100	63.3	313.9

For the CLT slab-on-grade system, Table 4.5 indicates that the most optimized insulation configurations are 100-100-100 for the HP and 300-100-100 for DH. Similar to the results observed for the concrete system, both uniform and non-uniform insulation configurations achieve equivalent U-values, though they differ in their associated GWP values.

Table 4.6: U-value, zone-wise insulation configuration and total GWP-values for the Koljern system in the warehouse, organized by increasing U-value and divided by HP and DH.

Koljern system			
U-value [W/(m^2 · K)]	**Insulation configuration** [mm]	**GWP** [$kg\,CO_2\,e/(m^2\,A_{gross})$]	
		HP	**DH**
0.07	200-200-200	108.8	346.1
	200-200-150	107.3	344.6
0.08	150-150-150	102.1	340.2
	200-150-50	100.2	338.3
0.09	100-100-100	95.4	335.1
	100-100-50	94.0	333.7
0.10	100-50-50	89.8	331.1
0.11	50-50-50	89.0	331.5

The insulation configurations and corresponding U-values for the Koljern slab-on-grade system are presented in Table 4.6. The most optimized configurations are identified as 50-50-50 for the HP and 100-50-50 for DH.

The configurations shown in Figure 4.4 comprise all uniform insulation configurations and the most optimized combinations for each slab-on-grade system, highlighted in red in the respective tables presented above. HP and DH results are represented by solid and dashed lines, respectively. A low-carbon concrete alternative with a 20% reduction is included, evaluated using the same insulation configurations, and demonstrates lower GWP outcomes due to reduced embodied emissions.

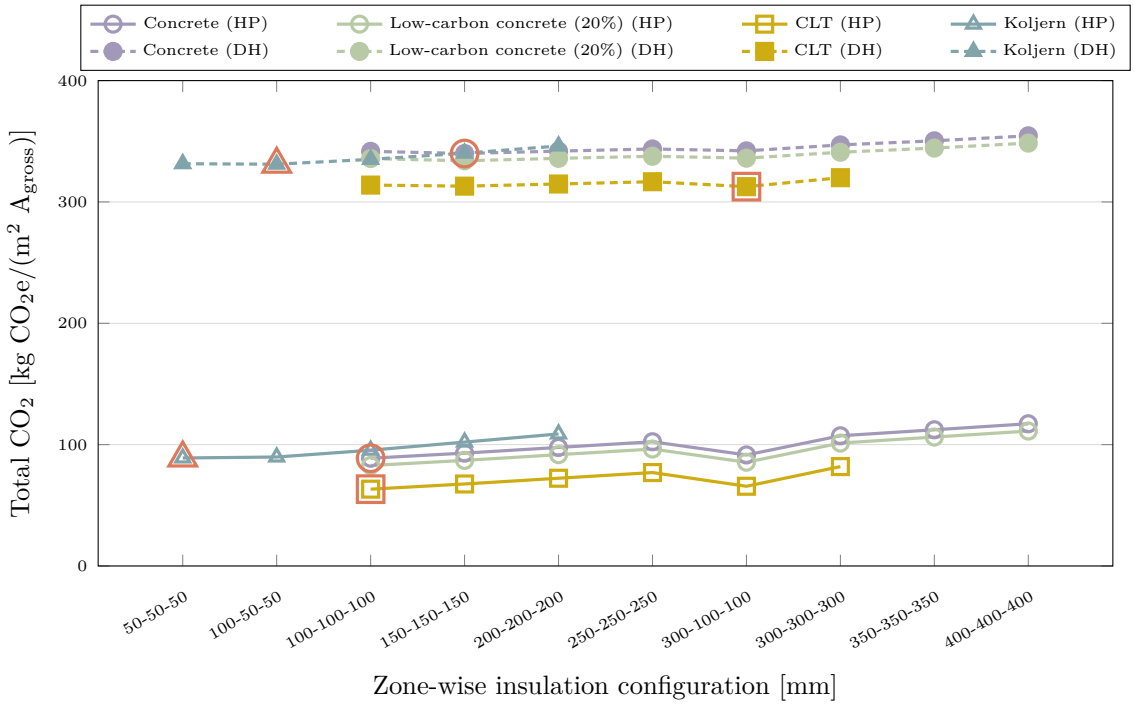

Figure 4.4: Line plot of total GWP as a function of zone-wise insulation configuration for the warehouse, comparing HP and DH. The x-axis is ordered by increasing total insulation thickness across zones. The most optimized insulation configuration for each heating source and slab-on-grade system is marked in red.

As illustrated in Figure 4.4, total GWP values are markedly higher when DH is used compared to HP systems across all slab-on-grade constructions. Under DH, GWP ranges from roughly 310 to 355 kg CO_2e/(m^2 A_{gross}), while the HP systems remain lower, between 60 and 120 kg CO_2e/(m^2 A_{gross}). A clear upward trend is observed for both heating sources as insulation thickness increases, highlighting the trade-off between improved thermal resistance and increased material emissions. The figure also reveals differences in optimal insulation configurations depending on the heating source. For HP, minimal insulation levels tend to yield the lowest GWP across all systems, highlighting that the benefit of added insulation diminishes when operational emissions are already low. In contrast, the most favorable configurations for DH involve thicker insulation layers, especially for the concrete and CLT systems, although the Koljern system reaches its minimum GWP with a relatively low

insulation level (100-50-50). Across all configurations and heating sources, the CLT system consistently demonstrates the lowest GWP, while the Koljern system performs better than concrete only under specific DH configurations. Notably, none of the systems benefit from the highest insulation thickness, which consistently leads to increased GWP. For HP scenarios, a sharp increase in GWP is seen in the CLT and concrete systems at the 300-100-100 configuration, corresponding to a significant change in U-value performance, as detailed in Table 4.4 and Table 4.5.

Figure 4.5 and Figure 4.6 show the total GWP for the most optimized insulation configurations of each slab-on-grade system, for HP and DH respectively. The results are compared to the reference case that represents the conventional concrete slab-on-grade solution currently used in the warehouse. Each bar is divided into material and operational energy emissions.

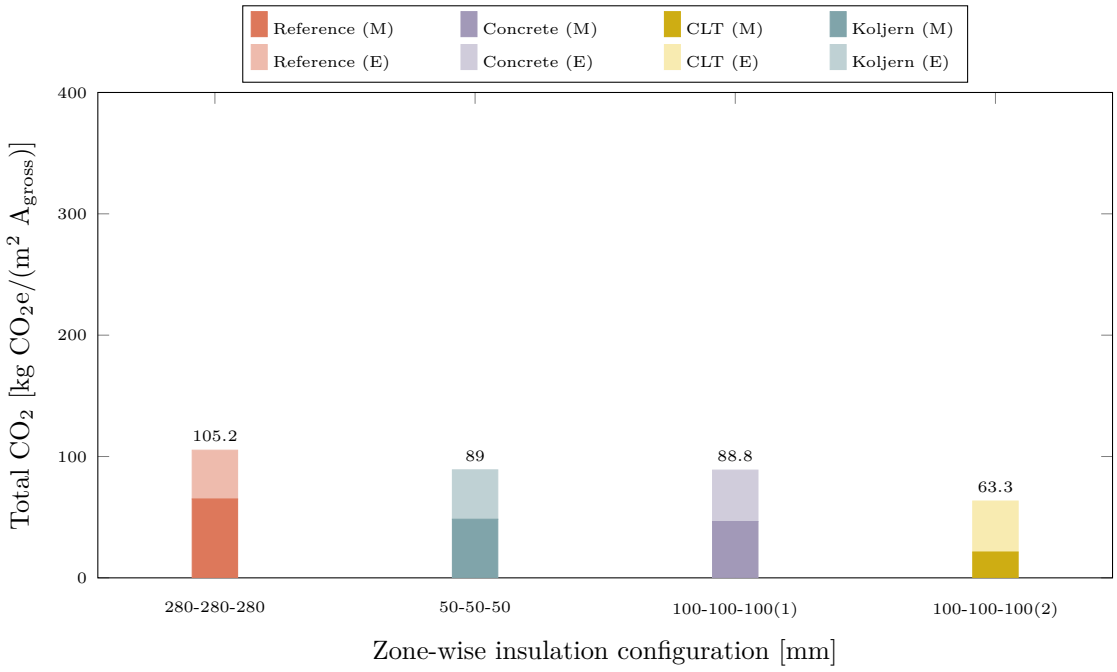

Figure 4.5: GWP for each optimized slab-on-grade system in the warehouse with a HP. (M) denotes material emissions; (E) denotes operational energy. The two cases labeled 100-100-100 represent different slab systems using the same insulation configuration: (1) refers to the concrete system and (2) refers to the CLT system.

Figure 4.5 further supports the trend shown in Figure 4.4, indicating that the CLT system has the lowest GWP among the evaluated slab-on-grade systems, 63.3 kg CO_2e/(m^2 A_{gross}), compared to approximately 89 kg CO_2e/(m^2 A_{gross}) for both the concrete and Koljern systems. However, all evaluated systems outperform the reference concrete slab-on-grade with a 280-280-280 mm insulation configuration. The figure also shows that the most optimized Koljern and concrete systems have nearly identical GWP values.

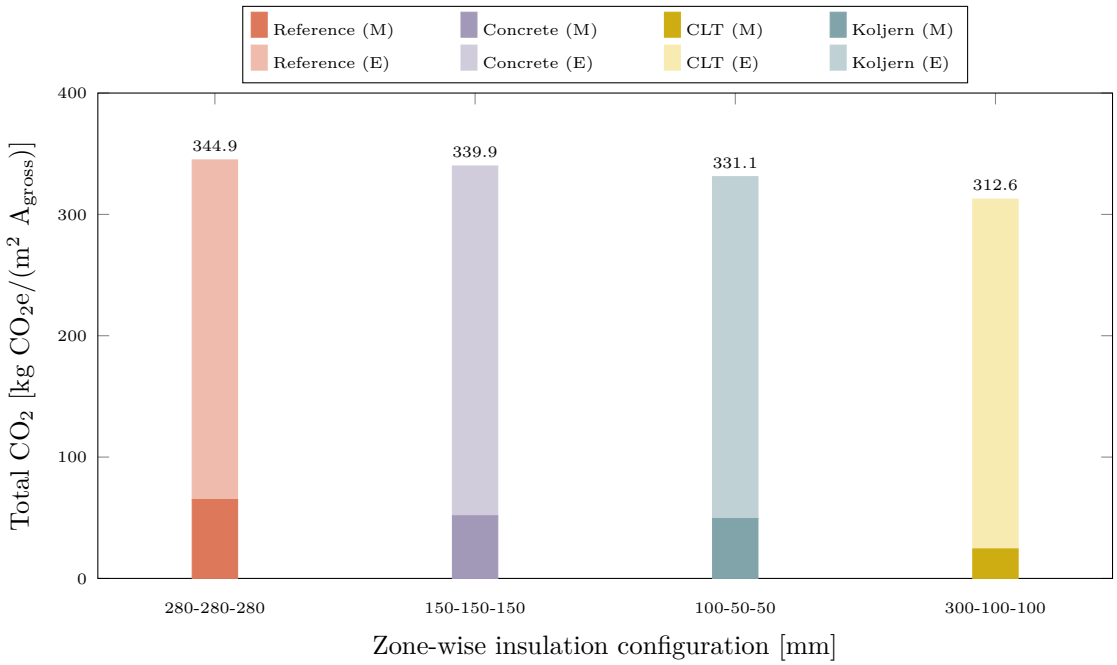

Figure 4.6: GWP for each optimized slab-on-grade system in the warehouse with DH. (M) denotes material emissions; (E) denotes operational energy.

Figure 4.6 demonstrates that, under DH conditions, the CLT system achieves the lowest total GWP among all optimized slab-on-grade configurations. Moreover, all evaluated systems perform better than the reference concrete slab-on-grade with a 280-280-280 mm insulation configuration. Additionally, a comparison of Figure 4.5 and Figure 4.6 reveals that the Koljern system achieves a lower GWP than the concrete system with DH, but not with a HP. This suggests that the high thermal performance of the Koljern system, due to its integrated insulation in the slab, offers greater benefits under DH conditions with higher energy use.

Further the two figures illustrates that using a HP, the relative contributions of operational energy and material-related emissions vary slightly between systems. The reference and standard concrete systems along with the Koljern system, display a higher proportion of emissions from material use compared to the CLT system, where operational energy use use accounts for the larger share of total GWP. In contrast, for DH, emissions from operational energy use dominate across all systems, including the reference slab-on-grade. This highlights the significantly higher climate impact of DH compared to HP in terms of energy-related emissions. It is also evident that, when using HP, the most favorable insulation configurations are all uniform. For DH, however, the optimal configurations for the CLT and Koljern systems involve non-uniform insulation, suggesting that uneven insulation distribution can be more effective in reducing GWP under district heating conditions for the warehouse. The low-carbon concrete variant is not shown, as it shares the same optimal configuration as the standard concrete system, but achieves a consistently lower GWP, about 6.8% for HP and 1.8% for DH, due to reduced embodied emissions.

4.4 Residential building

Table 4.7, Table 4.8, and Table 4.9 present the evaluated insulation setups for each slab-on-grade system, including the insulation thicknesses in the three thermal zones, the resulting U-values, and the corresponding GWP values for both HP and DH. The configuration with the lowest GWP per heating and foundation type is marked in red.

Table 4.7: U-value, zone-wise insulation configuration and total GWP-values for the concrete system in the residential building, organized by increasing U-value and divided by HP and DH.

Concrete system			
U-value [W/(m² · K)]	**Insulation configuration** [mm]	**GWP** [$kg\,CO_2\,e/(m^2\,A_{gross})$]	
		HP	**DH**
0.07	500-400-400	29.7	72.9
	400-400-400	29.6	72.8
0.08	400-400-300	29.3	72.6
	350-350-350	29.2	72.5
0.09	400-300-300	28.9	72.3
	300-300-300	28.8	72.2
0.10	300-300-200	28.4	71.9
0.11	250-250-250	28.3	72.1
	500-200-200	28.2	72.0
0.12	200-200-200	27.9	72.0
	300-200-200	28.0	72.1
0.13	300-300-100	28.2	72.6
0.14	300-200-100	27.9	72.6
0.15	150-150-150	27.7	72.6
	200-200-100	27.8	72.7
0.17	300-100-100	27.6	72.8
0.18	200-100-100	27.6	73.3
0.19	100-100-100	27.6	73.3

Table 4.7 shows that the most optimized insulation configuration for the concrete system, is 100-100-100 for the HP and 300-300-200 for DH. These configurations correspond to GWP values of 27.6 kg CO_2e/(m² A_{gross}) and 71.9 kg CO_2e/(m² A_{gross}), respectively. As with the warehouse, the table shows that both uniform and non-uniform insulation configurations can achieve the same U-value, but with varying GWP outcomes. Notably, for the HP, three configurations with U-values of 0.17, 0.18, and 0.19 W/(m² · K) result in nearly identical GWP values. This highlights a case where the most optimized configuration was determined based on differences at the second decimal.

Table 4.8: U-value, zone-wise insulation configuration and total GWP-values for the CLT system in the residential building, organized by increasing U-value and divided by HP and DH.

CLT system			
U-value [W/(m^2 · K)]	**Insulation configuration** [mm]	**GWP** [$kg\,CO_2\,e/(m^2\,A_{gross})$]	
		HP	**DH**
0.07	400-400-400	24.7	67.9
	600-400-300	24.5	67.7
0.08	350-350-350	24.3	67.6
	400-300-300	23.9	67.2
0.09	300-300-300	23.8	67.2
	400-300-200	23.5	66.9
0.10	300-300-200	23.5	67.0
	250-250-250	23.4	66.9
0.11	300-200-200	23.0	66.8
	200-200-200	22.9	66.7
0.12	300-300-100	23.1	67.2
0.13	200-200-100	22.7	67.1
	150-150-150	22.6	67.0
0.15	200-100-100	22.4	67.3
0.16	100-100-100	22.4	67.4

For the CLT slab-on-grade system in the residential building, Table 4.8 indicates that the most optimized insulation configurations are 100-100-100 for the HP and 200-200-200 for DH. Similar to the results observed for the concrete system, both uniform and non-uniform insulation configurations achieve equivalent U-values, though they differ in their associated GWP values.

Table 4.9: U-value, zone-wise insulation configuration and total GWP-values for the Koljern system in the residential building, organized by increasing U-value and divided by HP and DH.

Koljern system			
U-value [W/(m^2 · K)]	**Insulation configuration** [mm]	**GWP** [$kg\,CO_2\,e/(m^2\,A_{gross})$]	
		HP	**DH**
0.07	200-200-200	27.9	71.1
	250-200-150	27.5	70.7
0.08	150-150-150	26.9	70.2
	150-150-100	26.4	69.7
0.09	100-100-100	25.8	69.2
	150-100-50	25.5	68.9
0.10	100-50-50	24.9	68.4
	50-50-50	24.8	68.3

Table 4.9 presents the insulation configurations and corresponding U-values for the Koljern slab-on-grade system. The most optimized configurations are identified as 50-50-50 for both the HP and DH.

The insulation configurations in Figure 4.7 include all uniform setups along with the most optimized configurations identified for each slab-on-grade system. Solid and dashed lines represent results for HP and DH, respectively. The most optimized insulation configuration for each system and heating source is highlighted in red. The low-carbon concrete variant (20% reduction) was assessed using the same insulation setups as the standard concrete and shows reduced GWP due to lower embodied emissions.

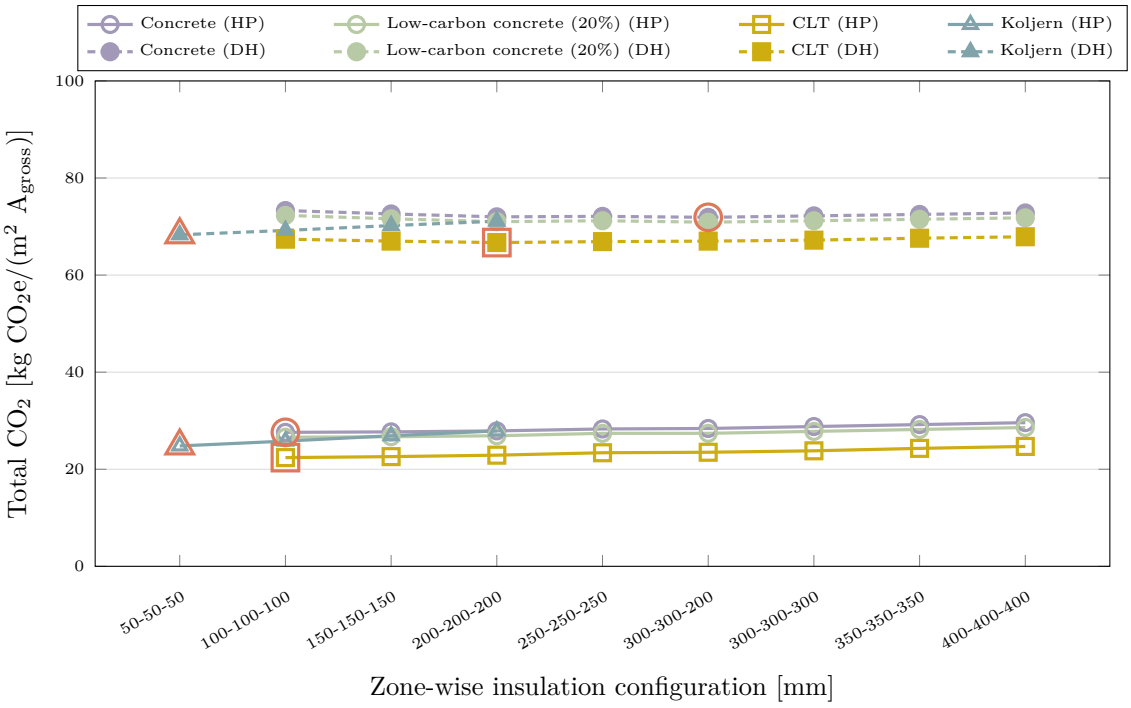

Figure 4.7: Line plot of total GWP as a function of zone-wise insulation configuration for the residential building, comparing HP and DH. The x-axis is ordered by increasing total insulation thickness across zones. The most optimized insulation configuration for each heating source and slab-on-grade system is marked in red.

Figure 4.7 illustrates that the GWP is higher for all slab-on-grade systems when DH is used, with values ranging from approximately 65–75 kg CO_2e/(m^2 A_{gross}), compared to 20–30 kg CO_2e/(m^2 A_{gross}) for HP systems. For both heating sources, the GWP increases only slightly with greater insulation thickness, as indicated by the low slope of the curves, indicating that insulation optimization has a relatively limited impact on the total GWP. For HP, configurations with the least insulation thickness yield the lowest GWP across all slab-on-grade systems. For DH, optimal configurations vary, Koljern performs best with 50-50-50, while the concrete and CLT systems require more insulation. However, the thickest insulation configurations never result in the lowest GWP. Furthermore, the figure also illustrates that

the CLT system consistently exhibits the lowest GWP across all insulation configurations for both heating systems. The Koljern system outperforms the concrete system in certain configurations, while in others, the two systems exhibit almost similar total GWP values.

Figure 4.8 and Figure 4.9 illustrate the total GWP for the most optimized insulation configurations of each slab-on-grade system using both a HP and DH. The results are compared against a reference case representing the concrete slab-on-grade currently used in the residential building. Each bar separates emissions from material use and operational energy, highlighting the relative contribution of each.

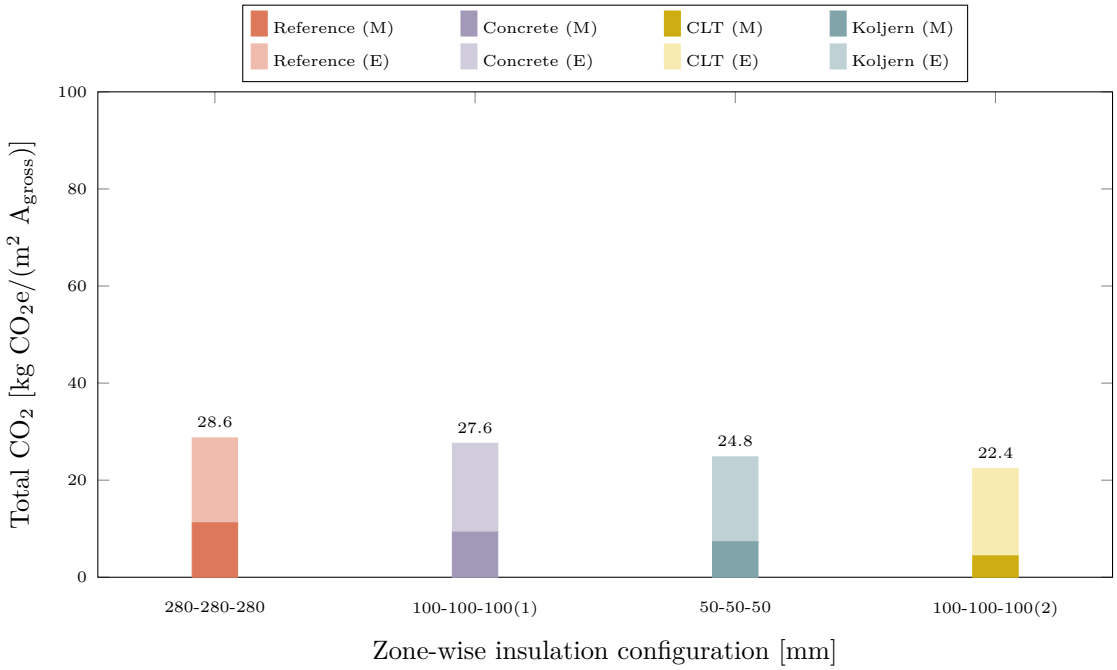

Figure 4.8: GWP for each optimized slab-on-grade system in the residential building with a HP. (M) denotes material emissions; (E) denotes operational energy. The two cases labeled 100-100-100 represent different slab systems using the same insulation configuration: (1) refers to the concrete system and (2) refers to the CLT system.

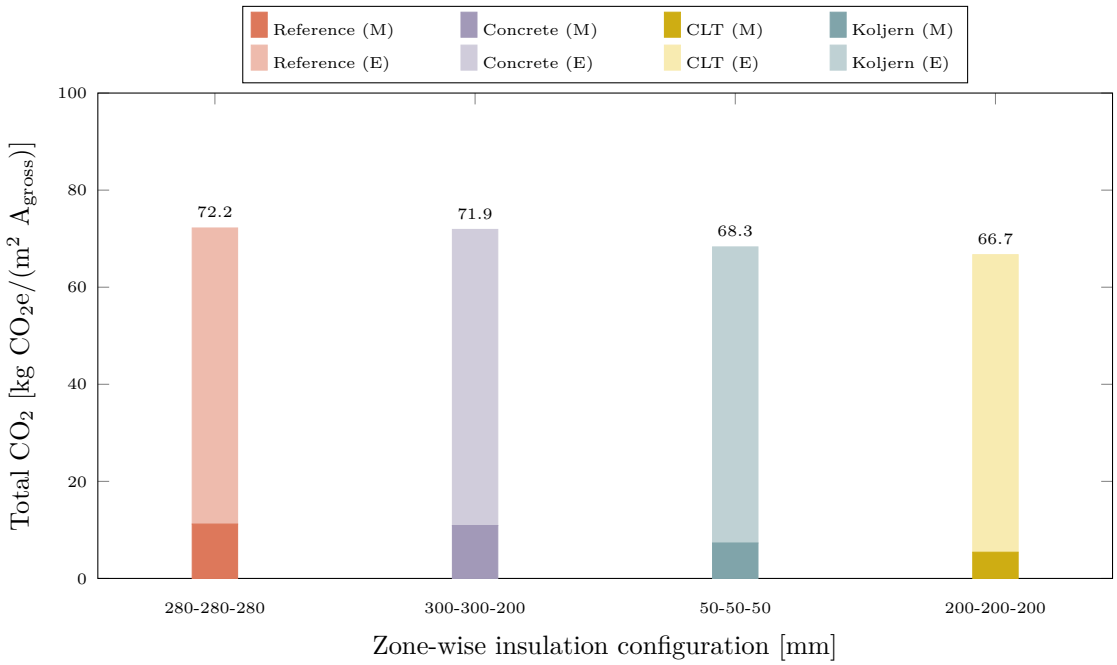

Figure 4.9: GWP for each optimized slab-on-grade system in the residential building with DH. (M) denotes material emissions; (E) denotes operational energy.

Figure 4.8 and Figure 4.9 demonstrate that the CLT system yields the lowest total GWP among all optimized slab-on-grade configurations. Furthermore, all systems exhibit slightly lower GWP values than the reference concrete slab-on-grade, independent of the heating source used. In both HP and DH cases, emissions from operational energy use exceed those from material use, with the contribution from energy use being notably larger for DH. Nearly all of the most optimized insulation configurations are uniform, the only exception is the concrete system using DH, which exhibits a non-uniform distribution. This suggests that for the residential building, the relatively small slab-on-grade area may limit the potential benefits of using non-uniform insulation to reduce GWP. The low-carbon concrete variant is not shown, as it shares the same optimal configuration as the standard concrete system, but achieves a consistently lower GWP, about 3.6% for HP and 1.4% for DH, due to reduced embodied emissions.

4.5 Cross-building comparison

Figure 4.10 and Figure 4.11 illustrate the variation in total GWP across all slab-on-grade systems for the three studied building types. The results are shown for the two heating sources, a HP and DH. For each building type, the lines represent the GWP range between the minimum and maximum insulation configurations for each slab-on-grade system, ordered by increasing total insulation thickness across thermal zones. Note that the two graphs have different maximum values on the y-axis, which should be considered when comparing absolute GWP levels between the two heating sources.

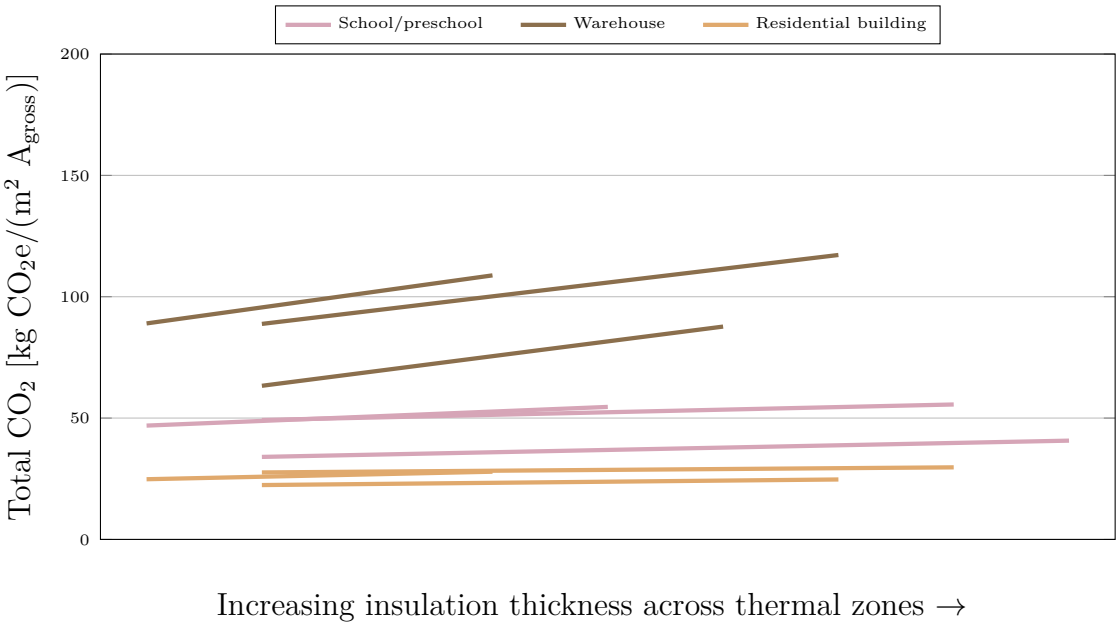

Figure 4.10: Variation in total GWP across all slab systems for all three buildings, using a HP. Each group of colored lines represents one building type, showing the GWP range across insulation configurations sorted by increasing total insulation thickness.

Figure 4.10 demonstrates that the warehouse exhibits the steepest slopes, indicating a higher sensitivity of total GWP to changes in insulation thickness. In contrast, the residential building shows a much flatter slope, meaning that increasing insulation thickness has a comparatively smaller effect on the total GWP. The school/preschool falls in between, showing a moderate increase in GWP as insulation thickness increases. Notably, all lines slope upward, showing that for all building types, increased insulation thickness leads to higher total GWP with a HP. This indicates that the reduction in operational energy use is not sufficient to compensate for the increasing embodied emissions from the additional insulation.

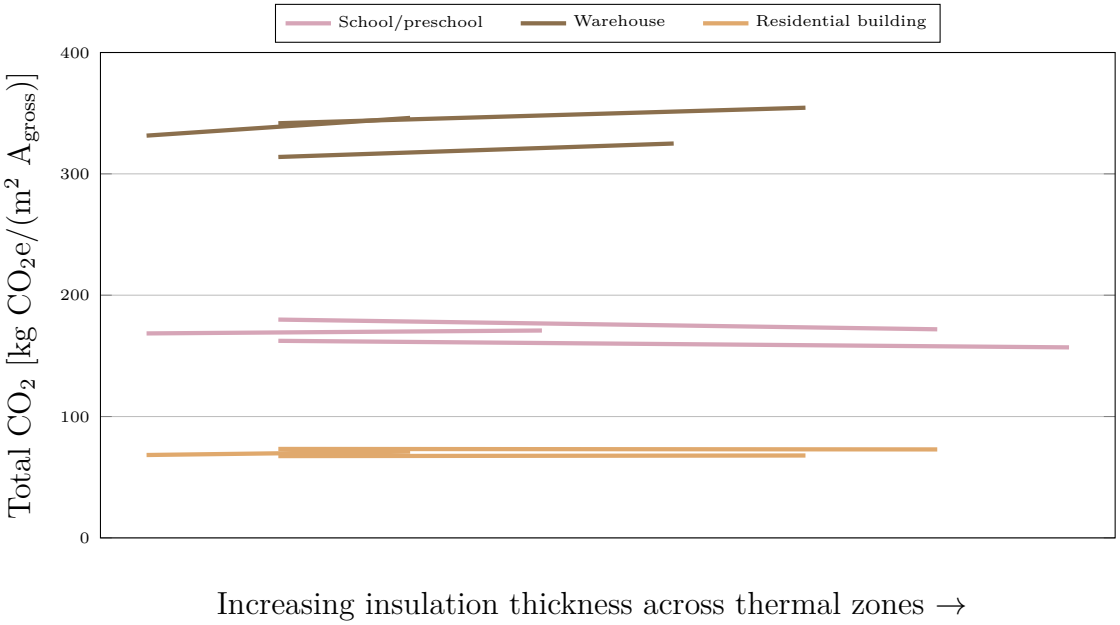

Figure 4.11: Variation in total GWP across all slab systems for all three buildings, using DH. Each group of colored lines represents one building type, showing the GWP range across insulation configurations sorted by increasing total insulation thickness.

As shown in Figure 4.11, the impact of increased insulation thickness on total GWP varies between building types under the DH scenario. For the school/preschool, the slope is slightly downward, indicating that total GWP decreases as insulation thickness increases, suggesting that operational energy savings outweigh the additional embodied material emissions. The residential building shows an almost flat slope, implying a near balance between the embodied emissions from more insulation and the reduction in operational energy use. In contrast, the warehouse still exhibits an upward slope, although it is less steep than in the HP case. The overall GWP levels are higher in the district heating scenario, especially for the warehouse, highlighting the importance of the energy source.

4.6 Slab-on-grade contribution to the building's total climate impact

Figures 4.12 and 4.13 illustrate the distribution of GWP from material production (stages A1–A3) across major building components for the school/preschool and the warehouse.

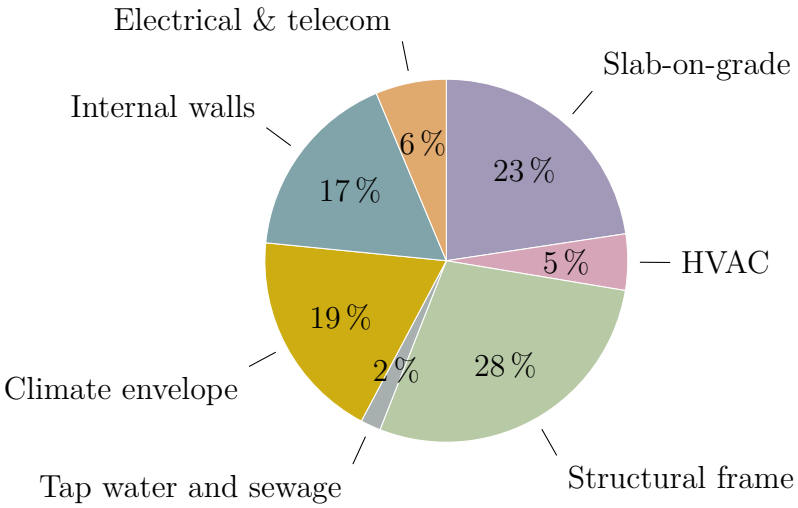

Figure 4.12: Distribution of GWP by component for the school/preschool.

Figure 4.12 shows that for the school/preschool, the structural frame is the single largest contributor, accounting for approximately 28% of total embodied emissions. The slab-on-grade foundation follows closely at 23%, highlighting its significant role in the building's overall climate impact. Combined, these two components represent more than half of the total GWP. Other notable contributors include the climate envelope (19%) and internal walls (17%), while technical systems such as HVAC and electrical installations make up smaller shares. Full values can be found in Table 3.18.

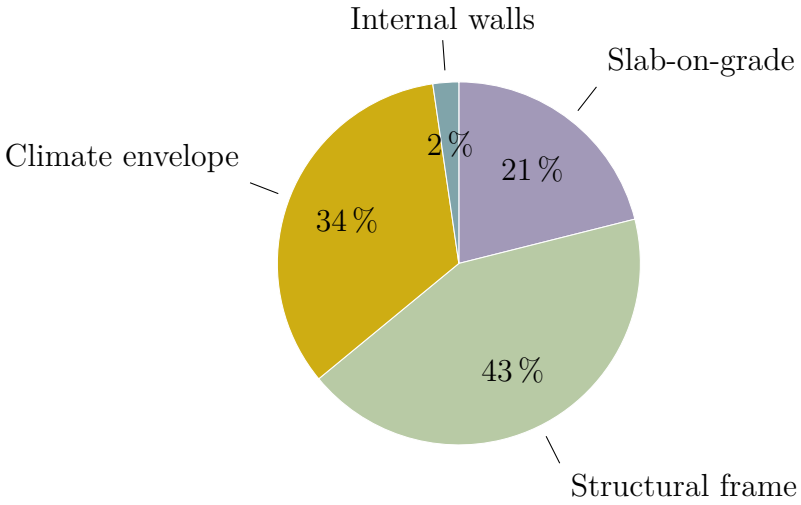

Figure 4.13: Distribution of GWP by component for the warehouse.

Figure 4.13 presents the corresponding breakdown for the warehouse. Here, the structural frame dominates even more clearly, contributing 43% of total GWP. The climate envelope follows at 34%, and the slab-on-grade accounts for 21%. The higher emissions from the structural frame in this case can likely be attributed to the use of a steel frame in the warehouse, compared to a timber frame in the school/preschool.

Despite the differences in building function, size, and structural system, the slab-on-grade contributes a similar proportion in both buildings, approximately 20%. This consistency is noteworthy considering the difference in slab area, indicating that foundations contribute significantly to climate impact regardless of building type. However, it should also be noted that the slab-on-grade is not the component with the greatest overall impact.

5
Discussion

This chapter reflects on the findings from the results chapter, discusses methodological strengths and limitations, and provides an overall conclusion in relation to the research questions. It begins with a discussion of observed trends in GWP across heating sources, slab-on-grade systems, insulation strategies, and building types. The chapter also includes a sensitivity analysis and outlines suggestions for future research and development.

5.1 Discussion of results

This section discusses the key findings from the results, with a focus on identifying patterns and drawing conclusions about GWP reduction strategies. While individual changes in insulation configuration within the same slab-on-grade system result in relatively small stepwise differences, comparing the configurations with the highest and lowest total GWP reveals more significant variations. Rather than identifying a single optimal solution, the overall trends observed, such as the influence of insulation thickness, material choice and heating source, offer a more solid foundation for understanding which design strategies most effectively reduce GWP.

One clear trend observed in the results is the significant difference in total climate impact between the two heating sources, HP and DH, which in turn influences the optimal design strategies for each case. This underscores the importance of defining the energy system early in the design phase, as it directly affects which slab-on-grade system and insulation configuration is the most appropriate. For HP systems, the trend is relatively straightforward: low insulation levels often result in the lowest GWP. This is because the operational energy emissions are already low, due to the high efficiency of the system. Adding more insulation in these cases has limited effect on reducing heating demand, while the embodied emissions from insulation materials continue to increase, raising the total GWP instead. In contrast, for buildings connected to DH, the relationship is less straightforward. Although thicker insulation is generally needed to reduce heating demand and compensate for higher operational energy emissions, the results show that increasing insulation does not necessarily lead to a lower total GWP. Instead, configurations with intermediate insulation levels perform better than those with the thickest insulation. This pattern is broadly consistent across the studied building types, although the optimal insulation level varies. Importantly, regardless of heating system, the data suggest a tipping point: a stage where more insulation leads to diminishing returns in energy

efficiency while embodied material emissions continue to increase. This reveals an important design consideration, achieving the lowest total climate impact requires careful balance, not just maximizing insulation thickness.

The results also suggest that the level of detail required in designing slab-on-grade insulation thickness varies depending on the heating source and building characteristics. For all building types analyzed, slab-on-grade systems with a HP generally show that a uniform insulation configuration is often the most optimal choice to reach the lowest GWP. In contrast, DH systems more frequently benefit from non-uniform insulation distributions, indicating that varying insulation thickness can help reduce total GWP in buildings with higher operational emissions. Additionally, building-specific factors, particularly the size of the slab-on-grade area, significantly influence the potential gains from insulation optimization. As shown in Figure 4.10 and Figure 4.11, the residential building with a relatively small slab area exhibits only a slight change in GWP regardless of insulation configuration. This suggests that for buildings with smaller slabs, detailed optimization of insulation thickness has a limited impact on overall GWP. Figure 4.10 further shows that the warehouse displays a much steeper GWP slope than the school/preschool, even though it has a smaller slab area. This indicates that in the warehouse, GWP increases considerably with thicker insulation. In this case, choosing a low insulation thickness becomes more important. This is explained by the lower operational energy use of the warehouse, so adding more insulation has minimal effect on reducing an already low heating demand, but still contributes to higher embodied material emissions.

Sandin's model supports using non-uniform insulation to account for variations in ground thermal resistance across the three zones, with the aim of optimizing the overall U-value. However, this approach does not necessarily lead to the most effective insulation setup when the goal is to minimize total GWP. In other words, optimizing purely for thermal performance might not align with minimizing climate impact. It is important to note that these conclusions are based on the specific building geometries and boundary conditions used in this study. Zone-specific insulation could become more relevant in buildings with larger slabs or under boundary conditions not included in this analysis. In summary, the need for detailed insulation design might increase for buildings with DH, larger slab-on-grade areas and higher operational energy use. It should also be noted that other components of the building envelope and their relative contributions to total transmission losses affect how beneficial it is to optimize the slab-on-grade in detail. In the buildings analyzed, windows and doors accounted for the largest share of transmission losses, followed by exterior walls, roofs, and thermal bridges, as shown in Table 3.2, Table 3.7, and Table 3.10. These findings suggest that prioritizing improvements in those areas could potentially yield greater reductions in operational energy use than refining slab-on-grade insulation thickness alone. Furthermore, the results indicate that the insulating properties of the ground mean that focusing insulation improvements on other parts of the building envelope can lead to more substantial overall energy savings.

When comparing slab-on-grade systems across all building types and both heating systems, the overall trends remain consistent. The CLT slab-on-grade demonstrates the lowest total climate impact across all evaluated insulation configurations and consistently achieves the lowest GWP values. For the Koljern system, the most optimized variants show a lower total climate impact than the optimized concrete slab-on-grade in all building types and for both heating systems, except in the warehouse scenario using a HP, where the Koljern and concrete systems display nearly identical GWP values. When considering all insulation thicknesses, the results vary as to whether Koljern or concrete achieves the lowest GWP. Notably, the Koljern system performs better in DH scenarios than in those using a HP, primarily because HP systems have lower energy use, reducing the potential benefits of the Koljern system's improved insulation performance. The low-carbon concrete (20% reduction) slab-on-grade results in slightly reduced GWP values compared to the standard concrete alternative but follows the same general trend in terms of relative performance across buildings and heating systems. Furthermore, all optimized slab-on-grade systems demonstrate a lower climate impact than the reference concrete slab-on-grade, though the extent of this reduction varies depending on the building type and heating system.

When looking at the building as a whole, the slab-on-grade accounts for approximately 20% of the total climate impact from material use in the warehouse and school/preschool cases analyzed in this study. This is a substantial share, indicating that the foundation is an important contributor to the building's embodied emissions. However, a closer examination shows that some design choices have a greater impact than others. While detailed adjustments to insulation thickness within a given slab system may only result in modest reductions, more significant improvements can be achieved by switching to an alternative slab system. For instance, in the school/preschool case, switching from a conventional concrete slab to the optimized CLT system reduces the climate impact from 52.8 to 33.8 $\mathrm{kg, CO_2e/(m^2\, A_{gross})}$. Across the building's total heated floor area of 4321 $\mathrm{m^2}$, this corresponds to a savings of approximately 82 tonnes $\mathrm{CO_2e}$. This highlights how even modest material choices at the component level can yield substantial emissions reductions at the building scale. In summary, the study shows that strategic choices, such as selecting a different slab system or aligning insulation strategy with the heating system, can meaningfully lower a building's overall climate impact. However, the results also indicate that in certain cases, such as buildings with a relatively small slab area, the benefits of insulation optimization are limited.

5.2 Discussion of other LCA stages

The construction methods used for the three slab-on-grade systems influence both transport and on-site emissions. The concrete system involves several labor- and equipment-intensive steps such as formwork, reinforcement, casting, and curing. This often results in higher A5 emissions, although widespread production across Sweden may help reduce A4-related impacts by shortening transport distances. Both the CLT and Koljern systems rely on prefabrication, which tends to lower on-site resource use and emissions. Koljern's elements are quick to install, but centralized production may lead to longer transport routes. Similarly, the CLT system benefits from modular construction, though it is more sensitive to moisture and may require additional protection during transport and assembly. As with Koljern, transport emissions for CLT depend on how close the production facility is to the site.

In the LCA, within the use stage phase, differences in durability and maintenance depend on material properties and environmental exposure. Concrete generally requires little maintenance and is resistant to biological degradation. The Koljern system uses cellular glass and protected steel beams, which could result in long service life with limited maintenance. The CLT system has potential for stable performance if moisture is effectively managed throughout its service life. Moisture ingress can lead to degradation, and while small repairs are possible, its uniform structure and biological sensitivity make preventive protection especially important.

At end-of-life, the systems differ in how easily they can be dismantled and whether their components can be reused or recycled. Concrete is often the most demanding to demolish and, while the crushed material can be reused as low-grade aggregate, this is generally considered downcycling. The reinforcement steel may be recoverable, depending on how well it's separated. CLT elements, particularly in modular systems, may be suitable for reuse or repurposing if kept dry. Otherwise, they may be directed toward incineration or low-grade recycling, and components like EPS and foil membranes pose recycling challenges. The Koljern system appears to support easier disassembly thanks to its mechanical assembly. Foamglas and steel may be reused or recycled multiple times, though this depends on their condition and whether future projects can accommodate reused elements. As with the other systems, making use of any circular potential depends heavily on early planning and suitable end-of-life handling.

5.3 Sensitivity analysis of the results

Several limitations and uncertainties have influenced the outcomes of this study. First, the analysis is based on only three case buildings, one per building category, which reduces the applicability of the results to buildings with differing scales, functions, or design characteristics. For example, in cases involving significantly larger structures, such as expansive warehouse facilities, the results may differ. Moreover, specific building characteristics, such as unconventional geometries, occupancy patterns, and indoor temperature settings, can significantly influence thermal performance and may lead to different results. Further, various geographical places where not evaluated. In addition, thermal bridges were only assessed at a general level, therefore more detailed evaluation of thermal bridges across slab-on-grade systems and insulation configurations could provide further insight into their performance. For example, non-uniform insulation distribution with increased edge insulation (zone 1) could reduce transmission losses compared to uniform insulation. This suggests that, in some cases, non-uniform configurations may result in a lower climate impact than considered, and could therefore represent a more effective design strategy in some cases.

The energy sources utilized for heating, along with their associated assumed GWP, represent a major source of uncertainty. Technological development and changes in energy policy have the potential to alter the GWP of energy systems over time. For example, future transitions toward more renewable or low-carbon energy sources could significantly reduce operational emissions, thereby diminishing the relative contribution of energy use to the overall climate impact. At the same time, such changes may also influence material-related emissions, as the adoption of innovative production technologies and alternative materials could lead to different environmental outcomes. Additionally, biogenic carbon uptake in timber-based materials has not been accounted for as negative emissions in this study. While timber has the potential to act as a carbon sink through long-term storage, the relatively short 50-year analysis period applied here and a conservative methodological approach have resulted in assigning timber products a zero net emission value rather than a negative GWP.

Furthermore, the GWP values from EPDs used for the different slab-on-grade systems and their materials also introduce uncertainty. There can be notable differences in GWP depending on the manufacturer. This means that the results are sensitive to the specific data used, and the total GWP could vary if different products or assumptions were applied. To explore this variability, a sensitivity analysis was carried out to assess how the results would change under different material scenarios. Specifically, the analysis included a low-carbon concrete with a 40% reduction in GWP, as well as concrete of higher strength class, C40/50. These alternatives were evaluated for the warehouse case, as shown in Figure 5.1, alongside a standard concrete slab-on-grade, another low-carbon variant with a 20% reduction, and the Koljern system. All scenarios were modeled with the same insulation configuration (100-100-100 mm) to isolate the effect of material choices on the total GWP.

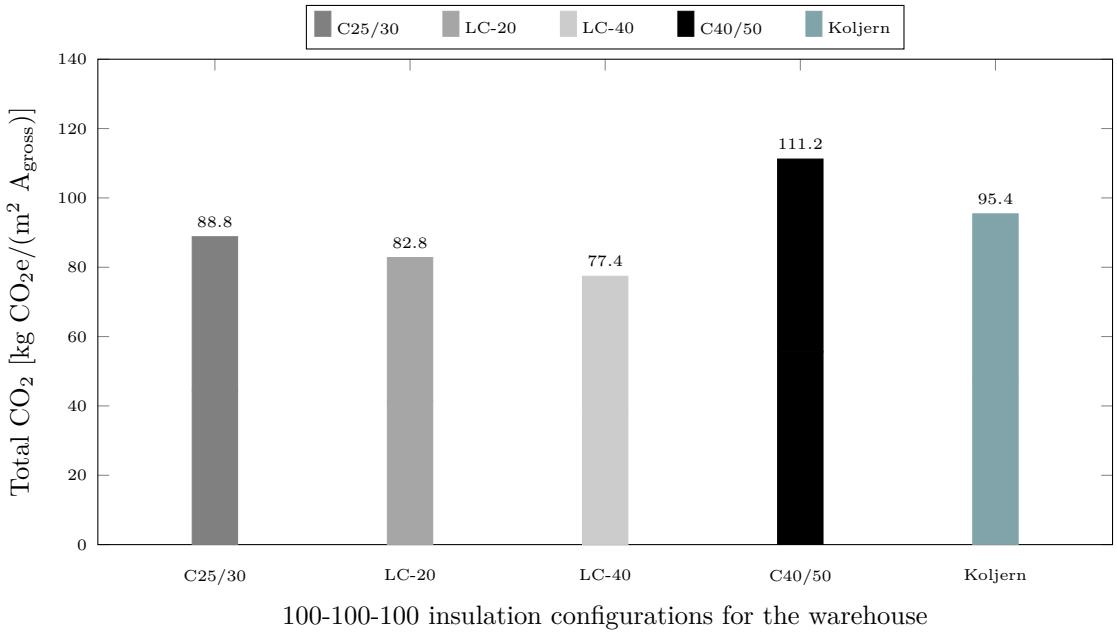

Figure 5.1: Total GWP from left to right: the optimized concrete system for the warehouse with insulation configuration 100-100-100, low-carbon concrete level 2 (20%), low-carbon concrete level 4 (40%), concrete with higher strength class (C40/50), and the Koljern system with insulation configuration 100-100-100.

.

Figure 5.1 demonstrates that both the standard concrete slab-on-grade and the two low-carbon concrete alternatives result in a lower total GWP than the Koljern system when using the same insulation configuration. However, when the concrete mix is replaced with a higher strength class (C40/50), which typically has a higher embodied carbon footprint due to increased cement content, the total GWP exceeds that of the Koljern system. This outcome highlights the importance of conducting detailed, case-specific analyses when comparing alternative slab-on-grade solutions. The results suggest that there is no generally optimal system in terms of climate impact, whether concrete or the Koljern system performs better depends on the specific material properties, structural requirements, and environmental data applied. Therefore, to achieve the lowest possible GWP, it is essential to evaluate different options under consistent conditions and consider the full range of influencing factors. It is also noteworthy that the concrete slab-on-grade systems analyzed in this study are based on a 120 mm thick load-bearing concrete layer, while the Koljern system includes a 168 mm thick structural element. This suggests that under alternative ground conditions requiring piling, the concrete slab may need to be increased in thickness to meet structural demands, while the Koljern system might already fulfill such requirements without modification. Consequently, in such scenarios, the GWP associated with the concrete solutions could increase more substantially than that of the Koljern system, highlighting the need for context-specific structural and environmental assessments.

The geographic location of a building significantly influences the climate data used in simulations within IDA ICE, as well as the thermal resistance values of different soil types applied in Sandin's model. Regional conditions, such as temperature, solar radiation and ground conditions surrounding the slab-on-grade foundation vary with location. These variations consequently affect the calculated energy demand and thermal performance. Therefore, conducting the analysis for an alternative geographic location with differing climate and soil characteristics could produce different results, highlighting the importance of incorporating site-specific data for accurate assessment and design of slab-on-grade foundations. Another aspect worth considering is the precision of U-values used in the simulations. In this study, U-values were applied with two decimal places, which aligns with industry standards. However, this level of rounding can result in relatively large jumps between configurations, potentially affecting the results. For instance, two slab configurations may have U-values of 0.096 and 0.14 $W/(m^2 \cdot K)$ respectively, which is both rounded to 0.10 $W/(m^2 \cdot K)$. In practice, however, the actual difference in energy performance between such values is likely minimal.

5.4 Evaluation of method

A large number of slab-on-grade configurations were analyzed in this study to investigate whether detailed optimization could lead to substantial improvements and to explore the balance between material emissions and energy efficiency. Initially, an even broader set of combinations was considered. However, to ensure the study remained feasible and focused, a set of constraints, outlined in Section 3.2, was applied to reduce the number of configurations. While these constraints excluded certain theoretical combinations, they were necessary to maintain a realistic design scope and reflect standard construction practices, such as the use of uniform insulation thicknesses and limiting large differences in insulation thicknesses between thermal zones.

To calculate heat transfer through the ground, the methodology developed by Sandin was chosen over the approach outlined in the standard SS-EN 13370:2017. This decision was based on both practical and methodological considerations. Sandin's method is used by PE Teknik & Arkitektur, which made it easier to compare and validate results. Additionally, the standard does not easily account for multiple thermal zones with varying insulation thicknesses, making it less suitable for configurations with non-uniform insulation. In contrast, Sandin's model allows for a more detailed representation of such variations, making it a well-suited and reasonable choice for this thesis.

Energy simulations were conducted in IDA ICE for each building and the various U-values. Due to limitations in the software, it was not feasible to apply different insulation thicknesses to individual thermal zones. Instead, a single U-value, calculated for each insulation configuration, was used uniformly across the model. This simplification was considered reasonable, as prior sensitivity analyses in IDA ICE have shown that, compared to using a single average U-value, applying different in-

sulation thickness between zones typically results in only minor differences in overall energy performance. Substantial time was spent on refining and validating the IDA ICE models. Through repeated adjustments and checks, the models were aligned with expected energy use, helping to ensure that the simulation results were both reasonable and reliable.

5.5 Further research

Several areas identified in this study present opportunities for further development and research to improve the accuracy and applicability of the results. One important aspect concerns moisture safety when reducing insulation thickness. For certain interior floor materials, the industry standard typically recommends 200 mm of insulation across all zones to ensure adequate moisture control. However, it is not yet clear whether thinner insulation layers, particularly for certain interior floor types, could sufficiently prevent moisture-related risks. Future studies should evaluate moisture performance with reduced insulation levels to determine the minimum thickness that still ensures long-term durability and safety. Reducing insulation may also help lower cooling demand in buildings with large temperature variations by utilizing the ground's thermal storage capacity. This can be explored further to understand how lower insulation amount can contribute to passive cooling and energy savings. The geographic location in this study influenced the climate data used in IDA ICE and the soil thermal resistance values in Sandin's model. Since climate and soil conditions vary regionally, conducting analyses for other locations could yield different results, highlighting the importance of site-specific data. Additionally, only a general assessment of thermal bridges was performed. A more detailed study, considering different materials for the slab-on-grade types, as well as the effect of increased edge insulation (zone 1), could reveal significant reductions in heat loss and affect the result. One potential area for further investigation is whether the additional layer of Foamglas beneath the Koljern element could be removed to reduce insulation thickness even more. Technically, it may be possible to remove this layer entirely. Although the Foamglas layer likely remains necessary for compressive strength and to provide protection for the steel profiles, it might not be essential for moisture control, given the Koljern system's high level of moisture resistance. Future studies could assess both the structural and hygrothermal consequences of removing this layer, and whether doing so could lead to further reductions in the total GWP of the Koljern system. In addition, other building types with different characteristics, as well as larger structures such as extensive warehouse facilities, could be analyzed to assess whether the results apply to a wider range of cases. A more comprehensive evaluation of all life cycle stages, not fully addressed in this thesis, would also offer a deeper understanding of the total climate impact of different slab-on-grade systems. Future research addressing these aspects would contribute to more accurate and sustainable slab-on-grade design strategies.

6
Conclusion

For all building types analyzed, the results indicate that when HP systems are used as the heating source, lower insulation thicknesses correspond to the lowest GWP. In contrast, buildings heated by DH typically require greater insulation thicknesses to achieve minimal GWP. Although reducing insulation can be favorable for GWP, it might increase moisture-related risks. Furthermore, the findings suggest that the level of detail in insulation placement becomes more important for buildings utilizing DH, those with larger slab-on-grade areas, and buildings characterized by higher operational energy demands.

The results indicate that, for all assessed building categories, the CLT slab-on-grade system consistently yields the lowest total GWP, considering both emissions from material use and operational energy. Furthermore, the most optimized Koljern configuration for each building and heating scenario generally outperforms both the most optimized conventional concrete system and the low-carbon concrete variant with a 20% reduction in material-related emissions. An exception is observed for the warehouse building when DH is applied, where the concrete alternative performs slightly better. However, looking across all insulation configurations, a comparison between the concrete and Koljern systems yields varying results, with neither system demonstrating consistently lower GWP. This variability underscores the importance of evaluating GWP performance on a project-specific basis, taking into account building-specific parameters and design choices.

The study shows that the reference concrete slab-on-grade contributes to approximately 20% of the building's total material-related GWP, indicating that optimization of the slab-on-grade can meaningfully reduce the overall climate impact. Although, detailed optimization of insulation placement does not always lead to significant GWP reductions. More substantial decreases in environmental impact can be achieved by selecting an alternative slab-on-grade system, for example, replacing a conventional concrete slab-on-grade with a CLT slab-on-grade. However, in cases where a change of material is not feasible, optimizing the insulation thickness may still be beneficial.

Bibliography

Boverket. (2017). *Boverkets föreskrifter om ändring av verkets föreskrifter och allmänna råd (2016:12) om fastställande av byggnadens energianvändning vid normalt brukande och ett normalår;* (Accessed: 2025-02-20). Yvonne Svensson. https://rinfo.boverket.se/BFS2016-12/pdf/BFS2017-6.pdf

Boverket. (2023a). Byggdelar som ingår - klimatdeklaration [Accessed: 2025-04-04]. https://www.boverket.se/sv/klimatdeklaration/gor-sa-har/byggdelar-som-ingar/

Boverket. (2023b). *Gränsvärde för byggnaders klimatpåverkan [Limit value for buildings' climate impact]* (Accessed: 2025-02-13). https://www.boverket.se/globalassets/publikationer/dokument/2023/slutrapport-gransvarde-for-byggnaders-klimatpaverkan.pdf

Boverket. (2024a). Direktiv för byggnaders energiprestanda [Accessed: 2025-02-13]. https://www.boverket.se/sv/byggande/uppdrag/direktiv-for-byggnaders-energiprestanda/

Boverket. (2024b). Vad visar en LCA? [What does a LCA show?] [Accessed: 2025-01-29]. https://www.boverket.se/sv/byggande/hallbart-byggande-och-forvaltning/livscykelanalys/vad-visar-en-lca/

Boverket. (2025a). Bygg- och fastighetssektorns energianvändning uppdelat på förnybar energi, fossil energi och kärnkraft [Accessed: 2025-03-06]. https://www.boverket.se/sv/byggande/hallbart-byggande-och-forvaltning/miljoindikatorer---aktuell-status/energianvandning/

Boverket. (2025b). District heating, swedish average [Accessed: 2025-03-06]. https://klimatdatabasen.boverket.se/detaljer/2/6000000014

Boverket. (2025c). Electricity, swedish mix [Accessed: 2025-03-06]. https://klimatdatabasen.boverket.se/detaljer/2/6000000008

Carl-Eric Hagentoft. (2001). *Introduction to building physics*. Studentlitteratur.

EQUA Simulation AB. (n.d.). IDA Indoor Climate and Energy (IDA ICE) [Accessed: 2025-03-12]. https://www.equa.se/en/ida-ice

EVIA. (2024). *Environmental product declaration, evia foundation with koljern technology* (Accessed: 2025-03-10).

https://api.environdec.com/api/v1/EPDLibrary/Files/5881ee26-3117-4f51-3a6d-08dc90836af3/Data

Evia. (2024a). Frequently asked questions - koljern foundation [Accessed: March 2024]. https://www.evia.se/faq

Evia. (2024b). *Koljern grund – prefabricated slab-on-grade system* [Accessed: 2025-02-18]. https://www.evia.se/produkter/koljern-grund

Finja Betong. (2021). *Product carbon footprint* (Accessed: 2025-03-04). https://www.finja.se/storage/ma/00b8b3bee3fb43b4b163907654f8d5b7/ff844e8eabb6403c8b2651f6b17f3060/pdf/4A13E30482781A7D1BC3DDB025BD06A4C3E736FC/EPS%20S200_LCA.pdf

Finja Betong. (2022). *Environmental product declaration, eps100* (Accessed: 2025-03-04). https://www.finja.se/storage/ma/fcea57833c6e4e50867d2b37f722e087/008678382d2340788c4aa03ca717d278/pdf/0881BAC90036DD3CE484FC7931D97C6D497CF10B/EPS%20S100_EPD.pdf

Finnfoam. (2021). *Environmental product declaration, ff-eps* (Accessed: 2025-03-04). https://finnfoam.fi/wp-content/uploads/2022/11/finnfoameps_rts-epd_FF-EPS_115-21.pdf

FOAMGLAS. (2025). Förskolan hoppet - sveriges första fossilfria förskola [Accessed: 2025-05-29]. https://www.foamglas.com/sv-se/referensprojekt/sweden/hoppet

Fossilfritt Sverige. (2024). *Färdplan för fossilfri konkurrenskraft bygg och anläggningssektorn* (Accessed: 2025-02-14). https://fossilfrittsverige.se/wp-content/uploads/2024/02/Bygganl%C3%A4ggning_fardplan_uppgraderad_2024.pdf

Gervasio, H., & Dimova, S. (2018). *Model for life cycle assessment (lca) of buildings* (Accessed: 2025-03-03). Publications Office of the European Union. https://data.europa.eu/doi/10.2760/10016

Göteborgs Stad. (2025). Förskola rosendalsgatan – nybyggnad [Accessed: 2025-05-29]. https://goteborg.se/wps/portal/start/goteborg-vaxer/hitta-projekt/stadsomrade-centrum/centrum/forskola-rosendalsgatan---nybyggnad

Gustafsson, A. (2017). *Kl-trä handbok*. Skogsindustrierna, Svenskt Trä.

Klara Byggsystem. (2025a). Klara byggsystem [Accessed: March 2024]. https://www.klarabyggsystem.se

Klara Byggsystem. (2025b). Kundreferenser - klara byggsystem [Accessed: 2025-05-29]. https://www.klarabyggsystem.se/kundreferenser/

Levin, P., Liss, M., Sayegh, S. A., Svensson, J., Falk, M., Olsson, H., & Westin, R. (2024). *Brukarindata bostäder: Svebyprogrammet* (tech. rep.) (Projekt finansierat av SBUF, projektnummer 14302, samt Energimyndigheten). Sveby. https://www.sveby.org

Lindab Profil. (2020). *Environmental product declaration, lindab construline* (Accessed: 2025-03-10). https://www.lindab.se/globalassets/commerce/lindabwebproductsdoc/assets/production/mgu0nwizymmtzti2oc00mmm2lthkzmutotnmntu3mmu2n2zl/5249841218584053890/nepd-2269-1037_construline.pdf?v=1748347224

Makhnatch, P. (2014). *Något om hur gwp-värden bestäms* (tech. rep.) (Accessed: 2025-02-26). KTH. https://www.energy.kth.se/sv/applied-thermodynamics/key-research-areas/heating-systems/low-gwp-news/nagot-om-hur-gwp-varden-bestams-1.474589

Malmqvist, T., Borgström, S., Brismark, J., & Erlandsson, M. (2023). *Referensvärden för klimatpåverkan vid uppförande av byggnader* (tech. rep.) (Accessed: 2025-01-29). KTH Royal Institute of Technology. Boverket. https://www.boverket.se/contentassets/5c704bbb2b2f4bd1a31beecf355efaa4/referensvarden-for-klimatpaverkan-vid-uppforande-av-byggnader_kth-2021.pdf

Pittsburgh Corning Europe. (2021). *Environmental product declaration, foamglas t3+* (Accessed: 2025-03-10). https://www.foamglas.com/sv-se/download

Rantala, J. (2005). *On thermal interaction between slab-on-ground structures and subsoil in finland* (tech. rep.) (Accessed: 2025-02-06). Tampere University of Technology. Publication. https://urn.fi/URN:NBN:fi:tty-200810021109

RISE Research Institutes of Sweden. (2023). Biogen kolinlagring - material och processer [Accessed: 2025-04-04]. https://www.ri.se/sv/expertisomraden/expertiser/kolinlagring

Roots, P., & Hagentoft, C.-E. (2004). Frost heave in swedish slab-on-grade. *Proceedings of the Buildings IX Conference*. https://web.ornl.gov/sci/buildings/conf-archive/2004%20B9%20papers/151_Roots.pdf

Rydegran, E. (2023). Fjärrvärmeproduktion [production of district heating] [Accessed: 2025-03-06]. https://www.energiforetagen.se/energifakta/fjarrvarme/fjarrvarmeproduktion/

Sandin, K. (2010). *Praktisk byggnadsfysik* (1st ed.). Studentlitteratur AB.

SIGA Cover AG. (2022). *Environmental product declaration, wetguard 200 sa* (Accessed: 2025-03-10). https://ipmcdataprod.blob.core.windows.net/cdn/105902-EPDWetguard200SA4901110620271023.pdf

SIS. (2011). *Sustainability of construction works - assessment of environmental performance of buildings - calculation method* (Accessed: 2025-03-05). https://www.sis.se/produkter/byggnadsmaterial-och-byggnader/byggnader/ovrigt/ssen159782011/

SIS. (2017). *Building components and building elements - thermal resistance and thermal transmittance - calculation methods (iso 6946:2017)* (Accessed: 2025-02-10). https://www.sis.se/produkter/byggnadsmaterial-och-byggnader/skydd-av-och-i-byggnader/varmeisolering/ss-en-iso-69462017/

SIS. (2019). *Sustainability of construction works - environmental product declarations - core rules for the product category of construction products* (Accessed: 2025-03-05). https://www.sis.se/produkter/byggnadsmaterial-och-byggnader/byggnadsindustrin/ovriga-aspekter/ss-en-158042012a22019/

Stena Stål. (2024). *Environmental product declaration, reinforced steel mesh* (Accessed: 2025-04-02). Stena stål AB. https://www.stenastal.se/siteassets/sv/om-oss/documents/miljovarudeklaration/epd-reinforced-steel-mesh_2024_draft4.pdf

Svenska kyl och värmepumpföreningen. (n.d.). Värmepumpen - en ren energikälla [Accessed: 2025-03-06]. https://skvp.se/om-varmepumpar/fakta-om-varmepumpar

Swedish Standards Institute [SIS]. (2017). *Thermal performance of buildings – heat transfer via the ground – calculation methods* (Accessed: 2025-02-03). Swedish Standards Institute, [SIS]. https://www.sis.se/produkter/byggnadsmaterial-och-byggnader/byggnadsdelar/inredning/ss-en-iso-133702017/

TräGuiden. (2020). Grundläggning – platta på mark [Accessed: 2025-02-03]. https://www.traguiden.se/konstruktion/konstruktiv-utformning/grundlaggning/grundlaggning/platta-pa-mark/

A

School/preschool

A.1 Concrete system

Table A.1: Zone-wise insulation configurations for the concrete system in the school/preschool, grouped by resulting U-value.

U-value [W/(m^2 · K)]	**Insulation thickness** [mm]
0.07	400-400-400
	500-400-400
	500-500-400
	600-400-400
	600-500-300
	600-500-400
	600-600-300
0.08	350-350-350
	400-400-300
	500-400-300
	500-500-300
	600-400-300
0.09	300-300-300
	400-300-300
	500-300-300
	500-400-200
	500-500-200
	600-300-300
0.10	250-250-250
	400-300-200
	400-400-200
	500-300-200
0.11	300-300-200
0.12	200-200-200
	300-200-200
	400-200-200
	400-400-100
	500-200-200
0.13	300-300-100
	400-300-100
0.14	400-200-100
0.15	150-150-150
	200-200-100
	300-200-100
0.17	300-100-100
	400-100-100
0.18	100-100-100

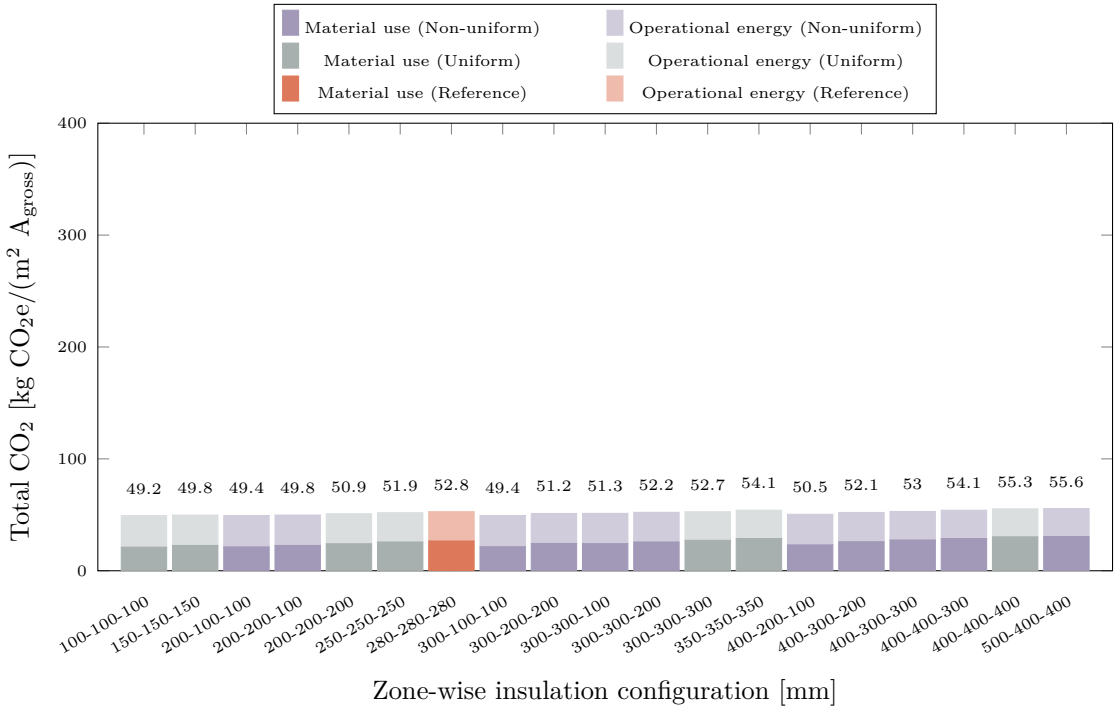

Figure A.1: Total GWP for each concrete system configuration in the school/preschool, based on a heat pump. Results are split into material use and operational energy.

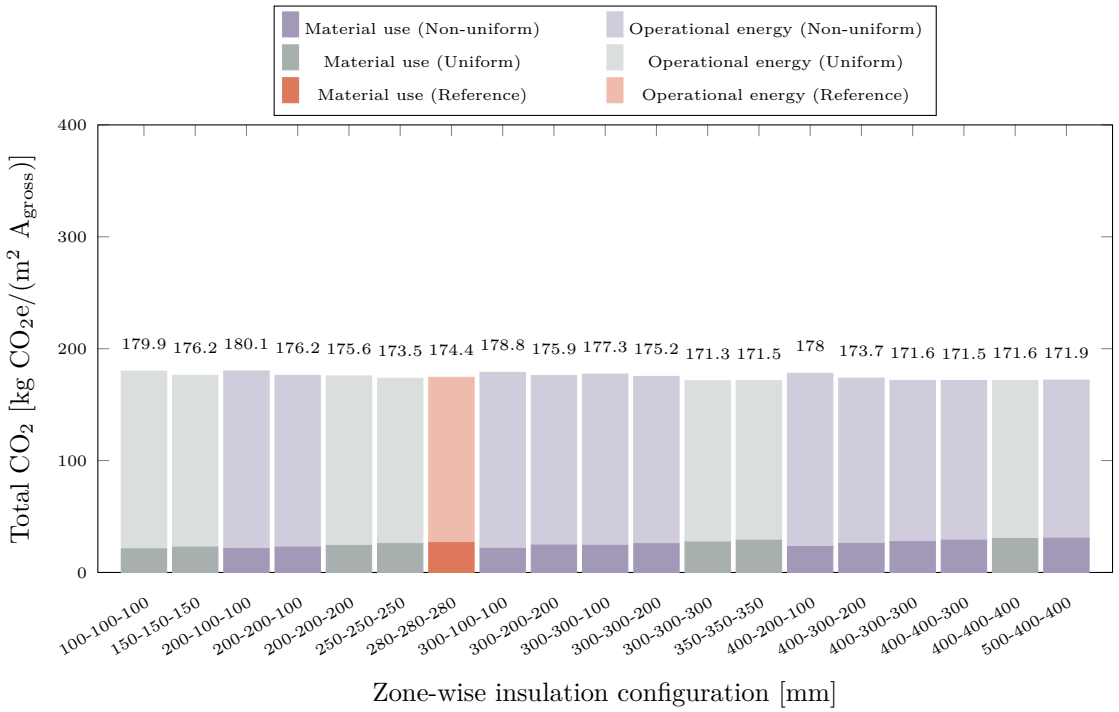

Figure A.2: Total GWP for each concrete system configuration in the school/preschool, based on district heating. Results are split into material use and operational energy.

A.2 CLT system

Table A.2: Zone-wise insulation configurations for the CLT system in the school/preschool, grouped by resulting U-value.

U-value [W/(m^2 · K)]	**Insulation thickness** [mm]
0.07	400-400-400
	500-400-400
	500-500-300
	600-400-400
	600-500-300
	600-600-300
0.08	350-350-350
	400-300-300
	400-400-300
	500-300-300
	500-400-300
	500-500-200
	600-300-300
	600-400-300
0.09	300-300-300
	400-400-200
	500-400-200
0.10	250-250-250
	300-300-200
	400-300-200
	500-300-200
0.11	200-200-200
	300-200-200
	400-200-200
	400-400-100
	500-200-200
0.12	300-300-100
	400-300-100
0.13	150-150-150
	200-200-100
	300-200-100
	400-200-100
0.15	200-100-100
	300-100-100
	400-100-100
0.16	100-100-100
0.18	200-200-0

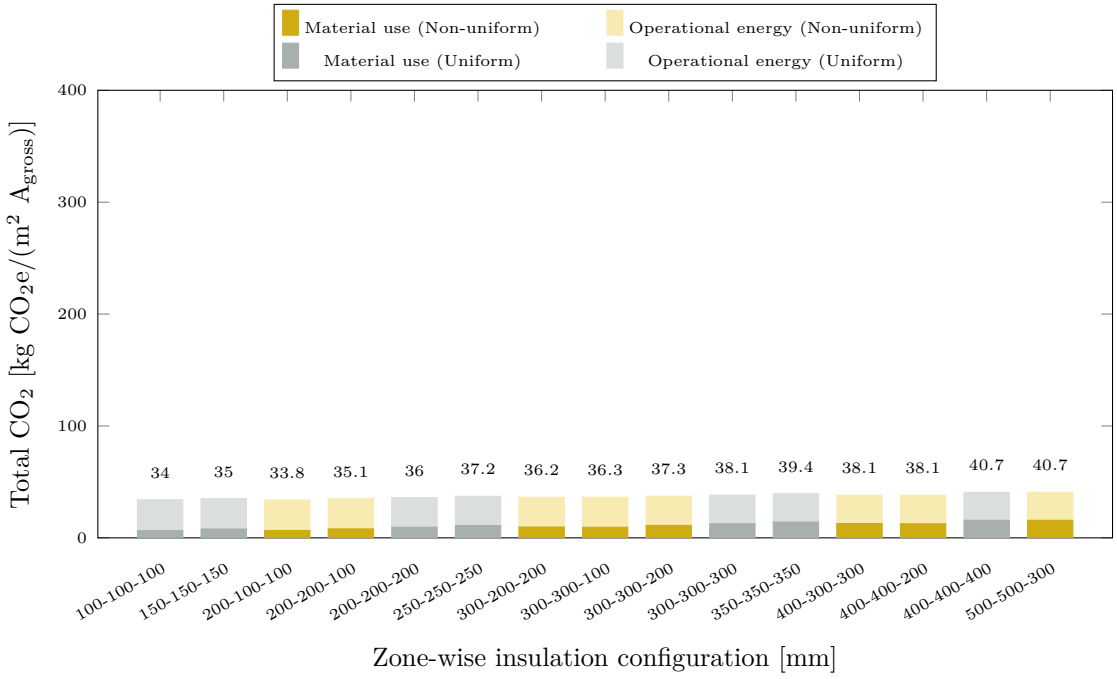

Figure A.3: Total GWP for each CLT system configuration in the school/preschool, based on a heat pump. Results are split into material use and operational energy.

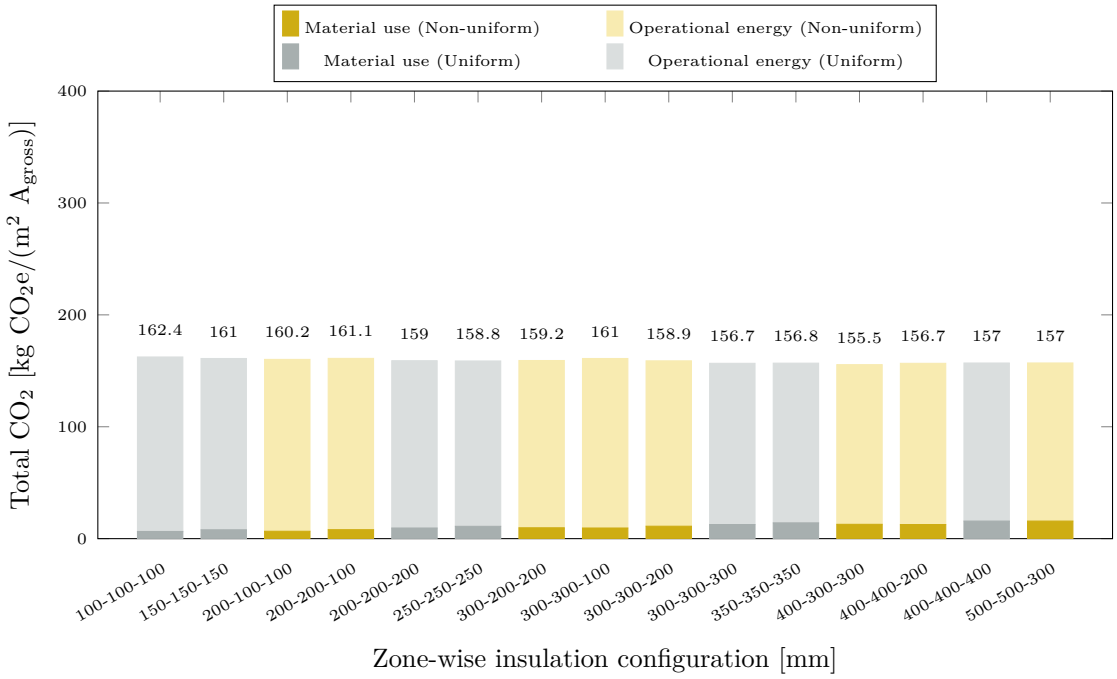

Figure A.4: Total GWP for each CLT system configuration in the school/preschool, based on district heating. Results are split into material use and operational energy.

A.3 Koljern system

Table A.3: Zone-wise insulation configurations for the Koljern system in the school/preschool, grouped by resulting U-value.

U-value [W/(m^2 · K)]	**Insulation thickness ranges** [mm]
0.07	200-200-200
	Zone 1: 200–500
	Zone 2: 200–400
	Zone 3: 100–200
0.08	150-150-150
	Zone 1: 150–450
	Zone 2: 150–350
	Zone 3: 50–150
0.09	100-100-100
	Zone 1: 100–400
	Zone 2: 100–250
	Zone 3: 0–100
0.10	50-50-50
	Zone 1: 50–350
	Zone 2: 50–150
	Zone 3: 0–50
0.11	
	Zone 1: 50–250
	Zone 2: 0–50
	Zone 3: 0
0.12	
	Zone 1: 50–200
	Zone 2: 0
	Zone 3: 0

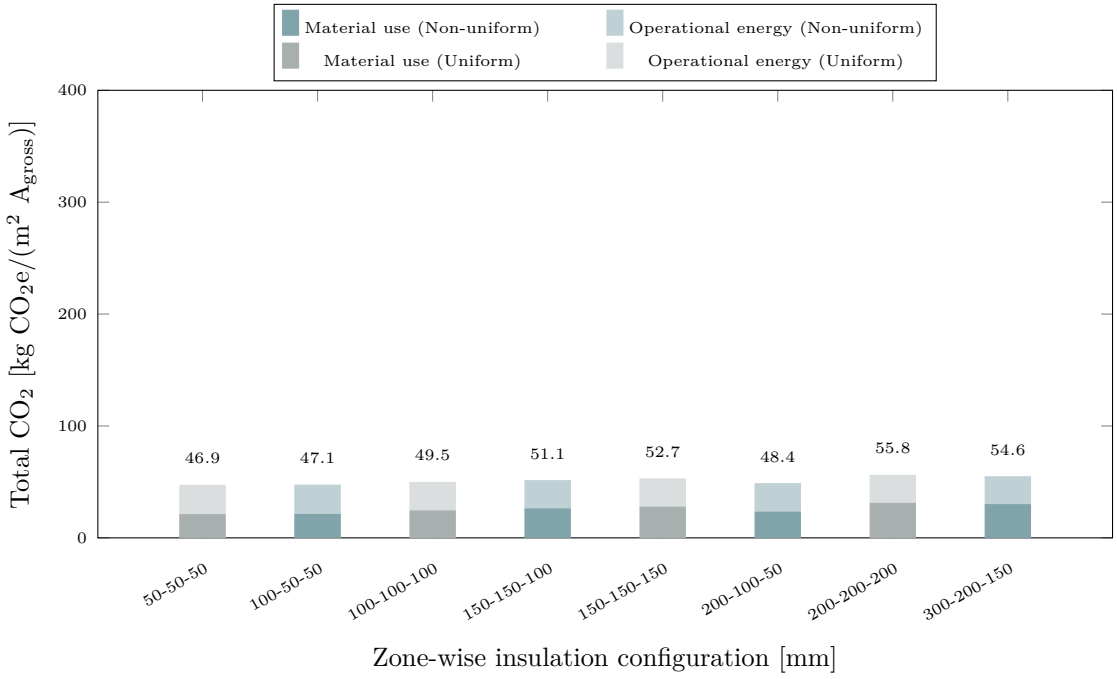

Figure A.5: Total GWP for each Koljern system configuration in the school/preschool, based on a heat pump. Results are split into material use and operational energy.

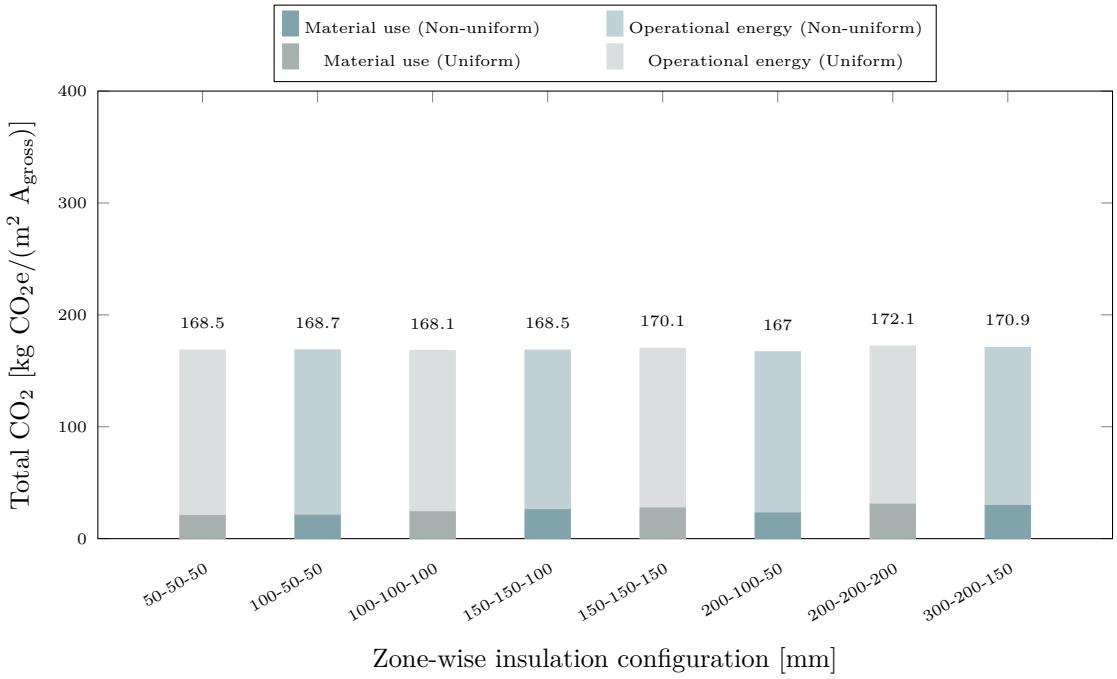

Figure A.6: Total GWP for each Koljern system configuration in the school/preschool, based on district heating. Results are split into material use and operational energy.

B

Warehouse

B.1 Concrete system

Table B.1: Zone-wise insulation configurations for the concrete system in the warehouse, grouped by resulting U-value.

U-value [W/(m^2 · K)]	**Insulation thickness** [mm]
0.07	400-400-400
	600-400-400
	500-400-400
	500-500-200
	600-400-300
	500-400-300
	400-400-300
0.08	350-350-350
	500-400-200
	400-400-200
	600-300-300
	500-300-300
	400-300-300
0.09	300-300-300
	500-300-200
	400-400-100
	400-300-200
	300-300-200
0.10	250-250-250
	400-300-100
	300-300-100
0.11	500-200-200
	400-200-200
	300-200-200
0.12	200-200-200
	400-200-100
	300-200-100
0.13	200-200-100
0.14	150-150-150
0.16	400-100-100
	200-200-0
	300-100-100
0.17	200-100-100
0.18	100-100-100

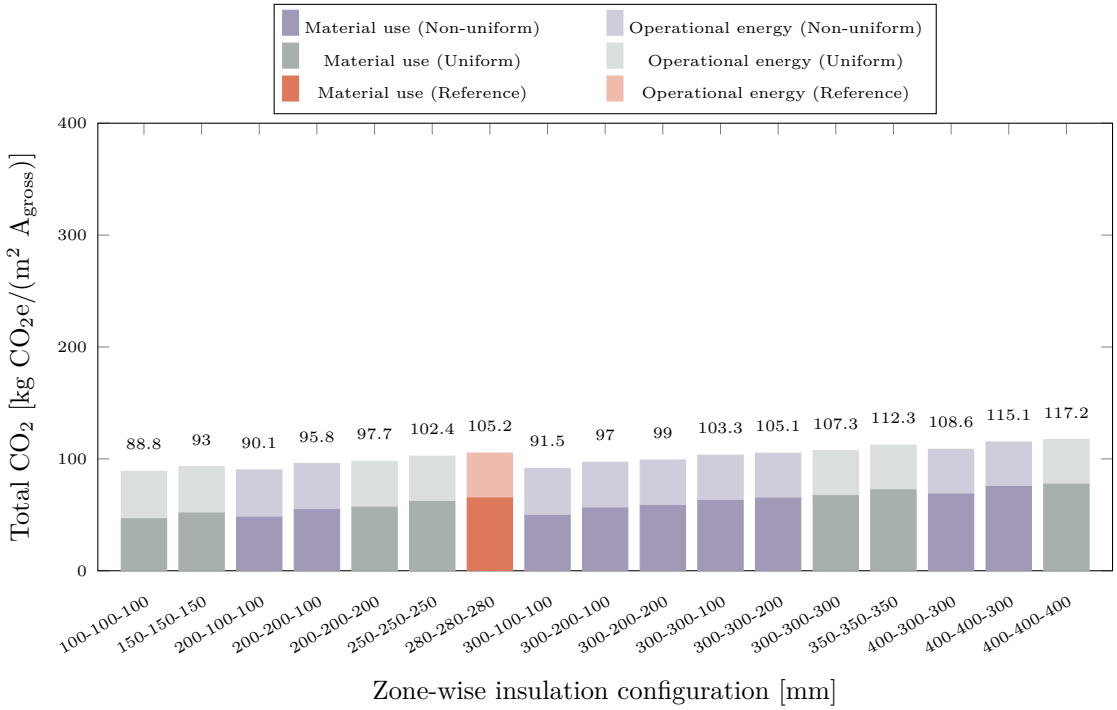

Figure B.1: Total GWP for each concrete system configuration in the warehouse, based on a heat pump. Results are split into material use and operational energy.

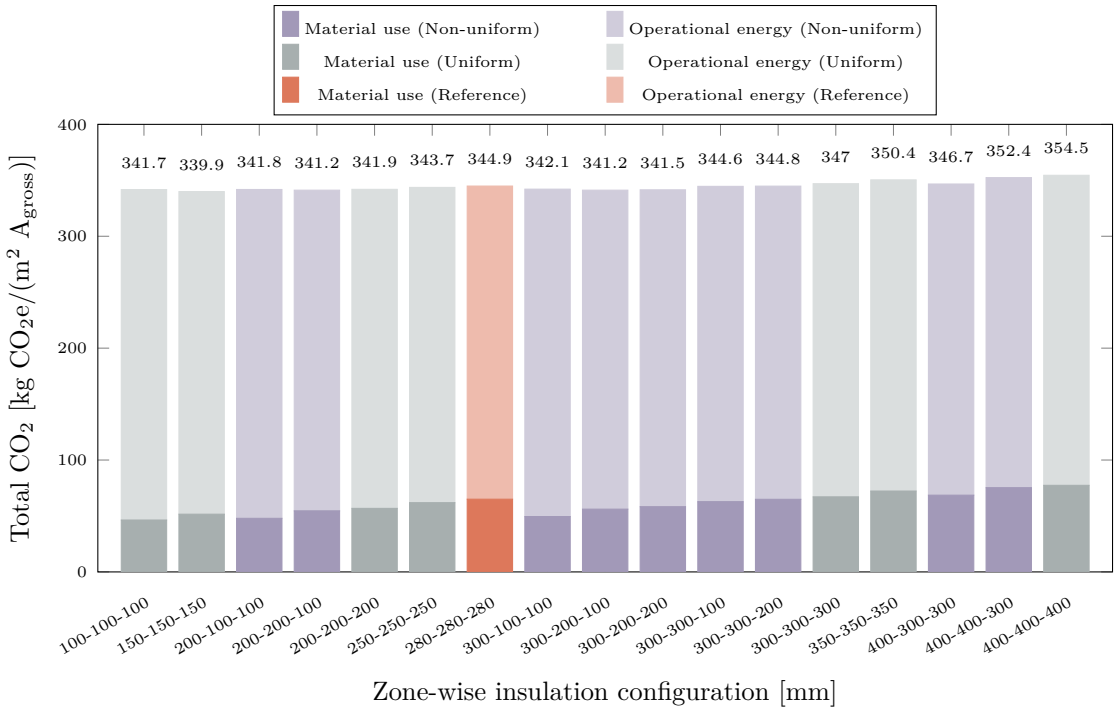

Figure B.2: Total GWP for each concrete system configuration in the warehouse, based on district heating. Results are split into material use and operational energy.

B.2 CLT system

Table B.2: Zone-wise insulation configurations for the CLT system in the warehouse, grouped by resulting U-value.

U-value [W/(m^2 · K)]	**Insulation thickness** [mm]
0.07	400-400-200
	400-400-300
	500-400-200
	500-400-300
	500-400-400
	500-500-200
	600-400-300
0.08	300-300-300
	400-300-200
	400-300-300
	400-400-100
	500-300-200
	500-300-300
	600-300-300
0.09	250-250-250
	300-300-200
	400-300-100
0.10	300-200-200
	300-300-100
	400-200-200
	500-200-200
0.11	200-200-200
	300-200-100
	400-200-100
0.12	200-200-100
0.13	150-150-150
0.14	200-200-0
	300-100-100
	400-100-100
0.15	200-100-100
0.16	100-100-100
0.17	200-100-0
0.18	100-100-0

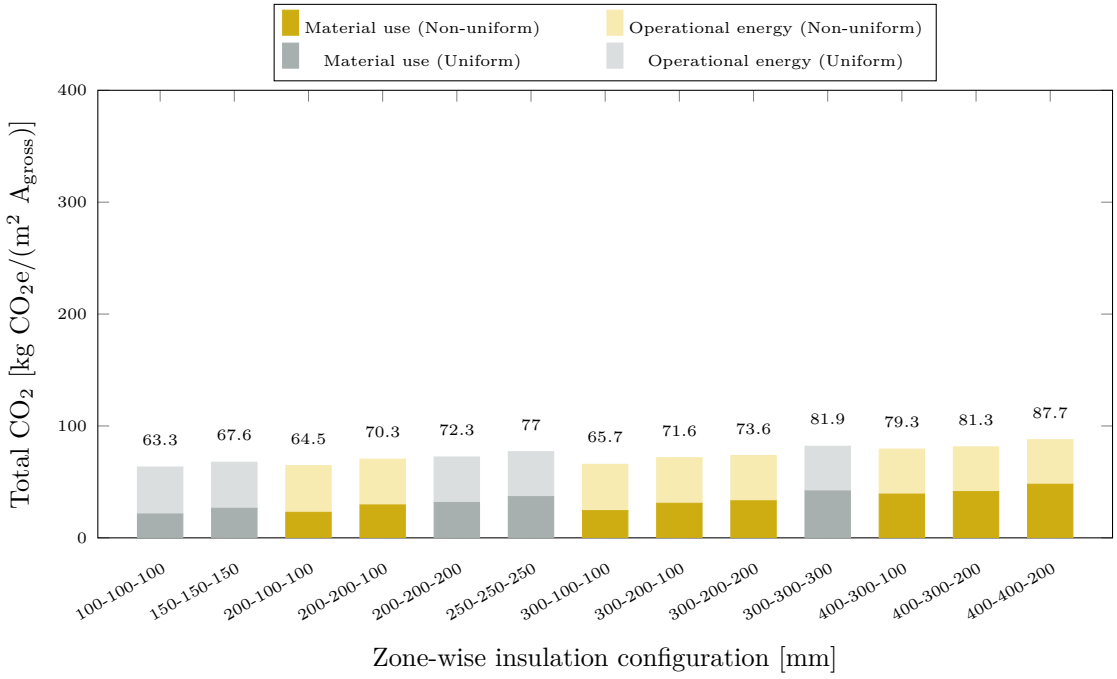

Figure B.3: Total GWP for each CLT system configuration in the warehouse, based on a heat pump. Results are split into material use and operational energy.

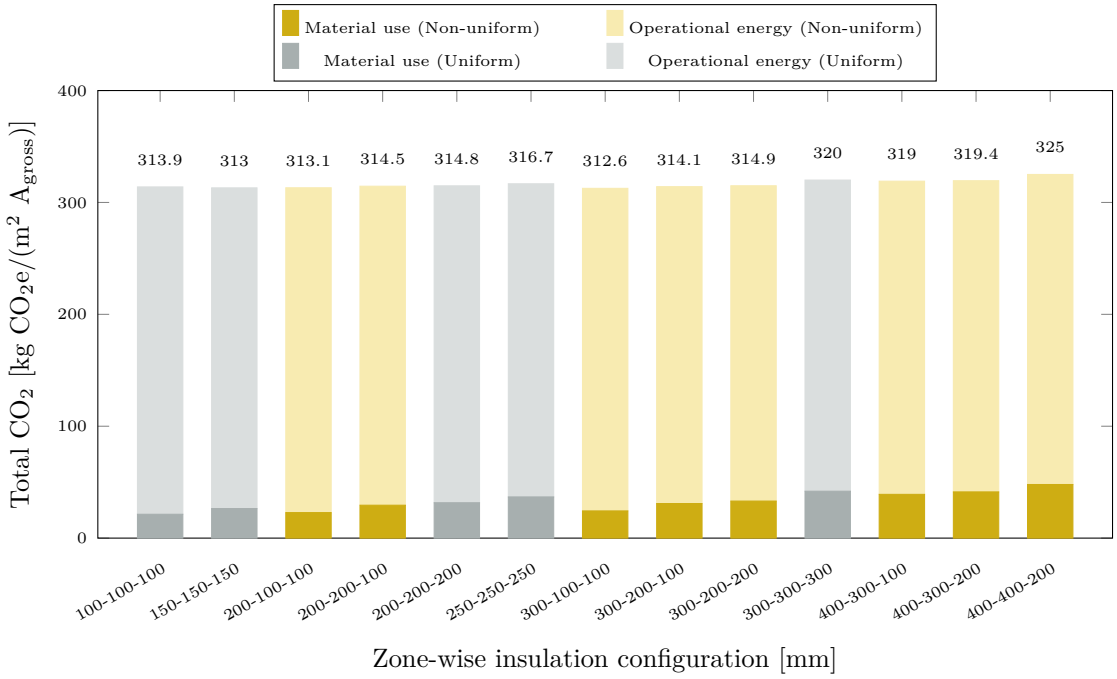

Figure B.4: Total GWP for each CLT system configuration in the warehouse, based on district heating. Results are split into material use and operational energy.

B.3 Koljern system

Table B.3: Zone-wise insulation configurations for the Koljern system in the warehouse, grouped by resulting U-value.

U-value $[W/(m^2 \cdot K)]$	**Insulation thickness ranges** [mm]
0.07	200-200-200
	Zone 1: 200–500
	Zone 2: 200–400
	Zone 3: 50–400
0.08	150-150-150
	Zone 1: 150–450
	Zone 2: 100–350
	Zone 3: 0–350
0.09	100-100-100
	Zone 1: 100–350
	Zone 2: 100–300
	Zone 3: 0–300
0.10	Zone 1: 100–350
	Zone 2: 50–250
	Zone 3: 0–250
0.11	50-50-50
	Zone 1: 50–250
	Zone 2: 0–50
	Zone 3: 0
0.12	Zone 1: 50–200
	Zone 2: 0–200
	Zone 3: 0–200

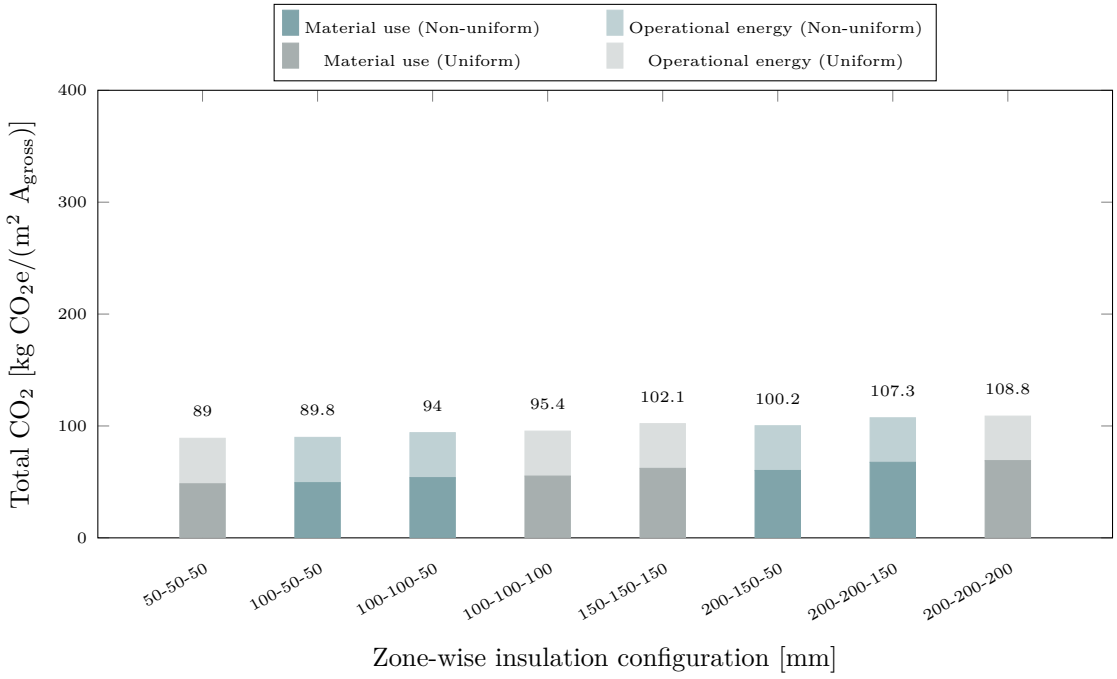

Figure B.5: Total GWP for each Koljern system configuration in the warehouse, based on a heat pump. Results are split into material use and operational energy.

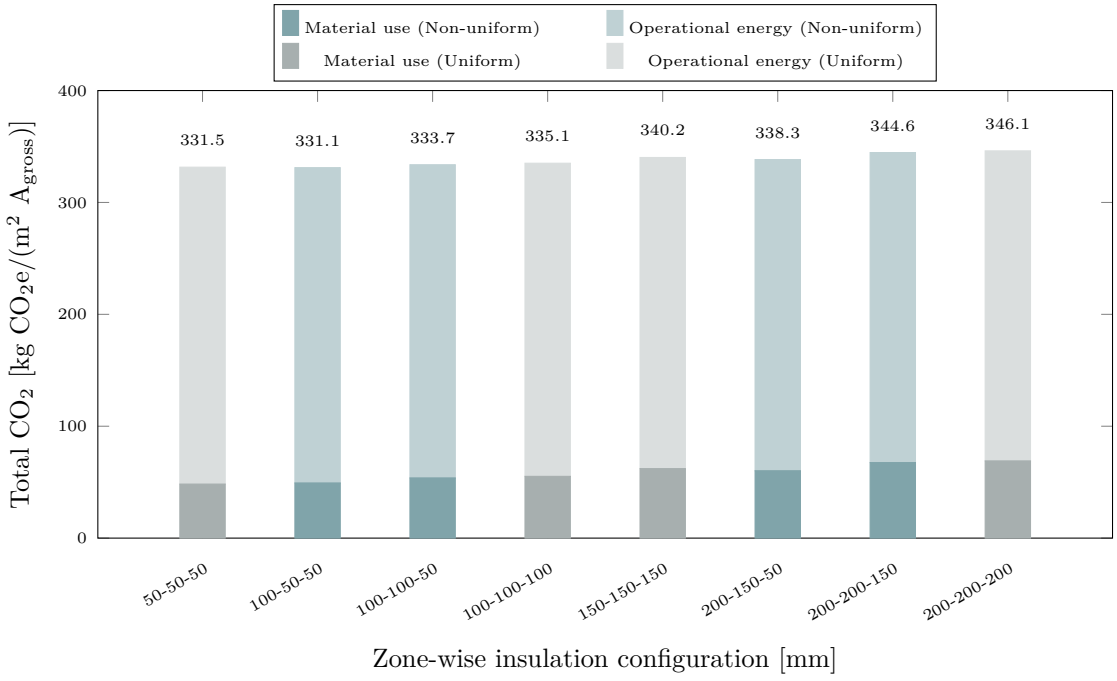

Figure B.6: Total GWP for each Koljern system configuration in the warehouse, based on district heating. Results are split into material use and operational energy.

C
Residential

C.1 Concrete system

Table C.1: Zone-wise insulation configurations for the concrete system in the residential building, grouped by resulting U-value.

U-value [W/(m^2 · K)]	**Insulation thickness** [mm]
0.07	400-400-400
	500-400-400
	500-500-300
	500-500-400
	600-400-400
	600-500-300
	600-500-400
	600-600-300
0.08	350-350-350
	400-400-300
	500-400-300
	600-400-300
0.09	300-300-300
	400-300-300
	400-400-200
	500-300-300
	500-400-200
	500-500-200
	600-300-300
0.10	300-300-200
	400-300-200
	500-300-200
0.11	250-250-250
	500-200-200
0.12	200-200-200
	300-200-200
	400-200-200
	400-300-100
	400-400-100
0.13	300-300-100
0.14	300-200-100
	400-200-100
0.15	150-150-150
	200-200-100
0.17	300-100-100
	400-100-100
0.18	200-100-100
0.19	100-100-100

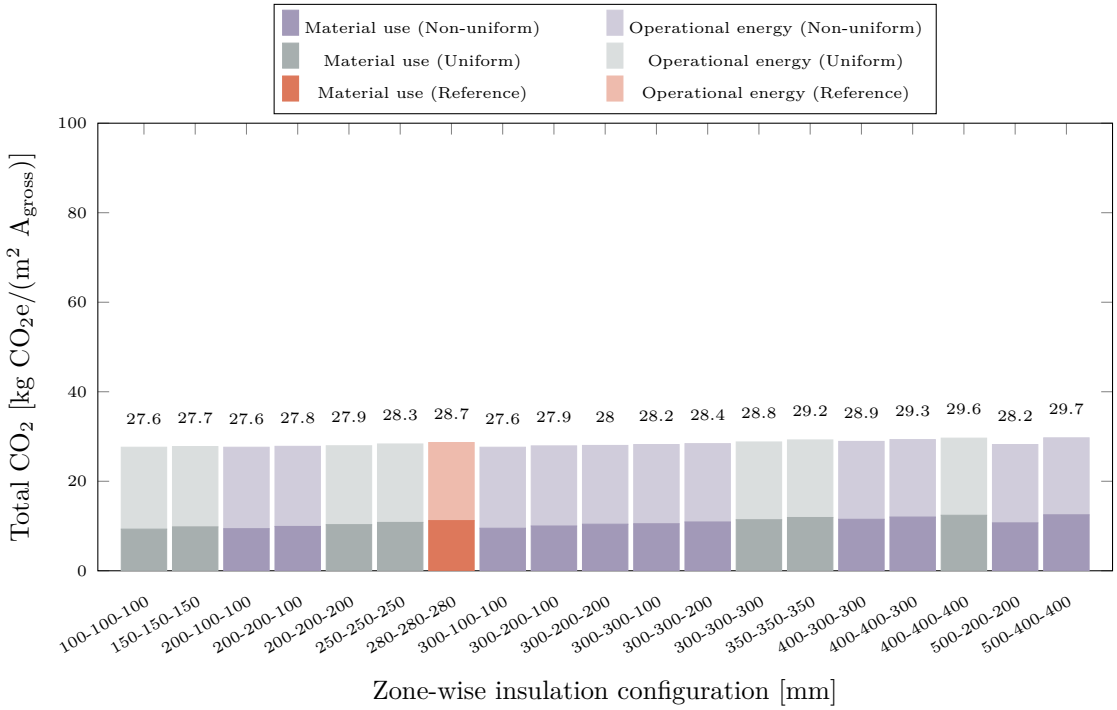

Figure C.1: Total GWP for each concrete system configuration in the residential building, based on a heat pump. Results are split into material use and operational energy.

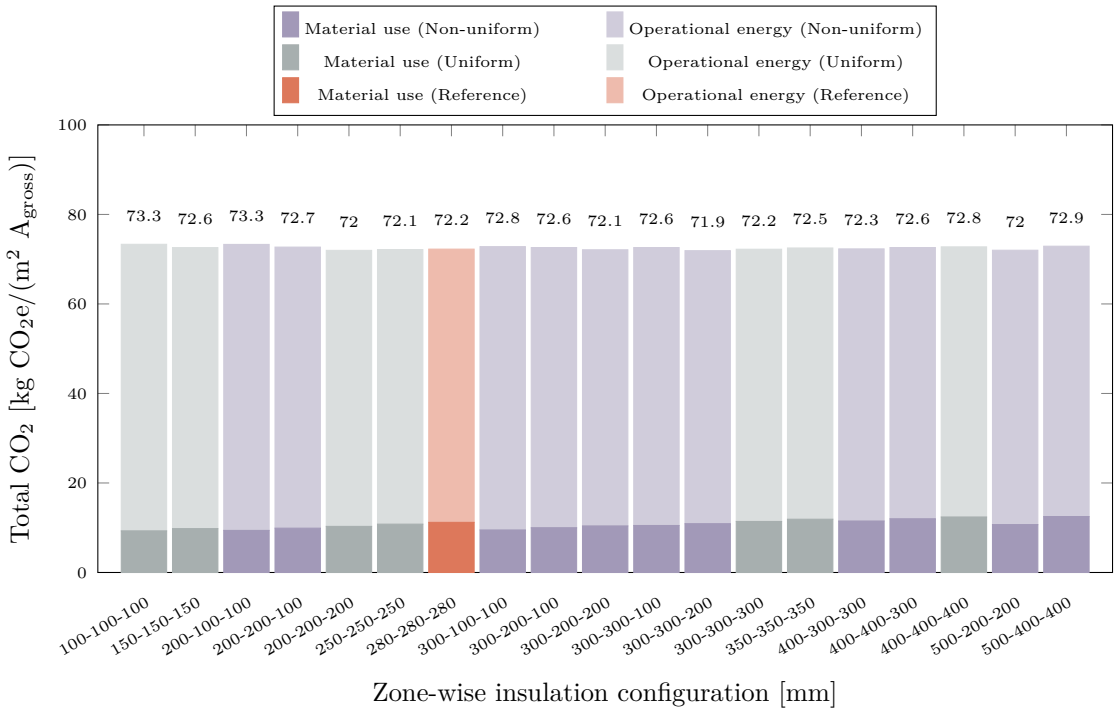

Figure C.2: Total GWP for each concrete system configuration in the residential building, based on district heating. Results are split into material use and operational energy.

C.2 CLT system

Table C.2: Zone-wise insulation configurations for the CLT system in the residential building, grouped by resulting U-value.

U-value [W/(m^2 · K)]	**Insulation thickness** [mm]
0.07	400-400-400
	500-500-300
	600-400-300
	600-500-300
0.08	350-350-350
	400-300-300
	400-400-300
	500-300-300
	500-400-300
	500-500-200
	600-300-300
0.09	300-300-300
	400-300-200
	400-400-200
	500-300-200
	500-400-200
0.10	250-250-250
	300-300-200
0.11	200-200-200
	300-200-200
	400-200-200
	400-300-100
	400-400-100
	500-200-200
0.12	300-300-100
0.13	150-150-150
	200-200-100
	300-200-100
	400-200-100
0.15	200-100-100
	300-100-100
	400-100-100
0.16	100-100-100
0.18	200-200-0
0.20	200-100-0

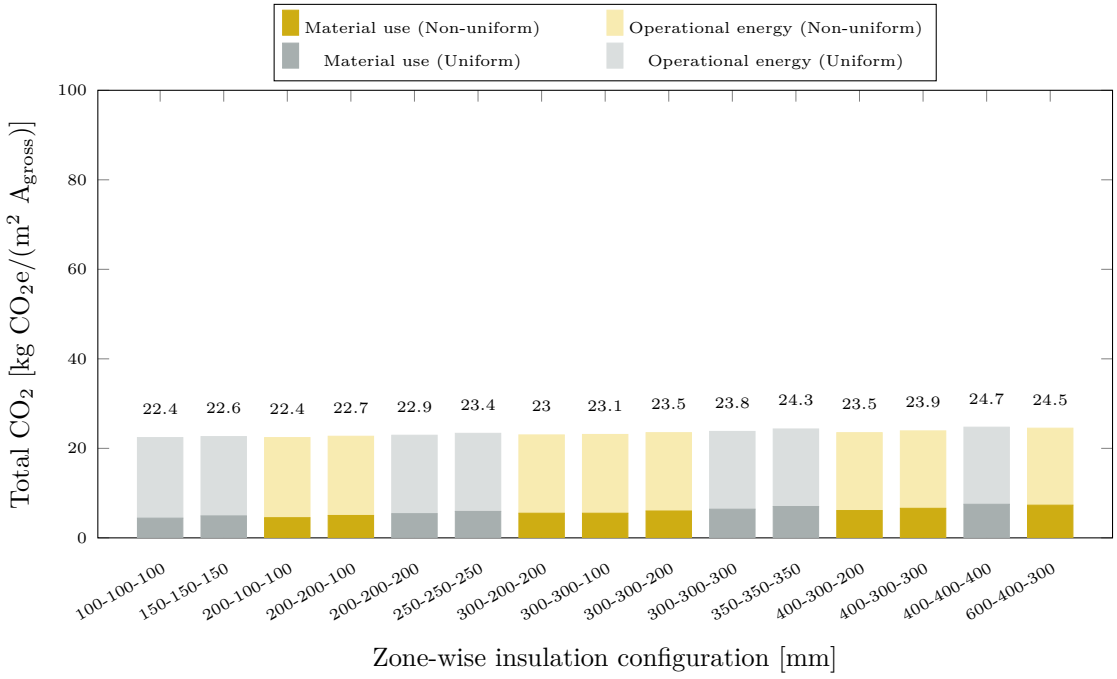

Figure C.3: Total GWP for each CLT system configuration in the residential building, based on a heat pump. Results are split into material use and operational energy.

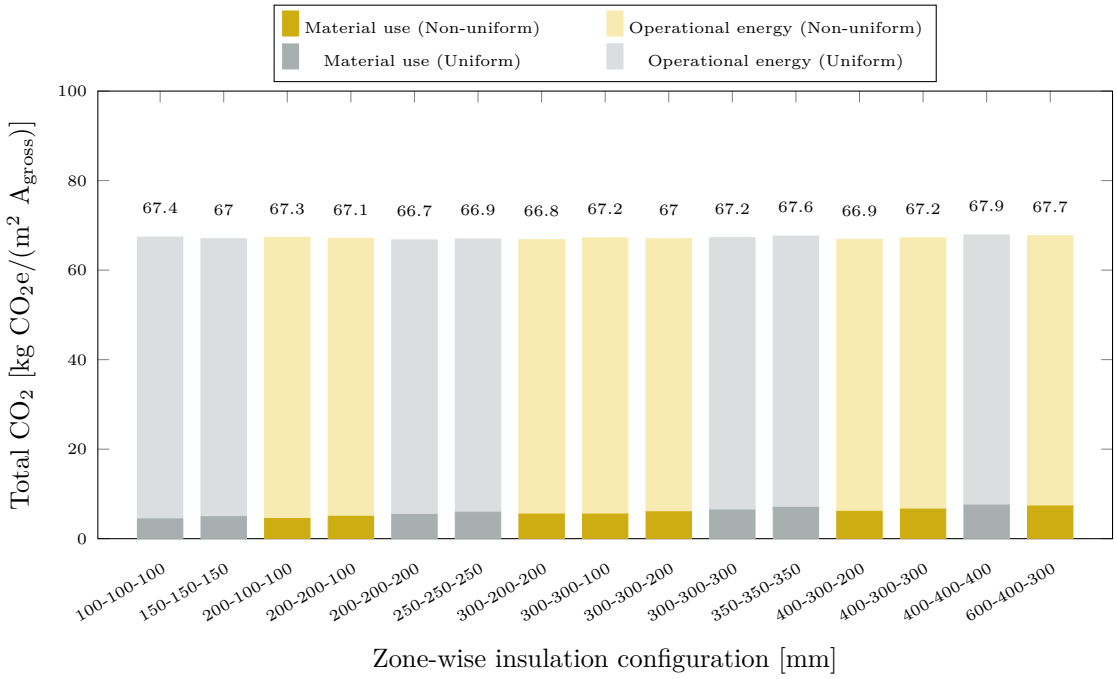

Figure C.4: Total GWP for each CLT system configuration in the residential building, based on district heating. Results are split into material use and operational energy.

C.3 Koljern system

Table C.3: Zone-wise insulation configurations for the Koljern system in the residential building, grouped by resulting U-value.

U-value [W/(m^2 · K)]	**Insulation thickness ranges** [mm]
0.07	200-200-200
	Zone 1: 200–500
	Zone 2: 200–400
	Zone 3: 100–250
0.08	150-150-150
	Zone 1: 150–150
	Zone 2: 150–150
	Zone 3: 150–150
0.09	100-100-100
	Zone 1: 100–100
	Zone 2: 100–100
	Zone 3: 100–100
0.10	50-50-50
	Zone 1: 100–50
	Zone 2: 50
	Zone 3: 50
0.11	
	Zone 1: 50–250
	Zone 2: 0–50
	Zone 3: 0
0.12	
	Zone 1: 150–150
	Zone 2: 0
	Zone 3: 0

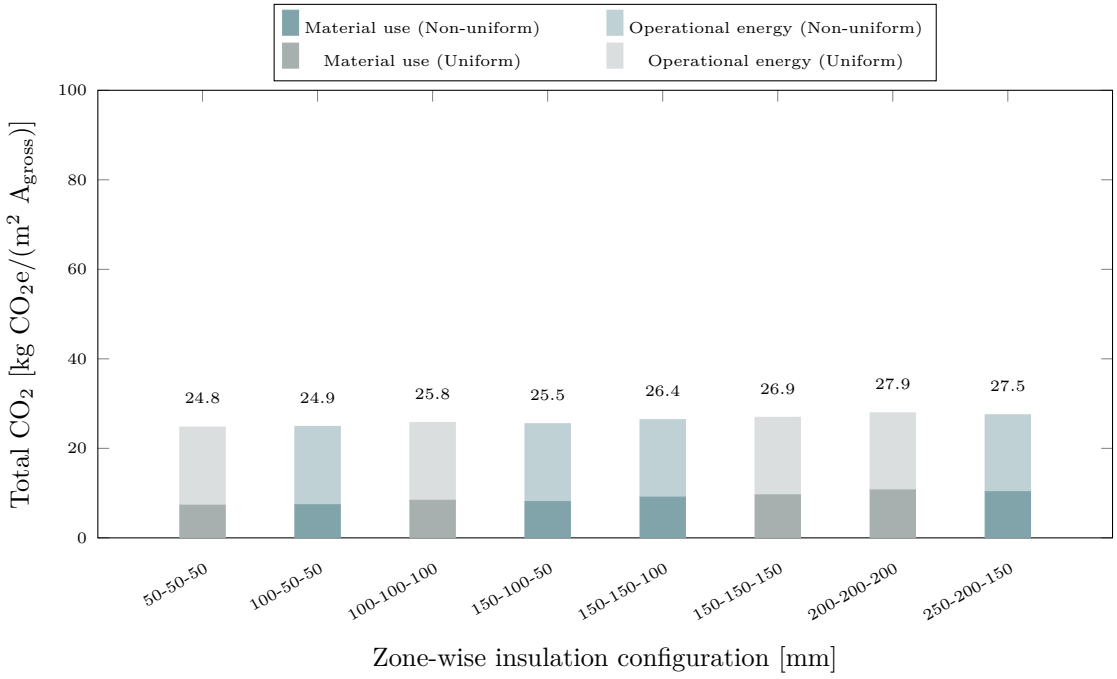

Figure C.5: Total GWP for each Koljern system configuration in the residential building, based on a heat pump. Results are split into material use and operational energy.

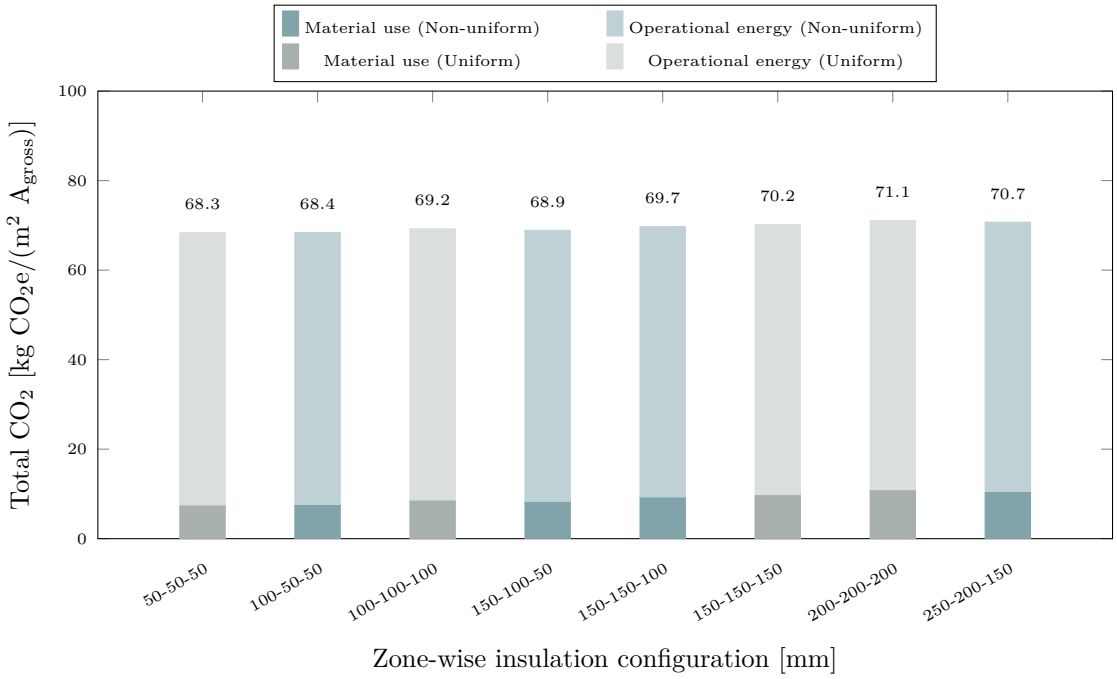

Figure C.6: Total GWP for each Koljern system configuration in the residential building, based on district heating. Results are split into material use and operational energy.

D

GWP-values

Table D.1: GWP-values for concrete and reinforcement.

Company	**Product**	**A1-A3** [kg CO_2e/m^3]
Skanska	Concrete C25/30	225
Skanska	Low carbon concrete 20% C25/30	175
Stena Stål	Reinforcement	557 (kg CO_2e/ton)

Table D.2: GWP-values for EPS S100 and the average used for calculations.

	Company	**A1-A3** [kg CO_2e/m^3]
	Finja	73.2
	Finnfoam	53
Average		63.1

Table D.3: GWP-values for EPS S200 and the average used for calculations.

	Company	**A1-A3** [kg CO_2e/m^3]
	Finja	127.3
	Finnfoam	79.5
Average		103.4

Table D.4: GWP-values for the weather protection layer used for calculations.

Company	**Product**	**A1-A3** [kg CO_2e/m^2]
SIGA	Wetguard	1.1

Table D.5: GWP-values for components in the Koljern system used for calculations.

Company	**Product**	**A1-A3**
Foamglas	T3+	137.8 kg CO_2e/m^3
Lindab	Galvanized steel beam	2.8 kg CO_2e/kg

DEPARTMENT OF SOME SUBJECT OR TECHNOLOGY
CHALMERS UNIVERSITY OF TECHNOLOGY
Gothenburg, Sweden
www.chalmers.se

CHALMERS
UNIVERSITY OF TECHNOLOGY